Interactive comment on "A CMEMS forecasting system for the marine ecosystem of IBI European waters" by Elodie Gutknecht et al.

Anonymous Referee #1
Received and published: 19 February 2019

Dear Referee,

Please find our comments/responses in blue throughout your text.
We have also attached a new release of the article.
This is a major revision of the initial article: the introduction has been completely revised, the sections are modified, a discussion section has been added. A synthesis of the results has been added by using a table and a Taylor diagram.
All your comments have been taken into account in the new release of the article.
If required we can also provide a version with the word track change, but I don't think that's helpful to you.
Thank you for your useful comments.

Elodie Gutknecht on behalf of co-authors.

General comments:

The manuscript "A CMEMS forecasting system for the marine ecosystem of IBI" by Elodie Gutknecht et al. aims to describe the skill performances of the CMEMS operational model system "IBI36" for the Iberia-Biscay-Ireland (IBI) area, with specific emphasis on the biogeochemical component. IBI36 is built on a physical-biogeochemical online coupling between NEMOv3.6 physical model and PISCESv2 biogeochemical model, at 1/36° horizontal resolution and with 50 vertical levels. The system is operational since April 2018, and consistently provides 7-days forecasts for ocean physics and biogeochemistry. The validation is applied over the "IBI Extended Domain", and is performed with a 2010-2016 simulation, using a suite of different reference data streams (from satellite and in situ, and 2 BGC-Argo floats), and then on a regional basis with comparison with in situ historical data (Northern Seas, North-East Atlantic waters, Bay of Biscay and Mediterranean Sea). IBI36 results generally consistent with the main properties of biogeochemical variables (chlorophyll, nutrients, oxygen and net primary production), in terms of spatial distribution and seasonal cycles. An indicator concerning oxygen deficiency is also proposed and assessed, which may be of great importance for the broad environmental communities, extending to the general public as well.

The manuscript is clear and well written, with a precise subdivision of the different sections (model configuration, reference data and validation, discussion). However, some major weaknesses can be highlighted:

1. The title specifically refers to the "CMEMS forecasting system": even if it may be acknowledged the goal of the work, the validation is here performed at seasonal or annual time scale on the period 2010-2016, computing monthly averages (as defined in P8, L29), and there is no reference to the forecasting skill of the operational system, that should be done on daily (or at least, weekly) averages. So, how the described validation may be suitable for the short-term forecasting system assessment? The reader would be interested in see results on how the IBI36 short-term forecast products compare with reference data (or with the background simulation). Which metrics, of the ones proposed, can then be used operationally to quantitatively evaluate the forecasting skill?

Author answer:
You are right; the title explicitly refers to the "CMEMS forecasting system". I realize that the title was not judiciously chosen and does not reflect the purpose of this paper. The purpose of this paper is to evaluate the biogeochemical component of the IBI coupled model system. This system has been developed to monitor and forecast the ocean dynamics and marine ecosystems of the European waters. But prior to its operational launch, a pre-operational qualification simulation is necessary to evaluate the performance of the coupled system. Here we evaluate this qualification simulation. It represents a substantial paper, with many figures. But it's necessary and voluntary. This paper represents the first validation of the biogeochemical component of the IBI36 system; it is intended to be complete and detailed, as it will serve as a basis for further studies. So the forecasting capability of the operational system will be studied and described in another paper. To avoid any misunderstanding, we propose to modify the title of the paper by: "Modelling the marine ecosystem of IBI European waters for CMEMS operational applications". We also modified the abstract and the Introduction to make clearer the objective of the paper.

2. The model system products are validated basically following consistency (Figs. 2 to 6, 8, 9, 10ab, 11, 12, 13, 15), providing BIAS and correlation. However, the uncertainty of products (i.e., forecast, see the previous point) seems not addressed. It may be interesting to quantitatively assess the capability of the model to represent the observed variability: did the author consider to evaluate the model uncertainty, e.g. by means of RMSE? The use of quantitative comparison may be even more useful in the NPP analysis, to estimate the spatial gradient. Further, is there any reason why Fig. 7 does not report the linear regression (as done in Figs. 11 and 14)? Moreover, on a higher level, given that the validation assessment is discussed following a regional subdivision (which is basically driven by the availability of data), I think it could be useful to provide the readers with a synthesis table with the mean values of the validation metrics (i.e. BIAS, correlation, uncertainty – e.g. as RMSE) per each region.

Author answer:
You are right, in order to complete the skill assessment, the RMSE was added in the Chl-a comparison to satellite estimate. The NPP analysis was also revised. It now presents the mean of

the three NPP products (VGPM, Eppley-VGPM and CbPM), the standard deviation of these three products and the bias between the IBI36 system and the averaged NPP products.

The regression lines are not discussed, so they are removed in all figures.

We also added a synthesis to summarize the performances for each region. It is presented in a Table for comparison to satellite estimates and in a Taylor diagram for in-situ observations.

3. The synthetic overview of the "IBI waters" (Section 2) in terms of the biogeochemical and ecosystem dynamics is interesting since gathers different regions with different properties in a single framework. However, it is not effectively used to define the areas then adopted in the validation (P9, L19). Authors should refer the definition of the 12 small boxes to this overview and then link the different model performances to the different biogeochemical properties of the specific areas. As an example, the availability of reference data may allow validating the consistency of the IBI36 system (or of a specific product) in a specific area/season. And this may be critical to provide indications on the quality of the model system to simulate eutrophication in the different areas (and again, the use of the synthesis table suggested at point 2 would be beneficial for this purpose).

Author answer:
You are right, the "IBI waters" (Section 2) has been revised in order to introduce the areas (the 12 small boxes) adopted in the validation section. Model performances are now better linked to the different biogeochemical properties of the specific areas.

Specific comments:

1. Are there other model applications to the IBI waters (also not operational)? Can the authors discuss how does the IBI36 perform in comparison with other operational systems (e.g. CMEMS Global)?

Author answer:

Within the framework of CMEMS, three other MFC share a part of their domain with IBI:
- GLO-MFC which covers the world's oceans at 1/4° resolution and is also using the PISCES biogeochemical model,
- MED-MFC which covers the Mediterranean Sea at 1/24° with the Biogeochemical Flux Model (BFM; Vichi et al., 2007a,b),
- NWS-MFC which covers the North-West European Shelf at 1/15° latitudinal resolution and 1/9° longitudinal resolution (~ 7km) with the ERSEM ecosystem model (Baretta et al., 1995).

For the physical component, two intercomparison papers have been submitted in ocean Science - Special issue "The Copernicus Marine Environment Monitoring Service (CMEMS): scientific advances". They are Lorente et al. (2019) and Mason et al. (2019).

For the biogeochemical component, the comparison of the different model applications is a work in progress and will be the subject of a separate paper, including the contribution of the regional in relation to the global, as well as the comparison of three distinct biogeochemical models.

The Introduction has been revised and now includes a state of the art part.

References:

Baretta, J. W., W. Ebenhoh, et al. (1995). "The European regional seas ecosystem model, a complex marine ecosystem model." Netherlands Journal of Sea Research 33(3-4): 233-246.
Lorente, P., García-Sotillo, M., Amo-Baladrón, A., Aznar, R., Levier, B., Sánchez-Garrido, J. C., Sammartino, S., De Pascual, Á., Reffray, G., Toledano, C., and Álvarez-Fanjul, E.: Skill assessment of global, regional and coastal circulation forecast models: evaluating the benefits of dynamical downscaling in IBI surface waters, Ocean Sci. Discuss., https://doi.org/10.5194/os-2018-168, in review, 2019.
Mason, E., Ruiz, S., Bourdalle-Badie, R., Reffray, G., Garcia-Sotillo, M., and Pascual, A.: Copernicus (CMEMS) operational model intercomparison in the western Mediterranean Sea: Insights from an eddy tracker, Ocean Sci. Discuss., https://doi.org/10.5194/os-2018-169, in review, 2019.
Vichi, M., Pinardi, N., and Masina, S.: A generalized model of pelagic biogeochemistry for the global ocean ecosystem. Part I: theory, J. Marine Syst., 64, 89-109, https://doi.org/10.1016/j.jmarsys.2006.03.006, 2007a.
Vichi, M., Masina, S., and Navarra, A.: A generalized model of pelagic biogeochemistry for the global ocean ecosystem. Part II: numerical simulations, J. Marine Syst., 64, 110-134, https://doi.org/10.1016/j.jmarsys.2006.03.014, 2007b.

A link with the global model is included only in Section 5 (P15, L15), where some more details (and relevant references) could be added. Also, the comment to the global performance at the eastern boundary (Skagerrak and Kattegat, P12, L16) could be more supported by some reference (again, the CMEMS Global).

Author answer:
The link with the global model is made in Section 3.2 as it is used at initial and open boundary conditions of the IBI system. The comment to the global performance at the eastern boundary (Skagerrak and Kattegat) has been modified. There is not particular evaluation of the Global system is this region. The CMEMS Baltic Sea regional configuration instead of the global product should be tested at the eastern open boundary of the IBI36 system.

2. GODAE Class metrics are widely recognized as references for the skill performance assessment of ocean operational systems and adopted also within the Copernicus community. Is there a specific reason why the authors did not include any mention to them?

Author answer:
You are right; it's an oversight on our part. GODAE metrics are introduced in Section 4.

3. Do you have any explanation of why the model anticipates the spring-summer bloom development and decrease in the north Atlantic (P9, L14-18)? Is it linked with physical forcing or with the biogeochemical parameterization?

Author answer:

The model anticipates the spring-summer bloom development and decrease in the north Atlantic. The bloom onset is in phase in the south part of the domain, but spreads more rapidly to the north as compared to satellite data. The summer decrease after the bloom is then earlier and sometimes more pronounced in the model. In fact, modelled chlorophyll-a is found deeper during summer with the formation of a Deep Chlorophyll Maximum while maximum Chl-a remains at the surface in BGC-Argo estimates.

I think that both phenomena (timing of the bloom and vertical migration of the maximum chlorophyll) are linked. As phytoplankton starts growing earlier in the model, the mixed layer becomes nutrient-depleted at the end of spring (oligotrophic conditions) in the model and phytoplankton migrates just below. This behavior is also present in the global model.

Several experiments on the physical and biogeochemical components are being carried out. The analysis of the BGC-Argo opens new doors for us to understand the vertical dynamics of phytoplankton. Another area for improvement is opened up with the assimilation of water color data.

This problem is now discussed in the Discussion section.

4. Fig. 4 and comment at (P9, L19-24): referring to "high correlation coefficient between the model and the data" I suppose the authors consider correlation values (r) larger than 0.7. However, box 12 (Gulf of Cadiz) has a correlation r=0.55, which is actually lower than the one for the English Channel (box 6, r=0.59). Please comment.

Author answer:
High correlation coefficient refers to values (r) larger than 0.7.
Boxes were slightly revised. As this box was not discussed, it has been removed in the revised version.

Further in Fig. 4: how the associated error to ESA OC-CCI product is estimated?

Author answer:
ESA OC-CCI distributes an estimation of the error associated to the chlorophyll-a concentration in sea water. The name of this variable is "CHL_error". But the term "error" is misleading. This is actually a standard deviation of the daily data when calculating the monthly average. It has to be analyzed jointly with the number of daily files that contained data incorporated into the monthly average. So to avoid any misunderstanding, it has been removed in the revised version.

5. Which specific products have been used from EMODnet? Please clarify the kind of "regional aggregated products" used (P7, L31-33). Further, you refer to EMODnet database as "in situ" (P10, L23; P13, L10, and P14, L25), but this looks in contradiction with the "aggregation" previously referred. Please clarify and reformulate.

Author answer:

In the two projects Seadatanet and EMODnet chimie, regional datasets are developed. They are "aggregated datasets" or "observation collections" by region, including one product in the North Atlantic and one in the Mediterranean basin. These datasets receive additional quality control of metadata and data.

They can be found here:

http://www.emodnet-chemistry.eu/products/catalogue#/search?fast=index&_content_type=json&from=1&to=20&sortBy=popularity&any=aggregated%20datasets

EMODnet website explicitly uses the term "aggregated dataset", and not "aggregated product" as referred in the paper. So to avoid any misunderstanding, the term "aggregated product" has been changed to "aggregated dataset" in the revised paper.

6. Fig. 10 is potentially very interesting, especially for communities more linked to environmental management. I suggest to enrich the discussion and provide some more information on this indicator: how is computed the minimum in Fig.10a and b (is this defined considering at least 1 daily value lower than the threshold as in P11, L17? is the minimum found along the vertical profile, or at the sea bottom? That should be defined at the beginning of the discussion at P11)? Do the two maps show the absolute minimum over the whole investigated period for each cell shown? What is shown in the time series of Fig.10c? Please clarify. Further, the deficiency threshold (at 187 umol/l) could be added to Fig.10c (e.g. with a dashed line): this may help to appreciate the model skill in representing the oxygen deficiency, and the fact that in 2011 and 2015 the model predicts higher levels than observed. To measure the skill of the model to overcome a specific threshold in comparison with observed data, authors may also consider using the statistics based on the relative operating characteristic (ROC), as for example shown in Sheng and Kim (J. Mar. Sys. 76, 212-243, 2009).

Author answer:

Fig. 10a present the absolute minimum oxygen concentrations for each 1°x1° grid point from ICES dataset (Fig. 10a left) and from IBI36 daily outputs co-located to ICES dataset (Fig. 10a right).

Fig. 10b presents the time series of the absolute minimum oxygen concentrations for each date from ICES dataset (red line) and from IBI36 daily outputs co-located to ICES dataset (black line).

So, in Fig. 10a, and b, we only catch low oxygen concentrations reported to the ICES database. We miss all other low oxygen events. But the objective is here to evaluate/validate the model estimates. The model performs in reproducing the spatial distribution and seasonal evolution of low oxygen concentrations.

After this positive evaluation, we are confident in the model results, so we can estimate the total surface area vulnerable to oxygen deficiency over the continental shelf (bathymetry <= 200m). In Fig. 10c, we do not restrict to the IBI36 daily outputs co-located to ICES dataset. We do not use ICES dataset anymore. But instead we use the full outputs of the simulation to give estimation over the whole IBI domain. We consider that a model grid point is an area vulnerable to oxygen deficiency if at least one daily value decrease below the threshold of 6 mg l^{-1} (or 187.5 µmol l^{-1}) during the simulation length, as in Ciavatta et al. (2016). The minimum is found along the vertical profile over the continental shelf (bathymetry <= 200m).

More information or clearer information is now given to describe Fig. 10 in the revised paper.
The deficiency threshold is now added to Fig.10b as a dashed line.

The model predicts higher levels than observed in 2011 and 2015 (Fig. 10b), but they come from a few measurement points very close to the coast in the vicinity of river mouth, not captured by the IBI36 system.

The ROC (relative operating characteristic) score is a very interesting skill assessment method to measure the skill of the model to overcome a specific threshold in comparison with observed data. I didn't know this metrics, and I think the biogeochemistry modelling community is not used to seeing this metrics. It therefore needs to be presented and explained in detail, as in Sheng and Kim (J. Mar. Sys. 76, 212-243, 2009). This would add complexity to the paper and this section. But I keep this metrics in mind carefully for a study dedicated to oxygen vulnerable areas.

7. Figs. 14 and 15 show the comparison with BGC-Argo floats data in Atlantic and West Mediterranean areas covered by the IBI system. May the authors add any comment on the systematic behavior of the model in comparison with the float also for nitrate and oxygen (as done for Chl-a at depth, see P14, L2, and then in the discussion, P15, L13)? Do the authors suspect that this behavior is related to possible errors of the model (due to representativeness or biogeochemical parameterization), or may be also related to uncertainty associated to float sensors? Further, does the white line in Fig. 15 represent the MLD? If so, it should be added to the caption, and briefly explained how it was computed.

Author answer:

Low oxygen concentrations are systematically overestimated and high nitrate are systematically underestimated. This systematic behavior of the model in comparison with the float is also observed when compared to other observational datasets. It can be related to possible errors of the model (due to representativeness, physical or biogeochemical parameterization).

But uncertainty associated to float sensors can not be excluded. An important work on the quality control is currently being done by the BGC-Argo teams, and the quality check process is evolving very rapidly. Temporal drifts, constant or even non-constant vertical bias, and negative concentrations (see the nitrate in Fig. 15d) are still observed in the BGC-Argo data.

Nitrate and oxygen are now more discussed in the revised paper.

Yes, the white line in Fig. 15 represents the MLD. It is now added to the caption, and its computation is now explained.

8. In the discussion (P15, L1-6) why do the authors write that the higher biases on the continental shelf are "no surprising"? Is this related to larger uncertainty given by the river input? Or is there any limits due to the physical drivers? If it seems obvious, please clarify. Secondly, is there any literature basis for the NPP (e.g. with in situ measurements) that can be used to establish which of the 3 referred products we should trust more?

Author answer:

Continental margins are very productive regions and play an important role in the biogeochemical cycle of nutrients and carbon. They are the site of complex interactions between physical, chemical and biological processes that include exchanges between shelf and the open ocean, sediment-water interactions, air-sea fluxes, and land-ocean freshwater inputs. In addition, coastal systems are locally strongly affected by human activities. All these interactions make the continental shelf a challenge to obtain realistic models.
It is now clarified in the revised paper.

Regarding the NPP, we are currently collecting the estimates reported in the literature in order to build an in-situ database. This work is very time-consuming, and unfortunately cannot be included in this paper.

9. At the end of the discussion, there is a reference to OMI (P16, L8-11): this might not be interesting for the general reader. However, since there is a specific indication of the "IBI-MFC biogeochemical forecast service", this should be properly validated before providing OMI (see major point n.1).

Author answer:
The text has been modified to avoid confusing the reader.

Technical/other corrections:

In the webpage of OSD (https://www.ocean-sci-discuss.net/os-2018-161/#discussion), the correct author's surname should be "Sotillo" and not "Sottilo".

The author's surname has been corrected.

P2, L8 and P4, L31. The "IBI-MFC Team" has not been defined.

The “IBI-MFC Team” is now defined in the Introduction.

P3, L14-15. “The annual primary production is then limited its seasonal variations are limited”: not clear, please correct or reformulate.

The sentence has been reformulated to : “The annual primary production is then limited and so is its seasonal variations”.

P3, L29. References about N:P ratio around 20 in the Western Mediterranean are also found in the recent work of Lazzari et al. (Deep-Sea Res. I 108, 39-52, 2016; see their Fig. 7), that may be added.

The reference Lazzari et al. (2016) is now added.

P5, L25-27. “Although PISCES was originally designed for global ocean applications, the distinction of two phytoplankton size classes and the description of multiple nutrient co-limitations allow the model to represent ocean productivity and biogeochemical cycles in the major ocean biogeographic provinces (Longhurst, 1998).” The reference seems not appropriate: PISCES is not used in Longhurst (1998), which only refers to the bio-provinces. Please reformulate.

The reference Longhurst (1998) is now removed to avoid any misunderstanding.

P6, L1-2. “To respect the conservation of the tracers, the coupling between biogeochemical and physical components is done every other time.” Not clear, please clarify: what do the authors consider as “conservation of the tracers”? Is it mass conservation?

Yes, we refer to mass conservation. The sentence has been modified.

This question also relates to the reference to Aumont et al. (2015), at L19-L34: it would be clearer for the reader to add more details about the river inputs (which are very important in coastal regions). Please describe the specific inputs (also reporting from Aumont, Section 4.9.2, and the one from EEA), list the names of the rivers (or their total amount), specify what you consider as “natural” and what as “anthropic”, and describe their impact in the investigated region. Finally, please clarify the use of “reminder” the last sentence “For the other variables, a reminder of the initial conditions is given.”: does this mean the initial condition values are maintained constant during the simulation?

More details and clearer explanation is now given about the external inputs of nutrients linked to the river runoffs. We briefly describe the impact of additional nutrient inputs in the investigated region. The terms “natural” and what as “anthropic” have been removed to make the text clearer

and avoid any misunderstanding. The location of the 33 rivers considered in the IBI36 system is available in Maraldi et al. (2013).
Yes, the other variables are maintained constant during the simulation at the open boundary conditions that are the river points. This last sentence “For the other variables, a reminder of the initial conditions is given” is now removed. It is not useful because we are only talking about nutrient inputs here.
We are aware that river discharges could be greatly improved. But it is hampered by the lack of in situ observations.

P6, L8. “is” should be “are”.

“is” has been changed to “are”.

P7, L20. As done with VGPM and CbPM, please add a reference also to the “Eppley version”.

A reference is now added in the revised paper.

P8, L6-18. Could you provide which fields from the BGC-Argo repository have been used and whether additional calibrations were performed after?

The APEX float observations in the Atlantic are adjusted following Johnson et al. (2017). The three variables are "delayed mode" data. For the PROVOR float observations in the Mediterranean, oxygen and nitrate are "Real time" data and Chl-a is "adjusted" data. They are adjusted following Mignot et al. (2018).

P8, L18. “Johnson et al.” (dot missing).

The dot was added.

P11, L13. “Breitburg et al.” (dot missing).

The dot was added.

P11, L19. It should be “surface area in winter”.

It is now corrected.

P11, L20. The authors refer to “the west coast of France” but in Fig.10 a and b it looks like only the north-western French coast is covered by data, and with value larger than 200 umol/l. Please check.

As detailed above, Fig. 10a only catches low oxygen concentrations reported to the ICES database. All other low oxygen events are missed. In Fig. 10c, IBI36 outputs over the whole IBI domain are used to estimate the total surface area vulnerable to oxygen deficiency. So areas not detected by the ICES database may appear vulnerable due to simulation. It is now better explained in the text.

P12, L4. "The seasonal cycle is in phase for Chl-a but out of phase for ammonium" it is also possible to refer to Fig.7e, where correlation for NH4 is r=0.2.

The reference to Fig. 7e is added.

P14, L25. Instead of "is described here", it should be clearer to indicate the corresponding Section or Figure (Figs. 2, 4 for Chl-a and 5, 6 for NPP). Or are the authors here referring to the general approach of the manuscript? Please clarify. Further, it should be "are described".

"is described here" has been changed to "are described in this paper".

P17, L3. The fact that a co-author is also acknowledged sounds somehow strange. Please check.

The acknowledgement is removed.

P29, L3. Correct "Eppley".

Eppley is corrected.

P33, Fig. 10. Add the units for O2 minimum (umol/l).

The units was added to the legend of the figure.

Interactive comment on "A CMEMS forecasting system for the marine ecosystem of IBI European waters" by Elodie Gutknecht et al.

Anonymous Referee #2
Received and published: 13 March 2019

Dear Referee,

Please find our comments/responses in blue throughout your text.
We have also attached a new release of the article.
This is a major revision of the initial article: the introduction has been completely revised, the sections are modified, a discussion section has been added. A synthesis of the results has been added by using a table and a Taylor diagram.
All your comments have been taken into account in the new release of the article.
If required we can also provide a version with the word track change, but I don't think that's helpful to you.
Thank you for your useful comments.

Elodie Gutknecht on behalf of co-authors.

The main objective of the article "A CMEMS forecasting system for the marine ecosystem of IBI European waters" is to demonstrate the performances of the CMEMS operational 1/36° coupled NEMO/PISCES of the IBI (extended) area from a 2010-2016, 7 years model simulation. The authors state that the model is in relatively good agreement with observations (for the main biogeochemical variables) and reproduce the large scale main biogeochemical processes, with a focus on seasonal cycles. In addition, an interesting oxygen deficiency indicator is presented. The article includes a wide variety of comparisons (15 figures) computed from an impressive set of observation. The document is well written and a very valuable effort has been done to make it as clear as possible. It results in a complete review of PISCES ability to simulate large scale main biogeochemical features in the IBI domain. In my opinion, despite these undeniable qualities, the article misses some important points and there are several major issues that should be (at least mostly) addressed before publication. The "general recommendations section" describes major points that, in my opinion, need to be improved before publication. The second section only provides some specific comments that could help to address the general recommendation needs. I did not go into very specific details as I think some materials should be added (and modified) before going further.

General recommendations:

A) In the actual form, the article is rather a review (interesting) of results from a 7 years PISCES simulation in the IBI region. It not clear to me whether the objectives are 1) demonstrate the ability of this system for regional forecast applications or 2) to assess PISCES ability to represent the main biogeochemical features of the IBI region => suitable for operational applications. In any case, important modifications need to be made and the introduction should be extended to better mention the objectives and the means used to address these objectives. From the sentence p2, line27, I guess the main objective is more on point 2) but the way it is written gives the impression that the authors want to assess the relevancy of this configuration for operational 7 day forecasts which is clearly not at all demonstrated here (ex 4.1.1. first sentence "Predicted sea surface..." should be rather something like "the model sea surface chlorophyll...").

Author answer:
The IBI36 system has been developed to monitor and forecast the ocean dynamics and marine ecosystems of the European waters. But before considering operational applications, a pre-operational qualification simulation is evaluated to assess PISCES ability to represent the main biogeochemical features of the IBI region. The purpose of this paper is to evaluate this qualification simulation.
The title and the Introduction of the submitted version are confusing. So to avoid any misunderstanding, we propose to modify the title of the paper by: "Modelling the marine ecosystem of IBI European waters for CMEMS operational applications". We also modified the abstract and the Introduction to make clearer the objectives of the paper.

This comment also underlines a lack of focus. The result section is more a presentation of various diagnosis than a scientific analysis of the results which might be induced by too unclear objectives of the paper. I understand that the paper is more an analysis of "consistency" but the reader can sometimes be irritated when a figure is nearly not discussed. If you decide to mainly make this scientific analysis in the discussion part i would suggest to dedicate a full section to this discussion (instead of discussion and conclusion) and to clearly state this point in introduction. Finally, taking into account a focus on objective 2), we sometimes lose the purpose of the paper and i am not sure that the article really answer whether or not this PISCES simulation is well adapted to operational simulation in the IBI area (i am sure it is). In my opinion this it mainly the consequence of an efficient but also too straight way of writing with a lack of methodology: "the role of this figure is to show this point, which demonstrates this information, which is related to my main objectives in this way". Nevertheless, i am sure that this could be corrected quite easily as there is also a very robust amount of information.

Author answer:
The entire text has been revised in order to clarify the objectives of the paper. The objective of each figure, each section and sub-section is now better apprehended. Figures are now more discussed. And a full section is now dedicated to the discussion, and it is clarified in the Introduction.

B) One major issue is the total absence of informations regarding uncertainties (except in figure 4). In my opinion, this point is crucial to assess the performance of any simulation even if the authors decide to only focus on point 2). As this might be difficult (and not necessary) to consider uncertainty for every comparison, I suggest to add one section dedicated to uncertainties. It should both discuss uncertainties of the PISCES simulation and the observation products. One simple question that should be addressed: is the model simulation included within the range of observation uncertainty? For instance, first order uncertainties could be deduced from the statistical level of dispersion (in a specific radius representative of error correlations). This particular suggestion might probably be better adapted for comparison with ocean colour data (or when a large amount of data is available and could be presented with histograms).

Author answer:

The issue of uncertainty is a truly complex one. The model uncertainties can be supported by the use of ensemble simulations. Here, the IBI36 system is a deterministic model. Only one trajectory is described. The uncertainties of the data are also complex to access, and are not always accessible.

In order to complete the skill assessment and better apprehend the uncertainty of the model, the bias and RMSE with to the ESA OC-CCI is added for Chl-a evaluation. Uncertainties (in terms of bias and RMSE) are the greatest in the coastal areas, which also correspond to the areas where the uncertainty of satellite measurements is highest (100% uncertainty compared to 30% for the open ocean; Moore et al., 2009). For NPP, the standard deviation between the three NPP products (VGPM, Eppley-VGPM and CbPM) is compared to the bias between the model and the mean of the three NPP products. This comparison shows that the modelled NPP is included within the range of observation uncertainty (as standard deviation between the three NPP products is considerable). Uncertainty is discussed in the discussion section (Sect. 5).

The suggested analysis deduced from error correlations is a work in progress in the framework of the development of an assimilation system for ocean colour data and in-situ data. This analysis represents a significant work that will be described in detail when setting up the future system with assimilation of biogeochemical tracers.

C) Particularly using a 1/36° model resolution, it is quite a shame not to show simple weekly or monthly mean maps (at least for chlorophyll) highlighting this PISCES simulation ability to catch the variability existing in ocean colour data. This would be relevant to insist on the benefits of using a 1/36° resolution. Are there such 1/36 PISCES simulation elsewhere? What are the benefits compare to lower resolution models? Why do you need this resolution here? I really think that it would be of great importance to compare your results with other existing configurations or models. This would also be a great help to demonstrate that your configuration is well adapted to simulate the IBI biogeochemical features (to solve some of the general recommendation A)). If it is really not possible to perform comparisons this have to be clearly stated in introduction. More generally, the introduction completely misses the state of the art part. This definitely has to be corrected.

Author answer:

The PISCES model is intended to be used for both regional and global configurations at high or low spatial resolutions as well as for short-term (seasonal, interannual) and long-term (climate change, paleoceanography) analyses (Aumont et al., 2015). But to our knowledge and that of the PISCES developers, the PISCES model has never been used at such a resolution before.

Within the framework of CMEMS, three other MFC share a part of their domain with IBI:
- GLO-MFC which covers the world's oceans at 1/4° resolution and is also using the PISCES biogeochemical model,
- MED-MFC which covers the Mediterranean Sea at 1/24° with the Biogeochemical Flux Model (BFM; Vichi et al., 2007a,b),
- NWS-MFC which covers the North-West European Shelf at 1/15° latitudinal resolution and 1/9° longitudinal resolution (~ 7km) with the ERSEM ecosystem model (Baretta et al., 1995).

For the physical component, two intercomparison papers have been submitted in ocean Science - Special issue "The Copernicus Marine Environment Monitoring Service (CMEMS): scientific advances". They are Lorente et al. (2019) and Mason et al. (2019).

For the biogeochemical component, the comparison of the different model applications is a work in progress and will be the subject of a separate paper, including the contribution of the regional in relation to the global, as well as the comparison of three distinct biogeochemical models.

The Introduction has been revised and now includes a state of the art part.

References:

Baretta, J. W., W. Ebenhoh, et al. (1995). "The European regional seas ecosystem model, a complex marine ecosystem model." Netherlands Journal of Sea Research 33(3-4): 233-246.
Lorente, P., García-Sotillo, M., Amo-Baladrón, A., Aznar, R., Levier, B., Sánchez-Garrido, J. C., Sammartino, S., De Pascual, Á., Reffray, G., Toledano, C., and Álvarez-Fanjul, E.: Skill assessment of global, regional and coastal circulation forecast models: evaluating the benefits of dynamical downscaling in IBI surface waters, Ocean Sci. Discuss., https://doi.org/10.5194/os-2018-168, in review, 2019.
Mason, E., Ruiz, S., Bourdalle-Badie, R., Reffray, G., Garcia-Sotillo, M., and Pascual, A.: Copernicus (CMEMS) operational model intercomparison in the western Mediterranean Sea: Insights from an eddy tracker, Ocean Sci. Discuss., https://doi.org/10.5194/os-2018-169, in review, 2019.
Vichi, M., Pinardi, N., and Masina, S.: A generalized model of pelagic biogeochemistry for the global ocean ecosystem. Part I: theory, J. Marine Syst., 64, 89-109, https://doi.org/10.1016/j.jmarsys.2006.03.006, 2007a.
Vichi, M., Masina, S., and Navarra, A.: A generalized model of pelagic biogeochemistry for the global ocean ecosystem. Part II: numerical simulations, J. Marine Syst., 64, 110-134, https://doi.org/10.1016/j.jmarsys.2006.03.014, 2007b.

D) In order to make the document easier to read (in particular considering the probable adding figures (from my previous comments), i also suggest to add an annex section. Indeed some figures are only quickly and partially discussed (for instance : first paragraph of section 4,2,1 only 8 lines to described 3 figures ; in section 4,1,1, 4 figures are covered ; fig 7,8,9 f) are not discussed...). This would also allow to better focus the article on its objectives. (This comment is connected with the general recommendation 1)).

Author answer:
The objectives are now clearly presented in the Introduction, and figures are better discussed. We are aware that it is a substantial paper, with many figures. But it's necessary and voluntary. This paper represents the first validation of the biogeochemical component of the IBI36 system; it is intended to be complete and detailed, as it will serve as a basis for further studies.

Main Specific comments:

Considering the major recommendations, i here only specify, by section, the main specific comments as there will probably have a second review process. Generally, i do think that some accuracy is needed.

1) Introduction - See section major recommendations.

It has to be extended in order to clearly explain the objectives of the article and present a clear state of the art (in terms of existing forecast studies with PISCES and on models on the IBI region) in the area.

Author answer:
Introduction has been fully revised to clearly explain the objectives of the article. A state of the art in terms of existing forecast studies with PISCES and on models on the IBI region is now available.

2) IBI European waters

Interesting and quite complete part. It is a nevertheless a shame that the link between this part and the result section are nearly non-existent.

Author answer:
IBI European waters Section has been improved. It now introduce the boxes used for the evaluation of Chl-a and NPP. The link between this part and the result section in now improved.

3) The IBI36 configuration

- What is the influence of a 1/4° (bio) and 1/12° (physics) initialisation in the 1/36° simulation ? Do you have an idea how long this information is kept in the system, about the differences ?

Don’t you think it can strongly impact the first timing and intensity of the blooms (especially with an initialization in January ? Why don’t you make a few years spin-off ? - I would be very interested to have some informations on differences between a 1/4° and a 1/36° simulations. It would also help to justify the use of your configuration.

Author answer:

Initialization and open boundary conditions of the IBI36 system answer the CMEMS requirements. The physics comes from the CMEMS global physical component and the biogeochemical conditions come the CMEMS global biogeochemical system, this latter being also forced by the CMEMS global physical component.

The influence of a 1/4° (bio) and 1/12° (physics) initialisation and forcing in the 1/36° simulation is an interesting question. Impact analyses have been performed in the framework of the AMICO project, but only for short term simulations (1-2 years), and so the impacts were limited to the borders of the domain, but longer simulations would be necessary.

The date of the initialisation has been tested. The initialisation in January benefits from a low productivity. The seasonal dynamics triggered by seasonal warming and stratification has not yet begun. And so, the system is slowly being set up.

A few years spin-off are not performed here. The IBI36 system starts with the outputs of the global physical and biogeochemical systems, based on the same NEMO-PISCES model, and which has already turned 3 years. The main strengths and weaknesses of the model are found in both global and regional systems, such as the timing of the North Atlantic spring bloom. Systematic comparison between the global and regional systems is being performed, but we think that showing such metrics does not enter in the topic of this paper.

Some additional information about the nutrient forcing files would be welcome as i suppose that it could mainly explain most of the coastal deviations with observations. Do you have an idea of probable impacts of using 1/2_ data to 1/36_ grid, how do you deal with this ?

Author answer:

Nutrient inputs come from the annual climatology at ½° spatial resolution Global News 2. They are reported to the 1/36° grid at the river plumes considered in the IBI36 system (Rhone River and the German Bight) and along the coastline for all other inputs. Thus, we have endeavoured to conserve the nutrient flows between the original Global News 2 grid and the IBI36 grid. Mayorga et al. (2010) report that Global NEWS 2 underestimates nutrient runoffs in the Western Europe. Indeed, the only contribution of Global NEWS 2 is not sufficient to support the high coastal biological production of the IBI European waters. In order to reproduce the maximum Chl-a observed along the European coasts, additional inputs of nitrates and phosphates are provided into the IBI36 system at source points of the 33 main rivers and are linked to the physical flow. Location of the rivers can be found in Maraldi et al. (2013). They come from rivers monitored and listed by the European Environment Agency (www.eea.europa.eu) on the basis of annual averages.

Nutrient forcing description was not clear and maybe confusing. The description is now improved in Section 3.2. Nutrient inputs from rivers are of primary importance for coastal ecosystems. Unfortunately, they are often introduced in a too simplistic way in regional models due to a crucial lack of available measurements. This is a weakness that really needs to be considered and improved, but that is not intrinsic to the IBI36 system.

4) IBI36 evaluation

4.1 Satellite estimations

- How is the temporal correlation figure 2d calculated ? From monthly averages ? - On which grid are the differences calculated (model or verification) ? Are there impacts resulting from this grid changing ? In particularly for Net primary production comparison (1/6 degree compared to 1/36 degree). Please clarify this point as non linearities can have significant effects. - It is difficult to see something in figure 3. The discussion on the bloom timing could also be done using different boxes of figure 4. This would permit to remove one figure (or in annex). - p6. lines 18-21 you say that Net primary production estimates are model products ? If it is true why do you include these data sets in a section 4,1 called satellite estimations ?

Author answer:

Temporal correlation is calculated from monthly averages between 2010 and 2016.). It is now clearly stated at the beginning of Section 4.1.

We have chosen to interpolate the model on the data grid, i. e. 1 km for the comparison to ESA OC-CCI ocean colour product and 1/6° for NPP.

Yes, the discussion on the bloom timing could be done only using different boxes of Figure 4, and we could remove Figure 3. But Figures 3 and 4 are complementary. Figure 3 clearly shows the seasonal phase shift and the high interannual variability in the data while the model is more seasonal. This is more evidenced than in Figure 4.

Net primary production estimates are model products because an algorithm (or model) is used to determine NPP from ocean colour data. But it is considered primarily as a product derived from satellite estimates. To avoid any misunderstanding, the term “NPP product” instead of NPP model” is used in the revised version.

4,2 In situ historical data

- In fig 8, for oxygen, it would be clearer if you could modify the colorbar. At a first view we think that the data and the model are very different while the bias is only 4% - It is a shame you do not discuss at all some possible reasons why the model does not catch the low oxygen period in 2014-2015. Especially when you thereafter discuss about oxygen deficiencies: : : -Don ’t you think that one of the main limitation comes from the nutrient forcing files ? Could you specify a

little bit more (than it is in 3.2) as it seems to be quite important ? Where are the anthropic inputs located in the model ? What is the impact of these additional anthropic inputs ? It could be relevant to go a little bit deeper into this point.

Author answer:
The colorbar of Figure 9 has been modified.

The model does not catch the lower oxygen concentrations observed in ICES in 2014-2015. It can come from the Baltic Sea or from river inflows. But I didn't find any reference to this event in the literature.

The oxygen-deficient areas are quite well estimated by the model in terms of spatial distribution and extension. They are located mainly along the coastline and are certainly impacted by river inflows but also sedimentary processes. More realistic external forcing files would obviously improve the estimation of vulnerable areas. But as explained above, they are introduced in a too simplistic way due to a crucial lack of available measurements.

Nutrient forcing description was not clear and maybe confusing. The terms "natural inputs" and "anthropogenic inputs" are now removed because they are not really accurate and could be confusing. The description is now improved in Section 3.2.

This adaptation was necessary to simulate higher coastal Chl-a and reproduce the maximum Chl-a observed along the European coasts. But it is not totally satisfactory because a strong seasonal signal seems to emerge from ICES comparisons. The future system will improve this external forcing.

4,3 Argo data
How are the Argo data co-located with the model data ? Do you grid Argo data on the model grid ? Could you re-precise dates ? Although correlations are still high, results are much less good than previously. Do you have an idea why ? Small scale features ? Have you compared the Argo data with some of the previous observations ? (it also could help in defining uncertainty levels).

Author answer:
As for the satellite comparison, we have chosen to interpolate the model on the BGC-Argo data grid. We used daily averaged model outputs at the nearest model grid point, and a linear interpolation for the vertical.

BGC-Argo float comparisons open new perspectives. Bu the comparison should be considered with some cautions because the product quality procedures are on-going work. They are not fully established or homogenized for all floats. Temporal drifts, constant or even non-constant vertical bias, and negative concentrations (see the nitrate in Fig. 15d) are still observed in the BGC-Argo data.

4,4 Discussion and conclusion

- I would suggest to separate the discussion and the conclusion since the authors have clearly decided not to deeply analyze the results in the result section. The discussion proposed here is interesting but should be extended and also make a clear link better with the objectives that should be first clarified in introduction.

Author answer:

Discussion and Conclusions are now separated, and the link with the objectives of the paper as clarified in introduction is now improved.

We decided to only describe the results in Section 4, and then deeply analyse the results in the Discussion section. This structure seems simpler because some aspects come up several times in the evaluation (smoothed vertical profiles, rivers, sediments…). So we discuss them once and for all in the dedicated section.

~~A CMEMS forecastingoperational system for the marine ecosystem of IBI European waters~~
Modelling the marine ecosystem of IBI European waters for CMEMS operational applications

Elodie Gutknecht[1], Guillaume Reffray[1], Alexandre Mignot[1], Tomasz Dabrowski[2], and Marcos G. Sotillo~~[1,]~~[3]
[1] Mercator Ocean, Parc Technologique du Canal, 8-10 rue Hermes, 31520 Ramonville St-Agne, France
[2] Marine Institute, Rinville, Oranmore, Co. Galway, H91 R673, Ireland
[3] Puertos del Estado, Av. Partenón, 10, 28042 Madrid, Spain

Correspondence to: Elodie Gutknecht (elodie.gutknecht@mercator-ocean.fr)

Abstract. As part of the Copernicus Marine Environment Monitoring Service (CMEMS), ~~an operational ocean forecasting system~~ a physical-biogeochemical coupled model system ~~was~~has been developed to monitor and forecast the ocean dynamics and marine ecosystem~~s~~ of the European waters; and more specifically on the Iberia-Biscay-Ireland (IBI~~ (Iberia-Biscay-Ireland~~) area. The CMEMS IBI ~~physical-biogeochemical~~ coupled ~~system~~ model covers the North-East Atlantic Ocean from the Canary Islands to Iceland, including the North Sea and the Western Mediterranean, with a NEMO-PISCES 1/36° model application. The coupled system ~~.~~ has provided 7-day weekly ocean forecasts for CMEMS since April 2018. Prior to its~~Since~~ operational launch, ~~Prior to its operational launch in April 2018,~~ a pre-operational qualification simulation~~a retrospective simulation~~ (2010-2016) has allowed ~~to assess~~assessing the ~~system~~model's capacity~~ability~~ to reproduce the main biogeochemical and ecosystem features of the IBI area.

~~This simulation begins on January 2010 and continues until real-time as the model currently provides 7-day weekly ocean forecasts for CMEMS. this CMEMS IBI system has provided a weekly short-term (7-days) forecast of the ocean dynamics and key biogeochemical variables of the marine ecosystem.~~

The objective of this paper is then to describe the skill performances of the PISCES biogeochemical ~~component~~model, using ~~the first 7 years of~~ this 7-year qualification simulation~~simulation (2010-2016)~~.

~~The main goal of this paper is to assess the performances of the IBI biogeochemical system, using a 7-year retrospective simulation that spans from 2010 to 2016.~~ The model results are ~~validated~~compared with available satellite estimates ~~and~~ as well as *in situ* observations ~~from the International Council for the Exploration of the Sea~~ (ICES, ~~), the European Marine Observation and Data Network (~~EMODnet~~)~~ and ~~the Biogeochemical Argo (~~BGC-Argo~~) float network~~). The ~~simulationIBI system~~simulation successfully reproduces the spatial distribution and seasonal cycles of oxygen, nutrients, chlorophyll-a~~,~~ and net primary production; and ~~.~~ confirms that PISCES is suitable at such a resolution and can be used for operational analysis and forecast applications. This model ~~simulation~~ system can be a useful tool to better understand the current state and changes in the marine biogeochemistry of European waters~~,~~ and ~~. It~~ can also provide key variables for developing indicators to monitor the health of ~~European~~ marine ecosystems. These indicators may be of interest to scientists, policy makers, environmental agencies and the general public.

1 Introduction

The ~~marine ecosystem of the~~ North-East Atlantic waters are~~is~~ subject to natural climate variability as well as intense human pressures that can have significant impacts for the marine ecosystem. In addition to intense fishing activity, human pressures also include aquaculture, agriculture, maritime transport, oil and gas extraction, tourism~~,~~ and urbanization. In order to regulate, sustainably manage, protect and conserve the maritime areas of the North-East Atlantic waters, t~~In order to~~

~~regulate, sustainably manage, protect, and conserve the maritime areas of the North East Atlantic waters, fifteen governments and t~~the European Union ~~have~~ adopted the OSPAR Convention in 1992. The European Union has also set up an Earth observation programme, the ~~To go further, Europe Union also wants~~ Copernicus European Programme, formerly known as GMES (Global Monitoring for Environment and Security). Copernicus aims for ~~to~~ developing an~~its~~ operational and autonomous Earth observation capacity of European Union to serve the general ~~European~~ interest and help public authorities and other international organizations to improve the quality of life. Its ~~In this objective, the Copernicus European Programme, formerly known as GMES (Global Monitoring for Environment and Security), manages Earth monitoring data from satellite observations, *in situ* measurements and numerical models on water, air and land. Its~~ marine monitoring component, ~~is~~ the Copernicus Marine Environment Monitoring Service (CMEMS; http://www.marine.copernicus.eu), is ~~implemented~~ coordinated and ~~operated~~ leaded by Mercator Ocean ~~International~~, a service provider of ocean information in real and delayed time (http://www.mercator-ocean.eu). Gathering ~~three kinds of data (~~satellite, *in situ* and model data~~s)~~, CMEMS provides regular and systematic information on the state and variability of the ocean dynamics and marine ecosystems for the g~~g~~lobal ocean and the European regional seas~~. The CMEMS service covers the European seas by defining~~ over six different areas: Arctic Ocean, Baltic Sea, European North-West Shelf Seas, Black Sea, Mediterranean Sea and Iberia–Biscay–Ireland (IBI) Seas.

The CMEMS IBI Monitoring and Forecasting Center (IBI-MFC) is in charge of delivering multi-decadal reanalysis and operational analysis and short-term forecasts over the IBI European waters. It is managed by a consortium of Centres, coordinated by Puertos del Estado and that includes Mercator Ocean, Meteo France, the Spanish Met office AEMET, the Irish Marine Institute and the CESGA Supercomputing Centre. The IBI area covers part of the North-East Atlantic Ocean from the Canary Islands to Iceland, the North Sea and the Western Mediterranean (IBI Extended Domain). However the IBI-MFC delivers IBI products to CMEMS end-users over a smaller area, extending from -19°E to 5°E and 26°N to 56°N (IBI Service Domain). IBI Extended and Service Domains are shown on Fig. 1a and further details on the IBI-MFC and the IBI region definition are available in Sotillo et al. (2015).

The IBI area is a complex region to simulate for numerical models because the highly variable bathymetry gives rise to a wide spectrum of physical and biogeochemical ocean processes. For monitoring and forecasting purposes, an analysis and forecast system has been developed and validated by Mercator Ocean (Maraldi et al., 2013; Sotillo et al., 2018). The IBI ocean dynamics is based on the 3.6 version of the NEMO modelling platform (Madec et al., 1998; Madec, 2008), constrained through data assimilation of *in situ* and satellite physical data, and coupled with the PISCES biogeochemical model (Aumont et al., 2015). NEMO-PISCES are "online" coupled on the same 1/36° model grid resolution, placing the model into the sub-mesoscale-permitting regime. The system, hereinafter referred to as IBI36, consists of a pre-operational qualification simulation that has served as initial conditions to start the operational analysis and forecast system. The system has provided on a weekly basis a short-term (7-days) forecast of the ocean dynamics and the main biogeochemical variables of the marine ecosystem for CMEMS, since April 2018. Such a model system represents a challenge in terms of numerical, computational and operational constraints.

PISCES simulates the lower trophic levels of the marine food web, from nutrients to mesozooplankton. It has already been successfully used in various biogeochemical studies at global, regional scales and up to process studies, at low and high spatial resolutions as well as for short-term and long-term analyses (e.g. Bopp et al., 2005; Gehlen et al., 2006, 2007; Schneider et al., 2008; Steinacher et al., 2010; Tagliabue et al., 2010, Séférian et al., 2013; Gutknecht et al., 2016). PISCES is also used in operational oceanography (Brasseur et al., 2009)~~:~~, for the CMEMS global ocean analysis and forecast system (Lellouche et al., 2016, 2018; Perruche et al., 2016) and ~~for~~ the Indonesian seas operational system (the INDESO project ; Gutknecht et al., 2016). While PISCES has so far been used to answer a wide range of scientific questions, it has never before been used at such a resolution. This makes particularly challenging its evaluation and validation in the IBI European

waters, where the biogeochemical processes of PISCES benefit from a bathymetry and an ocean dynamics at 1/36°. ~~This makes particularly challenging its evaluation and validation in the IBI European waters.~~

European waters are also covered by other biogeochemical models, as several MFC share a part of their model domain with IBI. The operational system for the Northwest European Shelf Seas (Edwards et al., 2012; O'Dea et al., 2017) is based on NEMO and the ERSEM biogeochemical component (Blackford et al., 2004; Butenschönet al., 2016) at 1/15° latitudinal resolution and 1/9° longitudinal resolution (~ 7km). The Mediterranean Sea forecasting system (Tonani et al., 2014; Teruzzi et al., 2018; Salon et al., 2019) is built on NEMO and the BFM biogeochemical model (Vichi et al., 2013) at 1/24° resolution. These regional coupled systems, and of course the NEMO-PISCES global ocean operational system at 1/4°, are the subject of inter-comparisons. Ocean dynamics forecast models, all of them based on NEMO, are already being compared in Lorente et al. (2019) and Mason et al. (2019). For the marine biogeochemistry and ecosystem dynamics, inter-comparison is initiated in the framework of CMEMS, but represents a significant work because the biogeochemical models differ in complexity (Gehlen at al., 2015).

~~This paper evaluates~~In this paper, the pre-operational qualification simulation (which extends from January 2010 to December 2016) of the IBI36 system is evaluated using different observational data sets (satellite, oceanographic historical databases and BGC-Argo float network). This paper represents the first validation of the biogeochemical component of the IBI36 system. The objective is to ~~evaluate~~assess the performance of the PISCES model in reproducing the main biogeochemical characteristics of IBI European waters, and ~~confirm~~verify that PISCES is suitable at such a resolution and can be used for operational analysis and forecast applications.

~~Concerning the latter region, tThe CMEMS Iberia Biscay IrelandIBI Monitoring and Forecasting Center (IBI MFC) is managed by a consortium of Centres, coordinated by Mercator Ocean International and that includes MeteoFrance, the Spanish Met office AEMET, the Irish Marine Institute and the CESGA Supercomputing Centre. covering part of the North-East Atlantic Ocean from the Canary Islands to Iceland, the North Sea and the Western Mediterranean (Fig. 1a).It is in charge of delivering physical and biogeochemical multi year products from reanalysis runs and forecast products from near real time systems for the physical dynamics and the main biogeochemical variables over the IBI region. The IBI MFC Team in charge of the development, production and the later validationevaluation of the products works on a model domain using a curvilinear grid, called IBI Extended Domain, covering part of the North East Atlantic Ocean from the Canary Islands to Iceland, the North Sea and the Western Mediterranean (Fig. 1a). However the IBI MFC delivers IBI products to CMEMS end users on a regular grid over a smaller area, called IBI Service Domain, extending from 19°E to 5°E and 26°N to 56°N (Fig. 1a). Further details on the IBI MFC and the IBI region definition are available in Sotillo et al. (2015).~~

~~The near real time system is developed by Mercator Ocean. It is based on the 3.6 version of the NEMO modelling platform (Madec et al., 1998; Madec, 2008) with a horizontal resolution of 1/36°. The PISCES biogeochemical model is coupled with the physical dynamics, and simulates the lower trophic levels of the marine food web, from nutrients to mesozooplankton (Aumont et al., 2015). This coupled system is hereinafter referred to as IBI36. In order to assess the system's ability to reproduce the main features of the IBI area, the last few years are modelled. Thus, the near real time simulation starts in January 2010 and runs until real time as the system currently provides on a weekly basis a short term (7 days) forecast of the ocean dynamics as well as the main biogeochemical variables (oxygen, nutrients, chlorophyll a, hereinafter denoted Chl a, and primary production) of the marine ecosystem for CMEMS.~~

~~In addition to have a very high level of human activity, the IBI waters are home to a wide range of physical and biogeochemical oceanic processes that must be understood in order to manage the area accordingly. In this objective, a physical biogeochemical coupled model system predicts the physical and ecosystem dynamics. The IBI NEMO PISCES model application, developed by Mercator Ocean, is based on the latest version of the NEMO modelling platform (Madec et al., 1998; Madec, 2008), version 3.6, with a horizontal resolution of 1/36°. The PISCES biogeochemical model simulates the~~

~~lower trophic levels of the marine food web, from nutrients to mesozooplankton (Aumont et al., 2015). This regional coupled system is hereinafter referred to as IBI36.~~

~~The IBI36 operational system provides, since April 2018, on a weekly basis a short term (7 days) forecast of the ocean dynamics as well as the main biogeochemical variables (oxygen, nutrients, chlorophyll a, hereinafter denoted Chl a, and primary production) of the marine ecosystem. A weekly update of physical and biogeochemical hindcast products (generated for the previous week) is also delivered as best historical estimates. The IBI36 system is described and evaluated in the CMEMS documents: Sotillo et al. (2018) for physics and Bowyer et al. (2017) for biogeochemistry.~~

~~This paper assesses the performances of the biogeochemical component in reproducing the main biogeochemical variables, using the firsta 7 years retrospective of this near real time simulation that covers the (2010-2016) period.~~ Oxygen, nutrients, chlorophyll-a (hereinafter denoted Chl-a) and net primary production (NPP) are assessed in terms of consistency and quality (or accuracy) using GODAE-like metrics (Hernandez et al., 2009, 2015). Despite some of the areas presented here are outside of the IBI Service Domain (where the IBI-MFC delivers IBI products to CMEMS end-users), the model is evaluated over the IBI Extended Domain in order to take advantage of the *in situ* observation coverage.

The paper is organized as follows. Section 2 presents a synthesis ~~n~~ overview of the IBI European seas with emphasis on the main drivers of the ecosystem dynamics. Section 3 describes the IBI36 ~~coupled configuration~~system, the model initialization and boundary conditions, the external forcing, the regional adaptations and the data used for evaluation. In Sect. 4, the biogeochemical tracers are compared to satellite and *in situ* observations. Finally, D~~a d~~iscussion and C~~c~~onclusions are provided, respectively, in Sect. 5 and 6.

2 IBI European waters

~~Phytoplankton dynamics is controlled by the complex interaction between ocean dynamics, nutrients and light availability.~~ Phytoplankton dynamics is controlled by the complex interaction between ocean dynamics, nutrients and light availability. The biogeochemical and ecosystem dynamics of IBI European waters are synthesized in this section, with an emphasis on several areas (please see the 12 black boxes added to Fig. 1). ~~with different properties.~~ These areas are ~~added to Fig. 1 (see the 12 black boxes), and~~ adopted in the validation framework (Section 4.1). They are named throughout the following description.

In the IBI European waters, phytoplankton dynamics usually follows a seasonal cycle typical of temperate seas, governed by the alternation between winter mixing and summer stratification of the water column (Barton et al., 2015). A rapid increase in phytoplankton biomass starts in spring, when seasonal re-stratification begins and, when the Mixed Layer Depth (MLD) becomes shallower (Sverdrup 1953; Behrenfeld 2010; Taylor and Ferrari 2011). This ~~event, called~~ spring bloom~~,~~ is followed by a summer decrease in biomass, when the increase in stratification of the water column reduces the vertical supply of nutrient to the euphotic layer (the layer where phytoplankton grows) (Barton et al., 2015).

In the North-East Atlantic Ocean, primary productivity increases from south to north (boxes 3, 2 and 1 in Fig. 1). ~~as a result of the main surface circulation. Near 50°W, the Gulf Stream splits into the North Atlantic Current (NAC) flowing northeastward and the Azores Current (AC) flowing east-southeastward (Rossby, 1996). The meandering Subpolar Front, an extension of the NAC, is a relatively wide region separating the subtropical gyre from the subpolar gyre (Rossby, 1996).~~ In the subtropical North Atlantic, wind stress induces Ekman downwelling that deepens the nutricline~~,~~ and the warm waters maintain a stratification of the water column throughout the year (Barton et al., 2015). The annual primary production is then limited and so is its seasonal variations ~~are limited~~. The subtropical gyre is separated from the subpolar gyre by the meandering Subpolar Front which covers a relatively wide region (Rossby, 1996), ~~which~~and represents a transition zone between the two regimes. ~~Moving~~ In ~~to~~ the subpolar North Atlantic, the seasonal surface cooling deepens the mixed layer in

winter~~, and~~, winds drive Ekman upwelling and make the nutricline shallower (Barton et al., 2015). However, light supply limits the phytoplankton growth in winter. A strong spring bloom is triggered by water column re-stratification in spring, while during summer the stratification limits the nutrient supply to the surface (Williams et al. 2000). This seasonal upward flow of deep and nutrient-rich waters triggers a higher productivity and a strong seasonal cycle.

Moving toward the coast, Moroccan and Iberian upwelling systems (boxes 10 and 8 in Fig. 1) are part of the Canary Current Upwelling System, one of the four main Eastern Boundary Upwelling Systems of the world~~,~~ and thus a very productive ecosystem and an active fishery (Aristegui et al., 2004). The season for upwelling along the Iberian coast begins in May-June with the establishment of northerly winds and continues throughout the summer (June-September; Wooster et al., 1976; Nykjær and Van Camp, 1994)~~, with periods of downwelling associated with wind relaxations (Torres and Barton, 2007)~~. Along the Moroccan coasts, upwelling intensifies from the north, where it is highly seasonal, ~~with higher activity in the summer and autumn,~~ to the south where it can be considered permanent and intense, with maximum activity from April to September (Pelegrí and Benazzouz, 2015).

The IBI European waters also cover part of the Western Mediterranean Sea (boxes 11 and 12 in Fig. 1). From a biogeochemical perspective, the Mediterranean Sea shows a high N:P ratio (N:P ~ 20 for the western basin; Ribera d'Alcalà et al., 2003; Lazzari et al., 2016)~~,~~ and relatively high oxygen consumption rates compared to the Atlantic and Pacific Oceans (Christensen et al., 1989; Roether and Well, 2001). Mediterranean Outflow Water (MOW) flows into the Gulf of Cadiz (box 9 in Fig. 1) and the Atlantic through a sill depth of only 290 meters at the Strait of Gibraltar. This salty and denser water flows out at the bottom of the sill and a northward-moving MOW core spreads on the continental slope of Portugal at 1000 meters depth, enters the Bay of Biscay~~,~~ and follow the shelf break further north.

The Bay of Biscay and Celtic Seas are moderately productive ecosystems (UNEP LME report). The seasonal cycle of phytoplankton in the Bay of Biscay (box 7 in Fig. 1) is typical of temperate seas (Fernández and Bode, 1991; Valdés et al., 1991; Lavín et al., 2006) but spatial variability is high. The bay is characterized by a weak anticyclonic circulation in the oceanic part, a coastal upwelling, the northerly flow of MOW (OSPAR, 2000; Lavín et al., 2006) and river discharges (Gohin et al., 2003). In the oceanic part of the bay, one biomass peak can be observed in spring due to oligotrophic conditions. However, in the coastal part of the bay, phytoplankton remains relatively high during winter for isobaths less than 100 meters in the Region Of Freshwater Influences (ROFI).

The continental shelf widens in the Bay of Biscay. It is quite narrow along the Spanish coast, but increases rapidly with latitude along the French coasts, from 10 km in the south to more than 200 km wide in the north of the bay. The most extensive continental shelf areas are in the Celtic Seas and the North Sea. The continental shelf along the European coasts is the site of intense tidal amplitude and turbulent mixing that prevent stratification (Piraud et al., 2003; Lam et al., 2003, Lavín et al., 2006). To the west of the Celtic Seas, a significant and permanent front can be observed in Chl-a at the edge of the shelf, extending from the northern Bay of Biscay to the Faroe-Shetland Channel~~,~~ and associated with the shelf edge current (Belkin et al., 2009; Aquarone et al., 2008). The English Channel (box 6 in Fig. 1), connecting the North Sea to the Atlantic, is generally mixed and strongly influenced by winds. The North Sea (boxes 4 and 5 in Fig. 1) is characterized by significant river discharges and permanently mixed water column in the south, supplying the highest coastal primary production rates. The north part is characterized by a seasonal stratification and a deep channel in the north-east. Finally, as eastern boundary of the IBI~~36~~ domain, the Skagerrak and Kattegat connect the North Sea to the Baltic Sea.

Discharges of fresh and nutrient-rich water from rivers are a strong forcing factor for European waters. In addition to natural inputs related to the watershed erosion, many European coastal ecosystems are damaged by eutrophication due to human activities such as wastewater, agriculture and fish farming (Valdés and Lavin 2002). Eutrophication affects coastal areas, fjords and estuaries, mainly within the Celtic Seas, the Bay of Biscay and the Iberian Coast (OSPAR, 2003). Excessive nutrient enrichment, usually due to increased nitrogen and phosphorous concentrations in rivers, leads to high primary

production rates and reduced oxygen concentrations in the bottom water. Oxygen deficiency was reported in the bottom waters of the North-West European shelf (OSPAR, 2013; Ciavatta et al., 2016) and can be used as indicator of the health of marine ecosystems.

3 The IBI36 configuration

3.1 The coupled model system

Within the framework of CMEMS, the IBI-MFC Team has deployed an operational forecast service based on a coupled physical-biogeochemical model application. The model domain covers part of the North-East Atlantic Ocean from the Canary Islands (26°N) to Iceland (64°N), and from 20°W to North Sea (14°E) and the Western Mediterranean (10°E), using a curvilinear grid (Fig. 1a) with a horizontal resolution of 1/36°, corresponding to ~2 km for latitudes covered by the IBI domain, and 50 vertical levels.

The physical model is based on the NEMO 3.6 hydrodynamic model (Madec et al., 1998; Madec, 2008), developed by the NEMO consortium. The NEMO modelling system is freely available (http://www.nemo-ocean.eu), and specific regional improvements include time-splitting and non-linear free surface to correctly simulate high frequency processes such as tides. The ocean dynamics is constrained through data assimilation of *in situ* and satellite physical data (temperature and salinity vertical profiles, sea surface height and sea surface temperature). The IBI36 physical component is described in Maraldi et al. (2013) and Sotillo et al. (2018).

The biogeochemical model PISCES v2 (Aumont et al., 2015), ~~which is~~ part of the NEMO 3.6 modelling platform, is an intermediary complexity model taking into account 24 prognostic variables. There are five nutrients that limit phytoplankton growth (~~:~~ nitrate and ammonium, phosphate, silicate and iron). ~~Phosphate and nitrate + ammonium are linked by a constant C/N/P Redfield ratio (122/16/1; Takahashi et al., 1985) in all organic compartments of PISCES.~~ The model distinguishes two phytoplankton size compartments (nanophytoplankton and diatoms) expressed ~~, for which the prognostic variables are the total biomass~~ in carbon, iron, Chl-a~~,~~ and silicon content (the latter only for diatoms) and ~~. Consequently, Fe/C, Chl/C, and Si/C ratios are variable and predicted by the model. T~~two zooplankton size classes (microzooplankton and mesozooplankton) ~~are considered, with constant ratios~~. ~~The total biomass in C is therefore the only prognostic variable for zooplankton.~~ The bacterial pool is not explicitly modelled. PISCES distinguishes three non-living detrital pools for organic carbon~~: small particulate organic carbon, big particulate organic carbon and semi labile dissolved organic carbon. Although the C/N/P composition of dissolved and particulate materials is related to Redfield stoichiometry, the iron content of the particles is computed prognostically. In addition to the three organic detrital pools, pa~~, ~~rticles~~particles of calcium carbonate ~~(calcite)~~ and biogenic silicate ~~are modelled~~. In addition, the model simulates the carbonate system ~~(dissolved inorganic carbon and total alkalinity)~~ and dissolved oxygen. Biogeochemical parameters are based on the standard parameters of PISCES v2. Please refer to Aumont et al. (2015) for the full description of the model.

~~Although PISCES was originally designed for global ocean applications, the distinction of two phytoplankton size classes and the description of multiple nutrient co-limitations allow the model to represent ocean productivity and biogeochemical cycles in the major ocean biogeographic provinces (Longhurst, 1998). PISCES has been successfully used in various biogeochemical studies at global and regional scales, at low and high spatial resolutions as well as for short-term and long-term analyses (e.g. Bopp et al., 2005; Gehlen et al., 2006, 2007; Schneider et al., 2008; Steinacher et al., 2010; Tagliabue et al., 2010, Séférian et al., 2013; Gutknecht et al., 2016). PISCES is also the biogeochemical model used for the IBI reanalysis product (Bowyer et al., 2018), the global ocean analysis and forecast product (Perruche et al., 2016) and the non-assimilative hindcast product (Perruche et al., 2018), all of them are developed at Mercator Ocean for delivery to CMEMS.~~

For this regional configuration, physics and biogeochemistry are running simultaneously ("on-line" coupling), with the same 1/36° spatial resolution. For reason of numerical cost (optimization of the computing time), the numerical scheme for

biogeochemical processes is forward in time (Euler) while the physical component uses the leap-frog scheme. To respect the mass conservation ~~of the tracers~~, the coupling between biogeochemical and physical components is done every other time. The time step of the biogeochemical model is therefore twice that of the physical component, i.e. 3~~9~~00 s. The advection scheme for biogeochemistry is the same QUICKEST scheme (Leonard, 1979) used for the physical part, but using the limiter of Zalezak (1979).

3.2 Model initialization, external forcing and boundary conditions.

The ~~physical biogeochemical coupled~~pre-operational qualification simulation starts on January 6, 2010 ~~and continues until real-time as the model currently provides 7-day weekly ocean forecasts for CMEMS. In this paper, only the first 7 years of simulation (~~and runs until December 31, 2016~~) is analysed~~.

~~The variables characterizing o~~Ocean dynamics (temperature, salinity, currents~~,~~ and free surface) ~~are~~ is initialized and forced to the open boundaries by the daily outputs of ~~the CMEMS~~ the NEMO global ocean analysis and forecasting system at 1/12° (Lellouche et al., 2016, Lellouche et al., 2018) of CMEMS. Both regional and global systems are forced every 3 hours with atmospheric fields from the ECMWF.

The biogeochemistry is initialized with ~~the CMEMS~~ the NEMO-PISCES global ocean analysis and forecasting system at ¼° ~~horizontal resolution (Perruche et al., 2016)~~ (Perruche et al., 2016) of CMEMS, for the same date~~.~~. Open boundary conditions come from this same global product on a weekly basis. The global biogeochemical system is also forced by the coarsened solution of the global physics~~al outputs~~ system mentioned just above, making the global~~different~~ and IBI components of CMEMS consistent.

Other boundary fluxes account for the external supply of nutrients ~~(N, P, Si, Fe)~~ and carbon from three different sources. The model includes the ~~:~~ atmospheric dust deposition of Fe, Si, P and N at the ocean surface (Aumont et al., 2015). ~~,~~ ~~r~~River discharges of nutrients come from the Global NEWS 2 data sets (Mayorga et al., 2010) and carbon comes from Ludwig et al. (1996). An iron source corresponding to sediment reductive mobilisation on continental margins is also considered. ~~s and marine sediment mobilization.~~ For more details on external nutrient supplies, please refer to Aumont et al. (2015).

Two adaptations are necessary in order to meet regional specificities. The first adaptation concerns vertical sedimentation. In PISCES, external input fluxes are compensated by a loss to sediments in the form of particulate organic matter, biogenic silica and CaCO3. These fluxes correspond to the matter definitely lost to the ocean system. The compensation of external input fluxes by the loss at the lower limit closes the mass balance of the model. While this balance is a valid assumption at ~~the~~ global scale ~~of the global ocean~~, it is not necessarily achieved at the regional level. In addition, strong tidal currents prevent organic matter from settling on the bottom and being stored in the sediments of much of the North-West European continental shelf (De Haas et al., 2002). Thus, no loss to sediment is ~~taken into account~~considered in the IBI36 system. The second adaptation concerns the supply of nutrients from rivers. As mentioned above, nutrient inputs come from the annual climatology at ½° spatial resolution of Global News 2. They represent a realistic hydrology for the reference year 2000, considered as representative of the contemporary conditions (Mayorga et al., 2010). Inputs are injected into the model in the form of surface runoff in the river plumes of the Rhone River and the German Bight and along the coastline for other rivers, with caution of conserving the nutrient flows estimated by Global NEWS 2. However Global NEWS 2 seems to underestimate nutrient runoffs in the Western Europe (Mayorga et al., 2010). The only contribution of Global NEWS 2~~are injected into the model in the form of surface runoff in the river plumes but also along the coast, using the annual climatology at ½° spatial resolution Global News 2 (Mayorga et al., 2010) which reproduces a realistic hydrology for the year 2000.~~is not sufficient to support the high coastal biological production of the IBI European waters (not shown). ~~To have a more realistic system~~A~~, two types of inputs are considered. Natural inputs are injected into the model in the form of surface runoff in the river plumes but also along the coast, using the annual climatology at ½° spatial resolution Global News 2 (Mayorga et al., 2010) which reproduces a realistic hydrology for the year 2000. A~~dditional ~~(anthropic)~~ inputs of nitrates

and phosphates are then introduced into the system ~~-~~ at source points of the 33 main rivers of the IBI Extended Domain~~,~~ (please refer to Maraldi et al. (2013) for the location of the rivers), and are linked to the physical flow. These additional nutrients come from rivers monitored and listed by the European Environment Agency (www.eea.europa.eu) on the basis of annual averages. This adaptation leads to higher coastal Chl-a and allows the model to reproduce the maximum Chl-a observed along the European coasts (not shown). It also allows representing the nutrients in excess likely to cause eutrophication in downstream coastal waters and oxygen deficiency in the bottom waters. ~~For the other variables, a reminder of the initial conditions is given.~~

3.3 Satellite and *in situ* observational data sources used for model validation

~~This paper evaluates the capacity of the IBI36 system to reproduce the surface and vertical distributions, as well as seasonal cycles of the main biogeochemical variables (Chl a, primary production, nutrients, oxygen).~~ The model results are ~~thus~~ compared with satellite and *in situ* observational data. Chl-a ~~concentrations~~ and ~~primary productivity~~NPP are derived from remote sensing estimations. Dissolved oxygen, nutrients (nitrate~~s~~, phosphate~~s~~, silicate~~,~~ and ammonium) and Chl-a concentrations are gathered in regional databases such as ICES (International Council for the Exploration of the Sea), EMODnet (European Marine Observation and Data Network), and the Biogeochemical-Argo (BGC-Argo) floats. Chl-a concentration is expressed in in mg Chl m^{-3}. NPP is expressed in mg C m^{-2} d^{-1}. Oxygen and nutrient concentrations, for standardization purposes, are converted in µmol l^{-1}. The spatial distribution of ICES, EMODnet and BGC-Argo data are presented in Fig. 1b.

Remote sensing estimations of surface Chl-a are provided by the Ocean Colour - Climate Change Initiative project of the European Space Agency (ESA OC-CCI product), distributed via CMEMS.

~~Chl-a concentration is estimated from ocean colour sensors.~~ The regional ESA OC-CCI ~~ESA Ocean Colour CCI~~ product for the North Atlantic ~~and Arctic~~ Ocean~~s~~ ~~with~~ has a resolution of 1 km ~~is distributed via CMEMS~~. ~~The~~ It product merges ~~multiple sensors:~~ SeaWiFS, MODIS-Aqua, MERIS and VIIRS sensors. ~~ESA OC-CCI surface~~ Chl-a ~~concentrations~~ (in mg Chl m^{-3}) is estimated from the OC5CI regional algorithm case1/case2, a combination of OCI (Hu et al., 2012) and OC5 (Gohin et al., 2008.). A combined algorithm is required because wide and shallow North-West European shelf seas are supplied in sediment and organic material by many estuaries, which makes the water turbid and disturbs the measurement of Chl-a concentrations. ~~Optically absorbent constituents other than Chl a are responsible for large uncertainties in coastal ocean colour estimations, (up to 100% uncertainty, compared to 30% for open ocean (; Moore et al., 2009).~~ A detailed description of the ESA OC-CCI processing system can be found in Sathyendranath et al. (2012).

~~Concerning net primary production estimates, we use t~~Three ~~primary production~~NPP products using the ocean colour data of the MODIS ocean colour sensor are distributed by the Oregon State University (www.science.oregonstate.edu/ocean.productivity): the Vertically Generalized Production Model (VGPM; Behrenfeld and Falkowski, 1997; usually recognized as the Standard product), an "Eppley" version of the VGPM product (Eppley-VGPM; Behrenfeld and Falkowski, 1997) and the Carbon-based Production Model (CbPM; Westberry et al. 2008). These global ocean estimates are monthly averages with a resolution of 1/6°~~,~~ and are expressed in mg C m^{-2} d^{-1}. Due to the high uncertainty in ~~production~~ NPP products (Henson et al., 2010; Emerson, 2014), PISCES ~~primary production~~ estimates are compared with the three products mentioned above.

The ~~International Council for the Exploration of the Sea (~~ICES~~)~~ oceanographic database (www.ices.dk/marine-data/data-portals) gathers quality-controlled *in situ* observational data for the North-East Atlantic Ocean, the North Sea, the Baltic Sea and the Arctic Ocean. Dissolved oxygen, nitrate, phosphate, silicate, ammonium are all expressed in µmol l^{-1}~~,~~ and Chl-a in mg Chl m^{-3}. Over the period of the IBI36 pre-operational qualification simulation, ICES data are mainly located in the shallow and coastal waters of the Northern seas.

~~The European Marine Observation and Data Network (~~EMODnet~~)~~ collects, validate~~s,~~ and provides access to relevant marine chemistry data to assess the state of ecosystems in accordance with the Marine Strategy Framework Directive. EMODnet Chemistry has adopted and adapted SeaDataNet standards and services. Regional aggregated ~~products~~ datasets are available for the North-East Atlantic and the Mediterranean (www.emodnet-chemistry.eu/products). The aggregated datasets are regional *in~~-~~ situ* observation collections receiving additional quality control of metadata and data. The North-East Atlantic Ocean regional ~~product~~ dataset is aggregated, standardized and quality controlled by IFREMER / IDM / SISMER - Scientific Information Systems for the SEA (2018) from France~~,~~ and the Mediterranean Sea ~~product~~ dataset by Hellenic Centre for Marine Research, Hellenic National Oceanographic Data Centre (HCMR/HNODC) (2018) from Greece. The regional datasets contain oxygen, nitrate, phosphate, silicate and ammonium profiles all in µmol l^{-1} and Chl-a profiles in mg Chl m^{-3}. The North-East Atlantic dataset includes data from ~~T~~the OVIDE section between Portugal and Greenland in spring 2010 and the PELGAS cruises each spring on the Bay of Biscay ~~are part of the North East Atlantic productdataset. The regional products datasets contain oxygen, nitrate, phosphate, silicate and ammonium profiles all in µmol l-1, and Chl-a profiles in mg Chl m-3.~~ For PELGAS comparison, Chl-a data come from Niskin bottles.~~-~~ For the Mediterranean Sea regional dataset, only Chl-a is presented as it has the best spatial cover as compared to other variables.

~~Biogeochemical Argo (~~BGC-Argo~~)~~ floats are autonomous profiling floats advected by currents (Biogeochemical-Argo Planning Group, 2016). These floats acquire vertical profiles of temperature, salinity~~,~~ and key biogeochemical variables over complete seasonal cycles. In this study, we use the vertical profiles of dissolved oxygen, nitrate (both estimated in µmol kg^{-1} and converted in µmol l^{-1}) and Chl-a concentrations (in mg Chl m^{-3}) collected with 2 BGC-Argo floats in the IBI region. The first float is an APEX profiler (World Meteorological Organization (WMO) number 5904479), deployed in the North Atlantic Ocean by the University of Washington (Seattle) in February 2014 and which provided biogeochemical measurements until December 2016~~active until December 2017~~. The second float is a PROVOR-II profiler (WMO number 6901648), deployed in the Western Mediterranean Sea by the French Villefranche Oceanographic Laboratory in July 2014 and recovered in May 2016. The float data can be downloaded from the Argo Global Data Assembly Centre in France (ftp://ftp.ifremer.fr/ifremer/argo; Carval, et al., 2017)**.** The CTD and trajectory data are quality-controlled following Wong et al. ~~(~~-2015). The raw BGC signals are transformed into Chl-a, oxygen and nitrate concentrations following Schmechtig et al. (2015), Thierry et al. (2016) and Johnson et al. (2016), respectively. Finally, corrections are applied on each variable to correct from calibration biases and sensor drifts. ~~The APEX float observations are adjusted following Johnson et al (2017) and the PROVOR float observations~~adjusted following Mignot et al. (2018). The APEX float observations are adjusted following Johnson et al. (2017). The three variables are "delayed mode" data. For the PROVOR float observations, oxygen and nitrate are "Real time" data and Chl-a is "adjusted" data. They are adjusted following Mignot et al. (2018). The first five months of nitrate measurement by the PROVOR float were masked due to spurious values. ~~are adjusted following Mignot et al. (2018).~~

4. IBI36 evaluation

The skills of the ~~model~~ pre-operational qualification simulation are ~~estimated~~ evaluated by comparing model results for the main biogeochemical variables (Chl-a, NPP, nutrients~~,~~ and oxygen) to satellite derived estimations and *in situ* observations between 2010 and 2016. In function of data availability, Daily to seasonal time scale is evaluated. The spatial distribution (two-dimensional longitude-latitude plots), time series, vertical profiles and statistics performance are presented, using GODAE-like metrics (Hernandez et al., 2009, 2015), in order to assess the quality of the PISCES biogeochemical component in terms of consistency and quality/accuracy. The GODAE "Class 1" metrics are a direct comparison to observed quantities and give a general overview of the model's ability to be consistent with the general features of the IBI European

waters. The GODAE "Class 4" metrics provide a series of statistics and quantify the differences between model and observations at their location and time. ~~Chl-a concentration is expressed in in mg Chl m^{-3}, net primary production is expressed in mg C m^{-2} d^{-1}, and oxygen and nutrient concentrations, for standardization purposes, are converted in µmol l^{-1}. The spatial distributions of ICES, EMODnet and BGC Argo data are presented in Fig. 1b. In function of data availability, the spatial distribution, seasonal cycle and statistics performance are presented.~~

4.1 Satellite derived estimations

For comparison to the satellite derived estimations (Chl-a and NPP), the model is interpolated onto the data grid. Satellite ~~data~~estimates are scarce north of 50°N during the winter season, especially between November and February due to omnipresent cloud coverage that dramatically limits the observation of Chl-a concentrations. Consequently, the model outputs (Chl-a and NPP) ~~is~~are masked based on data availability, thus the annual average is done on the same number of samples. The annual average is calculated using the 7 years of simulation, from 2010 to 2016. Time series, Hovmöller diagrams and time correlation are based on monthly averages. The time series are presented for several small boxes defined and presented in Section 2 and Fig. 1. ~~The first four~~Some of them ~~-~~are located offshore to the open ocean (boxes 1 to 4, 11 and 12) and the others follow the coastal areas ~~from North to South~~(boxes 5 to 10).

4.1.1 Chlorophyll-a

~~Predicted~~The model sea surface Chl-a concentration is compared to the ESA OC-CCI ~~estimates~~product. ~~(Fig. 2~~The annual average Chl-a spatial distribution, the~~,~~ bias and the root mean square error (RMSE) are~~is~~ presented in Fig. 2. ~~The uncertainties of the model with respect to the remote sensing estimations are determined by calculating the bias and the root mean square error (RMSE) (Fig. 2). averaged bias and root mean square error (RMSE) between the simulation and the satellite estimates are presented in Fig. 2.~~ The time evolution of Chl-a at 15°W longitude (Hovmöller diagram) is on Fig. 3 in order to discuss the seasonal dynamics of the North Atlantic part. Time series for the 12 boxes already introduced as well as ~~,~~ ~~completed by~~ the spatial distribution of the temporal correlation at each grid point are presented in Fig. 4. Global statistics are synthesised on Table 1.

~~). On annual average,~~ The averaged Chl-a over the IBI domain (0.615 ± 0.69~~337~~ mg Chl m^{-3}) is close to the ESA OC-CCI product (0.555 ± 0.63~~310~~ mg Chl m^{-3}) resulting in a low percent bias of 10.8~~839~~% and a high~~t~~ correlation of 0.81 (Table 1). ~~t~~The large-scale distribution of Chl-a is correctly reproduced: the North Atlantic subtropical gyre with low surface concentrations (< 0.1 mg Chl m^{-3}), increasing concentrations when moving to the north~~,~~ and the highest values on the continental shelf. The Chl-a signature of the shelf-slope front is well marked west of the British Isles to the Faroe-Shetland Channel. The maximum coastal Chl-a is supplied by nutrient input from rivers, resuspension by strong tidal currents in the Northern shelf~~,~~ and upwelling off the Iberian and Moroccan coasts.

Major biases are located on the continental shelf (Fig. 2c). The model simulates a higher annual average in the northern part (southern North Sea, English Channel, Irish Sea), the French coasts of the Bay of Biscay ~~, the Alboran Sea,~~ and the ROFI of the Ebro and Rhone rivers. The model underestimates Chl-a concentrations off the coast of Morocco (south of Agadir) and in the region linking the North Sea to the Baltic Sea (Kattegat and Skagerrak) (Fig. 2c). The spatial distribution of the RMSE (Fig. 2d) between the simulation and the satellite ~~data~~product is comparable to the annual average of Chl-a (Fig.2 a and b). ~~Temporal discrepancies between the simulation and ESA OC-CCI estimates explain to~~ RMSE increases from south to north in the North Atlantic part and is the highest ~~RMSE~~ in coastal areas~~. And an increasing RMSE from south to north is also present in the Atlantic part~~ (Fig. 2d). ~~Temporal discrepancies between the simulation and ESA OC-CCI product could explain part of high model uncertainties (bias and RMSE) in coastal areas. But coastal areas are also complicated areas for satellite sensors to measure because optically absorbent constituents other than Chl-a interfere, resulting in a 100% uncertainty in the estimate of Chl-a, compared to 30% for the open ocean (Moore et al., 2009).~~

The seasonal dynamics of the North Atlantic spring phytoplankton bloom,- expressed as Chl-a, is depicted by the ~~The simulated seasonal cycle is in phase with satellite estimates, particularly south of 50°N, in view of the strong temporal correlation (Fig. 2d). The~~ Hovmöller diagram at 15°W (Fig. 3) and the time series in boxes 1 to 3 (Fig. 4) ~~catches the North Atlantic spring phytoplankton bloom, expressed as Chl-a (Fig. 3)~~. In the subtropical North Atlantic, Chl-a concentrations are limited throughout the year. A moderate Chl-a peak develops in March in the southern part of the domain (peak to 0.4 mg Chl m^{-3} in box 3) and gradually moves northward while intensifying (peak to 1.3 mg Chl m^{-3} in box 1). The bloom onset is well reproduced in the south (r = 0.91 in box 3), but it spreads more rapidly to the north. The observed peak reaches Iceland in summer (June-July) while the simulated peak reaches Iceland in May. The summer decrease after the bloom is then earlier and sometimes more pronounced in the model, explaining the alternation of positive and negative biases in the Hovmöller diagram at 15°W (Fig. 3c), the -increasing RMSE from south to north (Fig. 2d) and the lower temporal correlation to the north of the domain (Fig. ~~2d~~4). The south part has limited seasonal variations while the north part shows a strong seasonal cycle. The ESA OC-CCI ~~estimates~~product also highlights a large inter-annual variability in the north part while the model ~~appears~~seems to be dominated by ~~-more~~the~~regular~~ seasonal dynamics (Fig. 3 and 4). ~~But o~~But ~~O~~one part of the ~~seasonal dynamics~~signal is ~~also~~ however missing due to cloud cover masking several months each winter.

~~The simulated seasonal cycle of Chl-a is in phase with satellite estimates, particularly~~ In the southern half of the IBI domain, ~~s~~south of 50°N in the Atlantic part and in the Mediterranean ~~parts~~, the simulated seasonal cycle of Chl-a is in phase with satellite product in view of the low RMSE (Fig. 2d) and high temporal correlation (Fig. 4).

~~Figure 4 presents the time series of surface Chl-a concentrations in 12 small boxes. In general, the model predicts the seasonal cycle of Chl-a quite well. South of 50°N,~~ C~~c~~ Coastal ecosystems of the Bay of Biscay (box 7) shows a peak biomass during spring bloom, the upwelling off Portugal and Morocco (boxes 8 and ~~9~~10) present a maximum in spring with more interannual variability off Morocco. T~~, t~~he Gulf of Cadiz (box 9)~~, the Alboran Sea and~~ and the ~~Gulf of Lions~~Western Mediterranean (boxes 1~~0~~1 ~~, 11~~ and 12) succeed in reproducing the seasonal cycle of Chl-a (Fig. 4), with a high correlation coefficient (~~-~~r > 0.71) between the model and the ~~data~~satellite product.

In shallow Northern seas, the model do~~es~~ not match satellite ~~estimates~~product (boxes 4 to 6 in Fig. 4~~; see boxes 4, 5 and 6, respectively, the open North Sea, southern North Sea and English Channel~~). In the open North Sea (box (4), the first peak is usually reproduced, but the data present a strong interannual variability. In the southern North Sea (box (5) and the English Channel (box 6), model and data are dominated by the seasonal dynamics. T~~; t~~he spring bloom is in phase but ~~not the rest of the year. H~~high ~~simulated surface~~Chl-a concentrations persist in summer in the model~~English Channel and the southern North Sea~~, while remote sensing ~~data~~estimates ~~predict~~show a sharp decrease after the spring bloom. These coastal regions ~~show~~present the highest biases, highest RMSE and low temporal correlation.

4.1.2 Net primary production

~~Ocean d~~Simulated depth integrated ~~Net Primary Productivity (~~NPP~~)~~ is compared to the three NPP ~~primary production~~ products (VGPM, Eppley-VGPM and CbPM). ~~:-~~Figure~~-~~ 5 presents the annual average distribution for the simulation and the mean of the three NPP products~~s, , . The uncertainties of the model with respect to the remote sensing derived estimations are apprehended by~~ the standard deviation of the three NPP products and the bias between the simulation and the mean of the three NPP products~~standard deviation of the three NPP products, and averaged bias between the simulation and the mean of the three NPP products~~. For time series (Fig. 6), the three products are presented separately because they do not all have the same seasonal behaviour, and therefore an average would ~~annihilate~~prevent any analysis. ~~Time series for the simulation and the three NPP products on the 12 boxes are presented in Fig. 6.~~Global statistics are synthesised on Table 1.

). On annual average, the IBI36 system (Fig. 5bd) provides for a NPP of 230 gC m^{-2} yr^{-1} at the western boundary of the domain that gradually increases towards the coasts (Fig. 5b). The highest NPP (1700 gC m^{-2} yr^{-1}) is found in the coastal regions of the North Sea, where rivers and mixed water columns supply the euphotic layer with nutrients. Compared to the mean of the three NPP products Standard VGPM product (Fig. 5a), the large-scale distribution is reproduced. The cross-shore gradients are reproduced; the signature of the shelf-slope front west of the British Isles to the Faroe-Shetland Channel is captured. However but the IBI36 system underestimates the NPP by a factor of 2 1.5 on average over the domain. This underestimation reaches a factor of 3-4 on the European coasts. The most important differences concern the Kattegat and the gat/Skagerrak area and the Norway current, with a factor of 3-4. HoweverOn the other hand, it should be noted that the dispersion between The spatial distribution of simulated NPP is in between the Eppley-VGPM and CbPM products instead (Fig. 5c). However, the dispersion between the three NPP productsVGPM, Eppley-VGPM and CbPM products is quite highis considerable (Fig. 5c), and. Except to the open boundaries, the bias of the model equals almost the variability of the NPP productsIt. is d). Finally, td).

So tin thes., except to the open boundaries where the model shows higher bias than the dispersion of the NPP products.

Figure 6 presents the time series of NPP in the same 12 small boxes as for Chl-a. The seasonal cycle time series of confirm the considerable spreading between the three NPP products (Fig. 6). The simulated NPP is generally in line with the two VGPM-based products (VGPM and Eppley-VGPM) with a time correlation higher than 0.7 in a majority of boxes. The very good correlation in the south part of the Atlantic (box 3, r = 0.91 with the VGPM) decreases northward (boxes 2 and 1), as IBI36 predictsproduces a moderate and above all an earlier production peak. In addition, the second peak, or at least the maintenance of highsignificant NPP in summer, is not reproduced. The behaviour of the NPP in the North Atlantic part is consistent with the seasonal dynamics of the sea surface Chl-a described in the previous section. The coastal waters of the Northern Seas and Atlantic part andas well as in the Mediterranean part (boxes 4 to 12; Fig. 6) also show a. The simulated seasonal cycle of NPP is very similarclose to the VGPM-based products. On the other hand, t in the shallow Northern seas (boxes 4 to 6) and in all coastal waters of the simulatedIBI domain and in the Mediterranean part (boxes 4 to 12; Fig. 6). The correlation is low compared to the CbPM product, but theis latter givingvesdelivers a seasonal cycle generally very distinctdifferent from the VGPM-based products. The CbPM signal is sometimes in phase opposition with IBI36 (boxes 3, 5, 9, 10 and 11) while the comparison with VGPM results in high correlation in these same boxes.

Spatial distributionThe standard deviation (Fig. 5c) and time series (Fig. 6) highlight the high variabilitydispersion of NPP products (Fig. 5 and 6)estimates derived from satellites. The VGPM is the most productive product. A well defined cross-shore gradient and , with the highest seasonal amplitude characterize it (Fig. 6). The Eppley-VGPM behaves the same way as the VGPM, but less productive (Fig. 6). The CbPM is the less productive, with the lowest coastal production, a more uniform rate over a large part of the domain including the open ocean, and a less pronounced seasonal cycle, sometimes out of phase with VGPM based products (boxes 3, 11 and 12; the subtropical gyre, Gibraltar strait and Gulf of Cadiz; Fig. 6).

Campbell et al. (2002) pointed out that the "best performing algorithms generally fall within a factor of 2 of the estimates derived from ^{14}C", and that NPP products have poor performances for water columns with depths less than 250 meters (Saba et al., 2011). Schourup-Kristensen et al. (2012) also reported that the VGPM product is twice as productive as biogeochemical models along the European coasts. This high uncertainty in NPP products prevents a quantitative assessment.

We can therefore only say that there seems to be an offset between the simulation and the satellite NPP products. The averages simulated NPP over the IBI domain (441.761 ± 203.5306.41 gC m^{-2} yr^{-1}) is close to CbPM (518.108 ± 660.9362.08

gC m^{-2} yr^{-1}) ~~)~~ and twice lower than VGPM (871.5~~49~~ ± 557.2~~306.41~~ gC m^{-2} yr^{-1}) (Table 1). But spatial distribution is better correlated with the VGPM-based products (Table 1). The VGPM is the most productive product, with a marked cross-shore gradient and the highest seasonal amplitude (Fig. 6). The Eppley-VGPM behaves the same way as the VGPM, but less productive (Fig. 6). The CbPM is the less productive, with a poorly marked cross-shore gradient, the lowest coastal production and a less pronounced seasonal cycle, sometimes out of phase with VGPM-based products (Fig. 6). A few extreme values near rivers increase the averaged NPP of CbPM and give rise to a high standard deviation.

In summary, ~~The model~~IBI36 provides an averaged NPP similar to CbPM. The spatial distribution, cross-shore gradients and seasonal variations are generally in good agreement with the VGPM-based products, but IBI36 is half as productive (mean factor of 1.5). The modelled NPP is thus within the range of variability of the satellite derived estimates. ~~estimates are included in the dispersion of the satellite NPP products and the seasonal variations are generally in good agreement with~~~~the simulated NPP lies between the three NPP products. IBI36 is in between the Eppley-VGPM and CbPM in terms of spatial distribution, and better correlated to the VGPM-based products with regard to seasonal variations.~~

4.2 *In situ* ~~historical~~ historical data

In the following, the simulation is compared to ICES and ~~and~~ EMODnet *in situ* historical ~~historical~~ databases using ~~The~~ daily average~~s of the~~d model outputs~~.~~. ~~are For compared ison to ICES and EMODnet datasetsbases, the daily averages of the modelled data are co-located with *in situ* data at the point closest of the model grid at the surface and using linear interpolation on the vertical dimension. These databases cover distinct areas, so the following evaluation is sub-divided by regions.~~ ICES data are mainly located in the shallow and coastal waters of the Northern seas (Fig. 1b) ~~where nutrients inputs from rivers are significant (Fig. 1b)~~. EMODnet regional ~~products~~ datasets cover the North-East Atlantic Ocean and the Western Mediterranean Sea. ~~Global statistics are summarised in a Taylor diagram (Fig. 7).~~~~The, the~~vertical distribution of ~~biogeochemical tracers in the open Atlantic is compared with the OVIDE section between Portugal and Greenland during spring 2010, and the surface distribution in the Bay of Biscay is compared with the PELGAS cruises in each year during May (Fig. 1b). For the Western Mediterranean Sea, Chl-a presents the best spatial coverage. Global statistics are summarised in a Taylor diagram (Fig. 16).~~

4.2.1 Northern Seas

Shallow Northern seas are assessed using oxygen, nutrients and Chl-a from ICES database. Dispersion diagrams for the full set of match-ups are presented on Fig. 8~~7~~. Sea surface spatial distribution and seasonal cycle are on Fig. 9~~8~~ and 10~~9~~.

~~-~~The oxygen match-ups are well aligned along the bisector with a ~~very~~ good correlation (r = 0.77) ~~of 0.81~~ and a normalized standard deviation ~~close to 1~~of 0.91 indicating that the model reproduces the amplitude and variability of the observations (Fig.~~7~~ 7 and 8~~16~~). ~~The temporal evolution at the s~~T~~S~~ea surface temporal evolution of sea surface concentrations (Fig. 9) ~~confirms~~shows the realistic amplitude and phase (Fig. 10~~9~~). ~~O~~Sea surface oxygen is slightly overestimated in the North Sea and English Channel, with an average bias of 10.7 µmol l^{-1}. ~~(~~corresponding to a percent bias of 4%~~)~~ (Fig. 9~~8~~). In addition, the model does not capture the lower sea surface oxygen ~~pool~~concentrations than that measured during 2014-2015 period (~~see the pool of overestimated oxygen in~~ Fig.~~7 and~~ 10~~9~~). This anomaly is located in the region linking the North Sea to the Baltic Sea (Kattegat and Skagerrak), the eastern open boundary of the domain. But n~~N~~o reference to this event has been found in the literature.

~~Ciavatta et al. (2016) worked on continental shelf areas vulnerable to oxygen deficiency, defining deficiency when at least one daily value is below the 6 mg l^{-1} (187.5 µmol l^{-1}) threshold. Using the same definition, ICES data and the IBI36 system identify vulnerable areas in the North Sea and in particular its eastern part (Fig. 10). The seasonal cycle of the minimum oxygen levels are well correlated (r=0.77). The waters are oxygenated in winter while they can deplete below the 2 µmol l^{-1} threshold or even reach anoxic conditions in summer (Fig. 10). But ICES data only permit identifying the North Sea because~~

~~the data density strongly decreases outside. So extending this analysis to the full set of simulated oxygen, minimum levels are also predicted in the Celtic Seas, Armorican shelf, coastal areas of Scotland and Western Ireland. Ciavatta et al. (2016) and the OSPAR commission point out these aforementioned regions as eutrophication problem areas, and Breitburg et al. (2018) also report low and declining oxygen levels in almost all coastal waters of the North-West European shelf.~~

~~Following this positive oxygen assessment, the IBI36 system can therefore be used to monitor the surface area exposed to oxygen deficiency. Using the same method as Ciavatta et al. (2016), the IBI36 system predicts a maximum extension of 280 000 km^2 by considering at least one daily value below the threshold. Vulnerable areas are similar to those reported by Ciavatta et al. (2016), while Celtic Seas and the English Channel are less affected. The seasonal extension varies from a very restricted and oxygenated surface area in winter to an average surface area of 85 000 km2 in summer (Fig. 10d), associated with deoxygenated waters that can reach anoxic conditions in the North Sea and along the west coats of France.~~

The distribution of nitrate~~s~~ also ~~is also well represented with a high correlation of 0.84~~follows the bisector~~ -~~, with a ~~higher~~noticeable dispersion (Fig. 8~~7~~) which deteriorates the statistics (Fig. 7). The model generally underestimates sea surface nitrate with an average bias of -1 µmol l^{-1} (9.6% percent bias) (Fig. 9~~8~~). The time series shows a seasonal cycle in phase, but excessive nitrate concentrations are simulated in spring and summer when the observed concentrations are very low (Fig. 10~~9~~). Very high values of 100 to 300 µmol l^{-1} are simulated throughout the year in the vicinity of river flows between the Rhine and Elbe~~. They are not visible on the dispersion diagram (Fig. 7) because a filter eliminates low-density points. But on other hand, these extreme values have an impact on the~~ and impact the ~~smoothed~~ time series ~~(Fig. 10~~9~~). The negative bias observed in space is masked in the time series by extreme values.~~

Phosphate and silicate are overestimated for low concentrations during spring-summer seasons, while higher concentrations during winter conditions are better captured (Fig. 8~~7~~ and~~ -~~ 10~~9~~). The phosphate dispersion diagram shows two high-density zones. The spring-summer over~~prediction~~estimation is mainly along the coasts. Winter conditions are better captured, although still a little high. The data show a marked seasonal cycle while simulated phosphate levels remain too high throughout the year. The average bias of 0.22 µmol l^{-1} or 48.3 % percent bias is reduced to 31.5% ~~if~~when the pathway to Baltic Sea is excluded. Silicate has an average bias of 2.1 µmol l^{-1} or 46.8% percent bias. They are overestimated in the open North Sea and underestimated along the coasts between the Rhine and the Elbe. In addition, percent bias decreases to 30.8% ~~if~~when the pathway to Baltic Sea is excluded. Ammonium shows a high dispersion~~,~~ but the magnitude is captured. The model does not reproduce the variability observed in data ~~-~~(Fig. 8~~7~~e), and the seasonal cycle is out of phase (Fig. 10~~9~~e). The statistics give thus poor performances for phosphate and silicate, even outside the Taylor diagram for ammonium (Fig. 7).

~~For ammonium and~~ Chl-a provides a satisfying distribution (Fig. 8~~7~~) but mean Chl-a concentrations along the coasts are underestimated (Fig. 9~~8~~). ~~- match ups show a high dispersion; the model does not reproduce the high variability observed in data (Fig. 7e et 7f). The~~The~~ -~~ seasonal cycle ~~is~~ is ~~in phase for Chl-a but out of phase for ammonium (Fig. 7e and Fig. 9).~~captured, but t~~On the other hand, the magnitude is captured for ammonium but not for Chl-a. Mean Chl-a concentrations along the coasts are underestimated (Fig. 8). T~~he model predicts a slow spring increase instead of a strong bloom in mid-march (Fig. 10~~9~~). ~~It should be noted that co~~Coastal Chl-a appears to be underestimated compared to ICES *in situ* data, ~~whereas it is~~while overestimated compared to satellite estimates (see Sect. 4.1.1 and Fig. 2)~~, which recalls the high uncertainties of remote sensing signal in coastal waters due to interference from Chl-a content and other optically absorbing elements such as suspended matter, coloured dissolved organic matter and bottom reflectance (Moore et al., 2009). -~~The statistics are low (Fig. 7) while the density plot, surface distribution and time series (Fig. 8 to 10) are positive.

~~Comparison with the ICES database in the Northern part of the IBI domain shows that the seasonal cycle of nutrients phosphate and silicate is not sufficiently marked, particularly for phosphate and silicate, and that the high spring bloom is not intense enough. Nutrient and Chl-a patterns are strongly influenced by river nutrient input. In the coupled IBI36 system, nutrient inputs at river points are prescribed using a constant value, while inputs usually follow a seasonal cycle related to precipitation and watershed erosion. In addition, sedimentary processes (i.e. remineralization of organic carbon and subsequent release of nutrients) are not considered here, this assumption may be too restrictive. The Kattegat and Skagerrak~~

~~are also complicated to reproduce. But the exit from the Baltic Sea is a very specific marine area probably not apprehended by the global product used at boundary.~~

Statistics are not really rewarding (Fig. 7) and they alone do not allow ~~us to understand~~understanding the characteristics of the IBI36 system. The spatial ~~distribution as well as the time series are~~distribution as well as the time series is necessary to interpret the statistics. The latter are strongly degraded by extreme values at the mouth of~~r~~ rivers or highly targeted areas such as Kattegat/Skagerrat, while the mean spatial distribution and temporal evolution ~~remain~~appear realistic. Oxygen is the best performing variable in the Northern Seas, and its satisfying statistics allow ~~to deepen~~deepening the analysis of oxygen match-ups between ICES and IBI36.

Oxygen content is a key element in biogeochemical cycles and can be an indicator of the health of marine ecosystems. So minimum oxygen concentrations are now analysed. For that, the absolute minimum is extracted for each pixel of ICES and col~~-~~located IBI36. The lowest concentrations are located in the eastern part of the North Sea (Fig. 11~~0~~a). The minimum remains high in winter while it sharply decreases or even reaches anoxic conditions in summer (Fig. 11~~0~~b). ~~-~~The minimum reported by ICES remain lower than usually during 2011 and 2015 winters, but they come from a few measurement points very close to the coast in the vicinity of river mouth ~~river~~, not captured by the IBI36 system. The spatial distribution of the simulated minimum as well as its seasonal evolution is consistent with the data (r = 0.77). ~~-~~But please remind that ICES data only permit identifying the North Sea because the data density strongly decreases outside. So extending this analysis to the full set of simulated oxygen over the IBI domain (not only the match-ups with ICES), IBI36 also simulates minimum levels ~~are also simulated~~ in the Celtic Seas, Armorican shelf, coastal areas of Scotland and Western Ireland. Ciavatta et al. (2016) and the OSPAR commission point out these aforementioned regions as eutrophication problem areas and Breitburg et al. (2018) also report low and declining oxygen levels in almost all coastal waters of the North-West European shelf.

Continental shelf areas vulnerable to oxygen deficiency were estimated by Ciavatta et al. (2016), considering vulnerable area when at least one daily value is below the 6 mg l^{-1} (187.5 µmol l^{-1}) threshold. Using the same method as Ciavatta et al. (2016), the IBI36 system predicts a maximum surface area exposed to oxygen deficiency of 280 000 km^2. The seasonal extension varies from a very restricted and oxygenated surface area in winter to an average surface area of 85 000 km^2 in summer (Fig. 11~~0~~c), associated with deoxygenated waters that can reach anoxic conditions in the North Sea and along the west coasts of France ~~(not shown)~~.

4.2.2 North-East Atlantic waters

The North-East Atlantic part ~~of IBI domain~~ is evaluated using the EMODnet regional dataset. Global statistics are very satisfying (Fig. 7) as *in situ* measurements cover the entire water column. However, performance between the vertical and sea surface distribution differs greatly. Comparison to OVIDE section and PELGAS data are detailed below using Fig. 12 and 13.

The OVIDE radial section sampled in June 2010 between Portugal and Greenland (Fig. 12) illustrate the vertical distribution of biogeochemical tracers in the open Atlantic. ~~the OVIDE radial section sampled in June 2010 between Portugal and Greenland (Fig. 11).~~ Oxygen and nutrients ~~correlate~~ show very ~~well~~ good statistics with OVIDE data, with coefficient correlation higher than 0.95. ~~5~~ (Fig. 7~~1~~6). ~~The model catches the main vertical distribution of biogeochemical tracers.~~ The dispersion diagram for oxygen shows two pools of high density: one for low oxygen values, and the other one for high concentrations. Throughout the OVIDE vertical section, the minimum oxygen level is around 1000 meter deep. Low oxygen content in the eastern part of the section is due to MOW on the shelf of the Iberian Basin. Oxygen maximum around 2500 meters relies on recently ventilated Labrador Sea Water (Garcia-Ibanez et al., 2015) that reaches the western part of the section. The three nutrients present a maximum around 1000 meters, the lower values at this depth being due to MOW. High silicate (45-50 µmol l^{-1}) near the bottom reflects the influence of Antarctic Bottom Water in the North-East Atlantic Ocean (Garcia-Ibanez et al., 2015).

However, vertical profiles of oxygen are somewhat smoothed. The minimum and maximum ~~oxygen~~ at respectively~~,~~ 1000 and 2500 meters~~,~~ are not pronounced enough, resulting in a normalised standard deviation of 0.74 (Fig. 7). ~~Also nutrient maximum around 1000 meters is weaker.~~ Nutrient profiles are also smoothed, but this is less visible (normalised standard deviation close to 1; Fig. 7) than on oxygen, as the latter has much stronger vertical gradients.

~~**4.2.3 Bay of Biscay**~~

The PELGAS spring data (Doray et al., 2018a, 2018b) are used to illustrate the mean sea surface distribution in the Bay of Biscay for spring conditions ~~(~~(Fig. 13). Surface statistics are significantly degraded compared to vertical statistics (Fig. 7). ~~The Bay of Biscay is assessed using the PELGAS data (Doray et al., 2018a, 2018b). These data allow evaluating the spring conditions of the bay. Sea surface oxygen concentrations are well correlated with PELGAS data (correlation of 0.74), which means that amplitude and variability are correctly simulated.~~ Simulated sea surface oxygen concentrations present an average bias of +16.4 µmol l^{-1} ~~(~~, which correspond~~s~~ing to a percent bias of 6.3% ~~(;~~ Fig. 13~~2~~). ~~Spring n~~Nutrient ~~concentrations~~ distribution is ~~are~~ realistically simulated, except at the ROFI of French rivers. Surface oxygen bias and excessive nutrient discharges were already highlighted in the Northern Seas using the ICES database. The mean surface Chl-a distribution is ~~very close~~similar to the data: the cross-shore gradient is realistic with ~~spring~~ concentrations of 0.3 mg Chl m^{-3} offshore, which increase to 6 mg Chl m^{-3} along the French coast.

4.2.3~~4~~ Mediterranean Sea

The Mediterranean Sea is assessed using EMODnet regional dataset~~base~~ that has a very good spatial coverage for oxygen and Chl-a tracers, while nutrient data are limited to the northern part of the domain. Oxygen comparison gives the same conclusions as for the North Sea and the ~~Bay of Biscay~~Atlantic: the model succeeds in reproducing the amplitude and variability of oxygen, but a constant bias persists. So only the sea surface Chl-a distribution is presented here (Fig. 14~~3~~). High coastal values are located along the Catalan coast, in the ROFI of the Ebro, along the Costa Blanca and along Algeria. Two highly productive areas are located further offshore: one in the convection zone of the Gulf of Lions and the other in the Algerian Basin between Sardinia and Algeria. Everywhere else, Chl-a is lower. The model simulates Chl-a higher than EMODnet in the Alboran Sea and in the ROFI of the Rhône River. ~~This overestimation was already highlighted by comparison with satellite estimates (see Sect. 4.1.1). EMODnet therefore confirms this tendency.~~ But in a general way, the model reproduces ~~very well~~ the mean spatial distribution of surface Chl-a in the Mediterranean.

4.3 BGC-Argo data

The evaluation is now enriched by a comparison to t~~T~~he free-drifting BGC-Argo profiling floats which allow continuous monitoring of dissolved oxygen, nitrate and Chl-a of the upper 1000 meters of the ocean. 2 BGC-Argo floats are used ~~here~~, one in the North Atlantic Ocean and the other in the Western Mediterranean Sea in order to discuss the model quality in reconstructing the seasonal vertical dynamics, and the key coupled physical-biogeochemical processes. Density plots between the BGC-Argo data and simulated fields are presented on Fig. 15 and time evolution of the vertical profiles of oxygen, nitrate and Chl-a along the float trajectory are on Fig. 16. The quantitative comparison is summarized by the statistics of Fig. 7.

Overall, the model predictions are in good agreement with the BGC-Argo observations with correlation coefficients greater than 0.8 for oxygen and nitrate profiles (Fig. 7). The model tends to overestimate low concentrations and underestimate high concentrations of oxygen and nitrate as shown by the distribution of match-ups which deviate from the bisector (Fig. 15). Time evolution of the vertical profiles in Fig. 16 shows that the deep oxygen minimum and nitrate maximum are not

pronounced enough in the model. Oxygen remains 20 µmol l^{-1} too high and nitrate 2 µmol l^{-1} too low. The smoothing of the vertical profiles of oxygen and nutrients was already highlighted by the comparison to OVIDE.

~~.~~

The IBI36 system succeeds in reproducing the winter vertically mixed water column that enriches the first few hundred metres of the water column with oxygen and supplies the surface with nutrients. Seasonal re-stratification and the shoaling of the MLD trigger the onset of the spring phytoplankton bloom (Fig. 16). ~~Figure 14 shows the density plots between the BGC-Argo floats and simulated fields of oxygen, nitrate and Chl-a concentrations in the two basins.~~

~~Overall, the model predictions are in good agreement with the BGC-Argo observations with correlation coefficients greater than 0.75 for all variables in the two basins (Fig. 714). For all variables, the model shows a gain lower than 0.7, suggesting that t~~The model tends to overestimate low concentrations and underestimate high concentrations of oxygen, nitrate and Chl-a ~~as shown by the distribution of match-ups which deviate from the bisector (Fig. 15). This is also~~ clearly evidenced in Fig. 16~~5 that shows the time evolutions of the vertical sections of oxygen, nitrate and Chl-a estimated from the BGC-Argo floats and the model. In particular, the deep oxygen minimum and nitrate maximum are not pronounced enough in the model. Oxygen remains 20 µmol l^{-1} too high and nitrate 5 µmol l^{-1} too low. The smoothing of the vertical profiles of oxygen and nutrients was already highlighted in by the comparison to OVIDE section. Additionally, the model simulates relatively high Chl-a concentrations at depths where there is no light and no phytoplankton is expected, indicating that the parameterization of Chl-a degradation in PISCES could be improved.~~

~~The skill of the model in representing the seasonal cycles of oxygen, nitrate and Chl-a concentrations in the Atlantic Ocean and Mediterranean Sea is also evaluated in Fig. 15.~~ In the Atlantic Ocean (Fig. 16~~5~~, left side), the MLD reaches 400-500 m depth during winter. Depth of the ventilation has a clear interannual variability, as shown by the deeper mixing during winter 2015 with respect to the following year. This ventilation also enriches the surface in nutrients. If winter processes are well reproduced, t~~he seasonal cycle of oxygen, nitrate and Chl-a concentrations are dominated by the spring bloom that dramatically increases oxygen and Chl-a concentrations and decrease nitrate concentrations in the surface layer when mixing stops and the MLD becomes shallower in spring, as clearly shown in the float observations. Overall, the model reproduces roughly the timing of thet~~he ~~simulated~~ onset of the simulated bloom ~~onset seems~~is however too early. The intensity of the bloom is misrepresented in the model as surface Chl-a concentrations remain significantly ~~too~~ lower than BGC-Argo data ~~in~~ during the spring bloom, ~~and become~~ decrease rapidly ~~depleted~~ after the bloom and remain at a low level during ~~in~~ summer. This behaviour as regards of the BGC-Argo data is consistent with ~~at sea surface is confirmed by~~ the comparison to ESA OC-CCI ocean colour product in box 2 of Fig. 4. The time evolution of vertical profiles highlights that t~~Here *in situ* and satellite data are consistent. T~~he high surface ~~concentrations~~Chl-a associated with the spring bloom migrate to the sub-surface during the ~~summer~~stratified season in the model while they remain at the sea surface in the data. Indeed~~Additionally~~, a Deep Chl-a~~orophyll~~ Maximum (DCM) develops is summer in the model simulation and is ~~. It is~~ not present in the observations ~~develops in the model simulation~~.

In the Mediterranean Sea (Fig. 16~~5~~, right side), the seasonal cycles of Chl-a and oxygen are characterized by the formation of a DCM (Mignot et al., 2014; Lavigne et al., 2015), which typically establishes during the stratified season. The DCM is associated to a Deep Oxygen Maximum (DOM) ~~(Estrada et al., 1985) in the lower part of the euphotic layer~~at the layer of the DCM due to intense phytoplankton production during spring and summer (Estrada et al., 1985). These maxima are also associated with the limit between nutrient-depleted and the nutrient-rich layers, termed nitracline (Estrada et al., 1993). The model correctly reproduces the time evolution of the nitracline, as well as the temporal evolution, vertical displacement ~~depth~~ and intensity of the DCM and DOM ~~from spring to fall~~. ~~-~~The IBI36 system compares well with the Mediterranean float to reproduce the vertical dynamics of the phytoplankton chlorophyll and oxygen. The seasonal succession of physical-biogeochemical processes is captured.

5 Discussion

An extended validation of the pre-operational qualification simulation has allowed understanding the strengths and weaknesses of the biogeochemical component of the IBI36 system, providing the trails for improvement to be explored. They are discussed now.

~~Differences~~Mismatches between simulated and satellite derived estimations of Chl-a and NPP increase when approaching the continental shelf. The uncertainties of the modelled Chl-a with respect to ESA OC-CCI product are determined by calculating the bias and RMSE. Highest uncertainties are located in coastal areas, and ~~could~~can be explained by temporal discrepancies between the simulation and ESA OC-CCI product. For NPP, the uncertainties are apprehended by the comparison of the standard deviation of the three NPP products and the bias between the simulation and the mean of the three NPP products. Bias of the model is included in the standard deviation of the NPP products. The modelled NPP is then included within the range of uncertainty of the satellite derived products.

Continental margins are very productive regions and play an important role in the biogeochemical cycle of nutrients and carbon. They are the site of complex interactions between physical, chemical and biological processes that include exchanges between shelf and the open ocean, sediment-water interactions, air-sea fluxes, and land-ocean freshwater inputs. In addition, coastal systems are locally strongly affected by human activities. All these interactions make the continental shelf a challenge to obtain realistic models.

~~The maximum coastal biological production is governed by a complex interplay between physical exchanges with the open ocean, local biogeochemical processes, input from river discharges, resuspension and sedimentary processes. It is thus a complex area to model in terms of dynamics, biogeochemical processes and external forcing.~~ These are also the areas where the uncertainties of satellite products are the greatest. Coastal areas are complicated areas for satellite sensors to measure due to interference from Chl-a content with other optically absorbing elements such as suspended matter, coloured dissolved organic matter and bottom reflectance, resulting in a 100% uncertainty in the estimate of Chl-a, compared to 30% for the open ocean (Moore et al., 2009). A good example is given in the North Sea example, where the model underestimates coastal Chl-a ~~are underestimated compared~~with respect to the ICES *in situ* data, which however appears in contrast with the ~~while~~ overestimation ~~ed~~ with respect to ~~compared to~~the satellite ESA OC-CCI product. The dispersion between the three NPP products is also considerable. Campbell et al. (2002) pointed out that the "best-performing algorithms generally fall within a factor of 2 of the estimates derived from ^{14}C", and that NPP products have poor performances for water columns with depths less than 250 meters (Saba et al., 2011). Schourup-Kristensen et al. (2012) also reported that the VGPM product is twice as productive as biogeochemical models along the European coasts. This high uncertainty in NPP products prevents a quantitative assessment. Additionally, they do not have the same seasonal dynamics. CbPM has a seasonal cycle distinct or event out of phase from the two others NPP models in a major part of the domain. An extensive dataset of measures of primary production in the IBI European waters would be necessary to evaluate the three NPP products and deepen the analysis.~~We can therefore only say that there seems to be an offset between the simulation and the satellite NPP products.~~

For oxygen and nutrients, s~~S~~tatistics are very satisfying when the entire water column is considered. The model preforms in reproducing the v~~V~~ertical ~~profiles~~structure of oxygen and nutrients ~~of oxygen and nutrients give statistics~~ but the profiles appear too smoothed. The deep minima and maxima are not pronounced enough. This behaviour is also observed in the global model ¼° (Perruche et al., 2016) used in the initial and open boundary conditions. It can originate from the physical or biogeochemical models. Different approaches are currently under study. Vertical diffusion could explain the loss of peaks and minima in vertical profiles, but b~~. B~~iogeochemical processes (parameterization of remineralisation processes, rate of sinking of particulate detritus, vertical migration of zooplankton which export organic matter at depth…) are also investigated.

~~But the regional model also inherits the qualities and weaknesses of the forcing global model, and the latter simulates a smoothed vertical distribution, so this default cannot be caught up in the regional model without improvements in the initial and open boundary conditions.~~

Performances decrease at sea surface and in the continental shelf area. Sea surface oxygen is slightly overestimated (around 4%). Surface ocean concentrations tend to balance with atmospheric concentrations, and here atmospheric oxygen concentrations are prescribed by a constant value over time and space. A spatial and temporal atmospheric oxygen forcing would be beneficial instead. ~~But~~ In addition, the continental shelf ecosystem ~~of Northern seas~~ is strongly driven by river discharges, especially in the Northern seas. The seasonal cycle of phosphate and silicate is not sufficiently marked, and the high spring bloom is not intense enough. ~~Nutrient and Chl-a patterns are strongly influenced by river nutrient input.~~ In the coupled IBI36 system, nutrient inputs at river points are prescribed using ~~a annually averaged values~~annually averaged values, while inputs usually follow a seasonal cycle related to precipitation and watershed erosion. The increased discrepancies when approaching the coasts are related to a poor representation of river nutrient discharges due to a crucial lack of available measurements. ~~Annually averaged nutrient inputs are injected into the ocean system, while~~ A~~a~~ time evolution or at least a seasonal variation would be necessary to apprehend the phytoplankton dynamics in the coastal areas triggered by rivers plume events. ~~As well, In addition~~Finally, sedimentary processes (i.e. remineralization of organic carbon and subsequent release of nutrients) are not considered ~~sedimentary processes are neglected~~ in the IBI36 system as strong tidal currents prevent organic matter from reaching and accumulating in sediments. This assumption may be too restrictive. As an alternative a sediment module should be coupled to the biogeochemical model to improve the representation of sedimentary processes, i.e. remineralization of organic carbon and subsequent release of nutrients.

For the coastal Northern Seas, t~~T~~he statistics ~~at sea surface~~ are strongly affected by extreme values at the mouth of~~r~~ rivers (discussed above) or highly targeted areas such as the Kattegat/Skagerrat area which is at the border of the IBI domain and so strongly dependant of the open boundary conditions used. The CMEMS ~~Batlic~~Baltic Sea regional configuration instead of the global product should be tested at the eastern open boundary of the IBI36 system.

BGC-Argo floats allowed better understanding the phytoplankton and oxygen vertical dynamics. The Mediterranean Sea is well capt~~r~~ured by the model, in terms of timing, vertical migration of the maximum chlorophyll and the formation of an oxygen maximum linked to the DCM. In the Atlantic part, winter processes are captured but the bloom onset is early. This earlier bloom is consistent with respect to the satellite estimates in the same area. In fact, the onset of the spring bloom is correct in the south part of the domain, but it spreads more rapidly to the north as compared to satellite data. The summer decrease after the bloom is then earlier and sometimes more pronounced in the model. BGC-Argo comparison highlighted that modelled Chl-a maximum is found deeper during summer with the formation of a DCM while maximum Chl-a remains at the surface in BGC-Argo estimates. As phytoplankton starts growing earlier in the model, the mixed layer becomes nutrient-depleted at the end of spring (oligotrophic conditions) and phytoplankton migrates just below. This behavior is also present in the global model (Perruche et al., 2016, 2018). Several experiments on the physical and biogeochemical components are being carried out. ~~a~~

~~This DCM develops while *in situ* maximum Chl-a remains to the surface. This DCM lets us suspect a distinct physical or biogeochemical behaviour at 50°N in the Atlantic between the model and the data. The formation of a DCM indicates that phytoplankton production has to deepen in order to reach the nitracline, and it is usually a typical feature of stratified water columns. Here, the physical model assimilates temperature and salinity profiles from Argo float network, so we can not suspect the model to overestimate the influence of stratified water masses of the subtropical gyre at 50°N. Instead, the biogeochemical distribution may constrain phytoplankton to grow deeper to find enough nutrients.~~ However, the validation of the Atlantic part is limited to only one BGC-Argo float measuring simultaneously ~~-~~oxygen, nitrate and Chl-a. Additional floats ~~measuring key the biogeochemical variables~~ would be required to understand the seasonal dynamics of phytoplankton, oxygen and nitrate on the Atlantic side and better apprehend the involved physical-biogeochemical coupled processes.

~~allow a detailed assessment to be made in order to understand the strengths and weaknesses of the model, providing the trails for improvement to be explored. They are discussed below.~~6 ~~and~~ C~~c~~onclusions

In the framework of CMEMS, the IBI-MFC Team has developed an operational system in order to monitor and forecast the ocean dynamics and marine ecosystems of the IBI European waters. A 7-year pre-operational qualification simulation (2010-2016) delivers the initial conditions to the analysis and forecast system. This paper provides a~~A~~n extended validation of th~~e~~is pre-operational qualification simulation~~.~~

~~This paper~~ in order to evaluate~~s~~ the capacity of the IBI36 system to reproduce the surface and vertical distributions, as well as seasonal cycles of the main biogeochemical variables (Chl-a, NPP, nutrients~~,~~ and oxygen)~~,~~ using GODAE-like metrics. The different ~~kind of metrics (direct comparison and statistics) are~~kinds of metrics (direct comparison and statistics) are necessary and complementary in order to have a complete vision of the model's performance in terms of consistency and quality/accuracy. This paper represents the first validation of the biogeochemical component of the IBI36 system. The objective is to show that PISCES can be used for operational applications, and that there is no contraindication to using the PISCES model at such a resolution.

~~of the model application used as base of the CMEMS IBI-MFC biogeochemical forecast service is provided. The IBI-MFC operational forecast system is based on the NEMO-PISCES modelling platform in its latest version 3.6, with a 1/36° horizontal resolution. It provides weekly a short-term (7 days) forecast of the ocean dynamics as well as the main biogeochemical variables. A weekly update of hindcast products (generated for the week before) is also delivered as part of the product, and configures the historic best estimates. The skills of the IBI36 configuration to reproduce the main biogeochemical variable distribution are assessed using a 7-year retrospective simulation starting in January 2010 up to December 2016.~~

~~The model results are evaluated using satellite estimates for~~ Chl-a and ~~net primary production~~NPP are compared to satellite estimates. The ~~annual averaged~~mean spatial distribution and seasonal cycle are~~is~~ described ~~here~~in the paper. Oxygen, nutrients and Chl-a concentrations are compared to ~~*I*~~*in situ* observations ~~come~~ from ICES, EMODnet and the BGC-Argo float network, using daily averages of the model outputs. ~~for oxygen, nutrients and Chl-a concentrations.~~ Observational data are available for the Northern Seas, the North-East Atlantic waters ~~, the Bay of Biscay, the Northern Seas~~ and the Western Mediterranean, and allow evaluating the vertical distribution as well as shallow and coastal distributions. Some of these areas are outside of the IBI Service Domain (that is the geographical domain covered by the CMEMS IBI-MFC products). But in order to take advantage of their *in situ* observational coverage, not only the IBI Service Domain is evaluated here but the IBI Extended Domain instead. ~~*In situ* data allow a detailed assessment to be made in order to understand the strengths and weaknesses of the model, providing the trails for improvement to be explored. They are discussed below.~~

The large-scale distribution of sea surface Chl-a is correctly reproduced, with ~~no surprising~~ higher errors (bias and RMSE) ~~biases~~ on the continental shelf. The seasonal cycle is in line with satellite estimates, particularly south of 50°N in the Atlantic and the Mediterranean. In the Mediterranean, a seasonal DCM develops below the MLD, and is associated with a MOC ~~just above the DCM. This is well caught by the model.~~ In the North-East ~~, while the North~~ Atlantic waters, the spring

phytoplankton bloom spreads more rapidly to the north and surface Chl-a are too low during the stratified season. In fact, phytoplankton migrates to the sub-surface with the formation of a seasonal DCM while maximum Chl-a remains at the surface in BGC-Argo estimates.

~~Primary production~~NPP is a complex field to evaluate, as NPP products give widely different estimates among themselves. Simulated NPP lies between the three NPP products. The averaged spatial distribution is ~~in between the Eppley-VGPM and~~close to CbPM product~~s~~, ~~and~~ but spatial distribution, cross-shore gradients and the seasonal variations are better correlated to the VGPM-based products. The modelled NPP is thus within the range of variability of the satellite derived estimates.

Vertical distribution of

~~Dissolved~~ oxygen and nitrate obtain~~s~~s very good statistics. ~~.~~The model is able to reproduce the amplitude and variability of the observations. However, t~~T~~he EMODnet and BGC-Argo comparison highlight a smoothing of the vertical profiles of oxygen and nitrate in the wider ocean. ~~in the open Atlantic, the Mediterranean but also on the continental shelf. However,~~ ~~s~~Sea surface and coastal comparisons present more uncertainties. Sea surface oxygen is slightly overestimated (around 4%). ~~Surface ocean concentrations tend to balance with atmospheric concentrations, and here atmospheric oxygen concentrations are prescribed by a constant value over time and space. A spatial and temporal atmospheric oxygen forcing would be beneficial instead. As well, the EMODnet and BGC-Argo comparison highlight a smoothing of the vertical oxygen profiles in the wider ocean. T~~t~~hat can originate from the physical or biogeochemical models. Different approaches are currently under study. Vertical diffusion could explain the loss of peaks and minima in vertical profiles. Biogeochemical processes are also investigated. But the regional model inherits the qualities and weaknesses of the forcing global model, and the latter simulates a smoothed vertical distribution, so this default cannot be caught up in the regional model without improvements in the initial and open boundary conditions.~~

~~The distribution of nutrients is also satisfying. In the wider ocean, vertical distribution presents the same default as oxygen one, i.e. the smoothed vertical profiles, already discussed above. In the coastal Northern seas, t~~he seasonal cycle of nutrients is not sufficiently marked in the coastal Northern seas, impacting the ~~. As well,~~ phytoplankton spring bloom ~~is not intense enough~~. ~~-~~ This evaluation shows the major importance of river nutrient discharges for the coastal ecosystems.

~~time evolution or at least a seasonal variation would be necessary to apprehend the phytoplankton dynamics.~~ ~~But continental shelf ecosystem of Northern seas is strongly driven by river discharges. Annually averaged nutrient inputs are injected into the ocean system, while a time evolution or at least a seasonal variation would be necessary to apprehend the phytoplankton dynamics. As well, sedimentary processes are neglected in the IBI36 system as strong tidal currents prevent organic matter from reaching and accumulating in sediments. As an alternative a sediment module should be coupled to the biogeochemical model to improve the representation of sedimentary processes, i.e. remineralization of organic carbon and subsequent release of nutrients.~~

~~Phytoplankton, oxygen and nitrate dynamics are evaluated using the BGC-Argo floats. In the Mediterranean, a seasonal DCM develops below the MLD, and is associated with a MOC just above the DCM. This is well caught by the model. But the model also simulates a seasonal DCM in the Atlantic around 50°N while maximum Chl-a remains at the surface in BGC-Argo estimates.~~ The continental shelf is also vulnerable to oxygen deficiency; such as the Northern seas and the Bay of Biscay. Maximum surface area can reach 280 000 km^2 when considering at least one daily value below the oxygen threshold during the time of the simulation. The vulnerable surface area is almost non-existent in winter because waters are well oxygenated due to strong mixing. It extends to an average surface area of 85 000 km^2 in summer, associated with deoxygenated waters that can reach anoxic conditions.

This extended evaluation has allowed understanding the strengths and weaknesses of the biogeochemical component in the IBI36 system. The pre-operational qualification simulation performs in reproducing the main biogeochemical characteristics

of IBI European waters. PISCES is then a suitable tool at such a resolution and can be used for operational analysis and forecast applications. Future improvements were also explored.

~~This DCM lets us suspect a distinct physical or biogeochemical behaviour at 50°N in the Atlantic between the model and the data. The formation of a DCM indicates that phytoplankton production has to deepen in order to reach the nitracline, and it is usually a typical feature of stratified water columns. Here, the physical model assimilates temperature and salinity profiles from Argo float network, so we can not suspect the model to overestimate the influence of stratified water masses of the subtropical gyre at 50°N. Instead, the biogeochemical distribution may constrain phytoplankton to grow deeper to find enough nutrients. However, the validation of the Atlantic part is limited to only one BGC Argo float measuring oxygen, nitrate and Chl a. Additional floats measuring key the biogeochemical variables would be required to understand the seasonal dynamics of phytoplankton, oxygen and nitrate on the Atlantic side.~~

Finally, ~~the European IBI shelf ecosystem can be exposed to oxygen deficiency. Vulnerable areas are well located in the Northern seas and Bay of Biscay, and seasonal variations are in phase with observations. Maximum surface area can reach 280 000 km^2 when considering at least one daily value below the oxygen threshold during the time of the simulation. T~~However, the vulnerable surface area is almost non existent in winter as ~~because~~ waters are well oxygenated due to strong mixing~~.~~ and ~~It~~ extends to an average surface area of 85 000 km^2 ~~in summer, associated with deoxygenated waters that can reach anoxic conditions in the North Sea and along the west coasts of France. This kind of estimation~~the operational analysis and forecast IBI36 system can be a useful tool to better understand and monitor the health of marine ecosystems ~~This IBI MFC biogeochemical forecast service is likely to give rise to an Ocean Monitoring Indicator (OMI). As an IBI MFC on-going work, it is currently being investigated the design of some IBI biogeochemical OMI, with the aim of publishing it in the context of the CMEMS Ocean State Report publication~~ (von Schuckmann et al., 2016, 2018).

Code availability

The IBI36 configuration is based on the NEMO 3.6 version developed by the NEMO consortium. NEMO modelling system is freely available at http://www.nemo-ocean.eu. The biogeochemical model PISCES v2 is part of the NEMO modelling platform and is available via the NEMO web site. Model initialization and boundary conditions are available via CMEMS (http://www.marine.copernicus.eu).

Data availability

The regional ESA Ocean Colour CCI product for the North Atlantic and Arctic Oceans with a resolution of 1 km is distributed via CMEMS (http://www.marine.copernicus.eu). Primary production products are distributed by the Oregon State University (www.science.oregonstate.edu/ocean.productivity). The International Council for the Exploration of the Sea (ICES) oceanographic database is available at www.ices.dk/marine-data/data-portals. The European Marine Observation and Data Network (EMODnet) is available at www.emodnet-chemistry.eu/products. EMODnet aggregated datasets ~~products~~ are generated by EMODnet Chemistry under the support of DG MARE Call for Tenders MARE/2008/03-lot3, MARE/2012/10-lot4 and EASME/EMFF/2016/006-lot4. Biogeochemical-Argo (BGC-Argo) float data can be downloaded from the Argo Global Data Assembly Centre in France (ftp://ftp.ifremer.fr/ifremer/argo).

Author contributio~~n~~

n

Elodie Gutknecht (Mercator Ocean) contributed to the ~~set up~~set-up of the IBI36 system, performed the evolution of model outputs by comparison to satellite and in-situ datasets, prepared the figures~~,~~ and is the main writer of the manuscript~~,~~. Guillaume Reffray (Mercator Ocean) has designed and developed the physical-biogeochemical coupled system~~,~~ and performed the simulations. Alexandre Mignot (Mercator Ocean) provided corrected BGC-Argo dataset. Tomasz Dabrowski (Marine Institute) is responsible of the evaluation and validation of the reanalysis and analysis/forecast systems in the CMEMS IBI-MFC. Marcos Garcia-Sotillo (Puertos del Estado) has the leadership responsibility of the CMEMS IBI-MFC.

Acknowledgments

The authors acknowledge financial support through CMEMS. CMEMS is implemented by Mercator Ocean International in the framework of a delegation agreement with the European Union. They thank their colleagues of Mercator Ocean for their contribution to the model development and ~~-~~evaluation (Bruno Levier, Mounhir Benkiran)~~ and especially Alexandre Mignot for his useful recommendations and advice on the BGC-Argo data and on the manuscript~~. The authors are grateful to the two anonymous reviewers for their relevant and constructive comments.

References

Aquarone, M. C., Adams, S., and Valdes, L.: XIII-37 Celtic-Biscay Shelf: LME #24. In Sherman, K. & Hempel, G. (eds) The UNEP Large Marine Ecosystem Report: A Perspective on Changing Conditions in LMEs of the World's Regional Seas. UNEP Regional Seas Report and Studies No. 182: 527–534. Nairobi: United Nations Environmental Program, 2008.

Aristegui, J., Alvarez-Salgado, X. A., Barton, E. D., Figueiras, F. G., Hernandez-Leon, S., Roy, C., and Santos., A. M. P.: Oceanography and fisheries of the Canary Current/Iberian Region of theeastern North Atlantic, Chapter 23 in The Sea, The Global Coastal Ocean: InterdisciplinaryRegional Studies and Syntheses, 14, A. R. Robinson and K. H. Brink, eds., Harvard UniversityPress, Cambridge, MA, 2004.

Aumont, O., Ethé, C., Tagliabue, A., Bopp , L., and Gehlen, M.: PISCES-v2: an ocean biogeochemical model for carbon and ecosystem studies. Geosci. Model Dev., 8, 2465–2513, http://www.geosci-model-dev.net/8/2465/2015/gmd-8-2465-2015.pdf,- 2015.

Barton, A. D., Lozier, M. S. and Williams, R. G.: Physical controls of variability in North Atlantic phytoplankton communities. Limnol. Oceanogr., 60: 181-197. doi:10.1002/lno.10011, 2015.

Behrenfeld, M.: Abandonding Sverdrup's crtical depth hypothesis on phytoplankton blooms. Ecology 91: 977–989. doi:10.1890/09-1207.1, 2010.

Behrenfeld, M. J., and Falkowski, P. G.: Photosynthetic rates derived from satellite-based chlorophyll concentration, Limnol. Oceanogr., 42(1), 1-20, 1997.

Belkin, I. M., Cornillon, P. C., and Sherman, K.: Fronts in Large Marine Ecosystems. Progress in Oceanography 81 (1-4), 223–236. doi:10.1016/j.pocean.2009.04.015, 2009.

Biogeochemical-Argo Planning Group: The scientific rationale, design and implementation plan for a Biogeochemical-Argo float array, https://doi.org/10.13155/46601, 2016.

Blackford, J. C., Allen, J. I., and Gilbert, F. J.: Ecosystem dynamics at six contrasting sites: a generic modelling study. J. Mar. Syst. 52, 191–215. doi: 10.1016/j.jmarsys.2004.02.004, 2004.

Bopp, L., Aumont, O., Cadule, P., Alvain, S., and Gehlen, M.: Response of diatoms distribution to global warming andpotential implications: A global model study. Geophys. Res. Lett.. 32, L19606, doi:10.1029/2005GL023653, 2005.

~~Bowyer, P., Dabrowski, T., Gutknecht, E., Lorente, P., Reffray, G., and Sotillo, M. G.: Quality Information Document (CMEMS-IBI-QUID-005-004), http://marine.copernicus.eu/documents/QUID/CMEMS-IBI-QUID-005-004.pdf, 2017.~~

~~Bowyer, P., Dabrowski, T., Gutknecht, E., Lorente, P., Reffray, G., Sotillo, M.G.: Quality Information Document (CMEMS-IBI-QUID-005-003), http://marine.copernicus.eu/documents/QUID/CMEMS-IBI-QUID-005-003.pdf, 2018.~~

Breitburg, D., Levin, L. A., Oschlies, A., Grégoire, M., Chavez, F. P., Conley, D. J., Garçon, V., Gilbert, D., Gutiérrez, D., Isensee, K., Jacinto, G. S., Limburg, K. E., Montes, I., Naqvi, S. W. A., Pitcher, G. C., Rabalais, N. N., Roman, M. R., Rose, K. A., Seibel, B. A., Telszewski, M., Yasuhara, M., and Zhang, J.: Declining oxygen in the global ocean and coastal waters, Science, 359 (6371), eaam7240, doi: 10.1126/science.aam7240, 2018.

Butenschön, M., Clark, J. R., Aldridge, J. N., Allen, J. I., Artioli, Y., Blackford, J. C., et al.: ERSEM 15.06: a generic model for marine biogeochemistry and the ecosystem dynamics of the lower trophic levels. Geosci. Model Dev. 9, 1293–1339. doi: 10.5194/gmd-9-1293-2016, 2016.

Campbell, J. W., Antoine, D., Armstrong, R., Arrigo, K., Balch, W., Barber, R., Behrenfeld, M., Bidigare, R., Bishop, J., Carr, M.-E., Esaias, W., Falkowski, P., Hoepffner, N., Iverson, R., Kiefer, D., Lohrenz, S., Marra, J., Morel, A., Ryan, J., Vedernikov, V., Waters, K., Yentsch, C., and Yoder, J.: Comparison of algorithms for estimating ocean primary production from surface chlorophyll, temperature, and irradiance, Global Biogeochem. Cycles, 16(3), doi: 10.1029/2001GB001444, 2002.

Carval, T., Keeley, R., Takatsuki, Y., Yoshida, T., Schmid, C., Goldsmith, R., Wong, A., McCreadie, R., Thresher, A., Tran, A.: Argo user's manual V3.2. https://doi.org/10.13155/29825, 2017.

Christensen, J. P., Packard, T. T., Dortch, F. Q., Minas, H. J., Gascard, J. C., Richez, C., and Garfield, P. C.: Carbon oxidation in the deep Mediterranean Sea: Evidence for dissolved organic carbon source, Global Biogeochem. Cycles, 3(4), 315–335, doi:10.1029/GB003i004p00315, 1989.

Ciavatta, S., Kay, S. Saux-Picart, S. Butenschön, M. and Allen J. I.: Decadal reanalysis of biogeochemical indicators and fluxes in the North West European shelf- sea ecosystem, J. Geophys. Res. Oceans, 121, 1824–1845, doi:10.1002/2015JC011496, 2016.

De Haas, H., Van Weering, T. C. E., and De Stigter, H.: Organic carbon in shelf seas: sinks or sources, processes and products, Continental Shelf Research, 22, 691–717, 2002.

Doray, M., Huret, M., Authier, M., Duhamel, E., Romagnan, J.-B., Dupuy, C., Spitz, J., Sanchez, F., Berger, L., Dorémus, G., Bourriau, P., Grellier, P., Pennors, L., Masse, J., Petitgas, P.: Gridded maps of pelagic ecosystem parameters collected in the Bay of Biscay during the PELGAS integrated survey. SEANOE. https://doi.org/10.17882/53389, 2018a.

Doray, M., Petitgas, P., Romagnan, J.-B., Huret, M., Duhamel, E., Dupuy, C., Spitz, J., Authier, M., Sanchez, F., Berger, L., Doremus, G., Bourriau, P., Grellier, P., Masse, J. : The PELGAS survey: ship-based integrated monitoring of the Bay of Biscay pelagic ecosystem. Progress In Oceanography, 166, 15-29, doi: 10.1016/j.pocean.2017.09.015, 2018b.

Edwards, K. P., Barciela, R., and Butenschön, M.: Validation of the NEMO-ERSEM operational ecosystem model for the North West European Continental Shelf, Ocean Sci., 8, 983-1000, https://doi.org/10.5194/os-8-983-2012, 2012.

Emerson, S.: Annual net community production and the biological carbon flux in the ocean, Global Biogeochem. Cy., 28, 14–28, doi:10.1002/2013GB004680, 2014.

Estrada M.: Deep Phytoplankton and Chlorophyll Maxima in the Western Mediterranean. In: Moraitou-Apostolopoulou M., Kiortsis V. (eds) Mediterranean Marine Ecosystems. NATO Conference Series (I Ecology), vol 8. Springer, Boston, MA, 1985.

Estrada, M., Marrasé, C., Latasa, M., Berdalet, E., Delgado, M., and Riera, T. : Variability of deep chlorophyll maximum characteristics in the Northwestern Mediterranean. Marine Ecology-progress Series - MAR ECOL-PROGR SER. 92. 289-300. 10.3354/meps092289, 1993.

Fernández, E., and Bode, A.: Seasonal patterns of primary production in the Central Cantabrian Sea (Bay of Biscay). Sci. Mar., 55 (4), 629–636, 1991.

Garcia-Ibanez, M. I., Pardo, P. C., Carracedo, L., Mercier, H., Lherminier, P., Rios, A. F., and Perez F. F.: Structure, transports and transformations of the water masses in the Atlantic Subpolar Gyre. Progress In Oceanography, 135, 18-36., doi: 10.1016/j.pocean.2015.03.009, 2015.

Gehlen, M., Bopp, L., Emprin, N., Aumont, O., Heinze, C., and Ragueneau, O.: Reconciling surface ocean productivity,export fluxes and sediment composition in a global biogeochemical ocean model. Biogeosciences. 1726-4189/bg/2006-3-521,521-537, 2006.

Gehlen, M., Gangstø, R., Schneider, B., Bopp, L., Aumont, O., and Ethé, C.: The fate of pelagic CaCO3 production in a highCO2 ocean: A model study. Biogeosciences., 4: 505-519, 2007.

M. Gehlen, M., Barciela, R., Bertino, L., Brasseur, P., Butenschön, M., Chai, F., Crise, A., Drillet, Y., Ford, D., Lavoie, D., Lehodey, P., Perruche, C., Samuelsen, A., and Simon, E. : Building the capacity for forecasting marine biogeochemistry and ecosystems: recent advances and future developments, Journal of Operational Oceanography, 8:sup1, s168-s187, DOI: 10.1080/1755876X.2015.1022350, 2015.

Gohin, F., Lampert, L., Guillaud, J.-F., Herbland, A., and Nézan, E.: Satellite and in situ observations of a late winter phytoplankton bloom, in the northern Bay of Biscay. Continental Shelf Research. 23. 1117-1141. 10.1016/S0278-4343(03)00088-8, 2003.

Gohin, F., Saulquin, B., Oger-Jeanneret, H., Lozac'h, L., Lampert, L., Lefebvre, A., Riou, P., and Bruchon, F.: Towards a better assessment of the ecological status of coastal waters using satellite-derived chlorophyll-a concentrations, Remote Sensing of Environment, 112, 3329-3340, 10.1016/j.rse.2008.02.014, 2008.

Gutknecht, E., Reffray, G., Gehlen, M., Triyulianti, I., Berlianty, D., and Gaspar, P.: Evaluation of an operational ocean model configuration at 1/12° spatial resolution for the Indonesian seas (NEMO2.3/INDO12) – Part 2: Biogeochemistry, Geosci. Model Dev., 9, 1523-1543, doi:10.5194/gmdd-9-1523-2016, 2016.

Hellenic Centre for Marine Research, Hellenic National Oceanographic Data Centre (HCMR/HNODC): Mediterranean Sea - Eutrophication and Ocean Acidification aggregated datasets 1911/2017 v2018. Aggregated datasets were generated in the framework of EMODnet Chemistry III, under the support of DG MARE Call for Tender EASME/EMFF/2016/006 - lot4, https://doi.org/10.6092/89576629-66d0-4b76-8382-5ee6c7820c7f, 2018.

Henson, S. A., Sarmiento, J. L., Dunne, J. P., Bopp, L., Lima, I., Doney, S. C., John, J., and Beaulieu, C.: Detection of anthropogenic climate change in satellite records of ocean chlorophyll and productivity, Biogeosciences, 7, 621–640, doi:10.5194/bg-7-621-2010, 2010.

Hernandez, F., Bertino, L., Brassington, G. B., Chassignet, E. P., Cummings, J. A., Davidson, F., Drévillon, M., Garric, G., Kamachi, M., Lellouche, J.-M., Mahdon, R., Martin, M. J, Ratsimandresy, A., and Regnier, C.: Validation and intercomparison studies within GODAE. Oceanogr Magazine. 22 (3):128–143. doi:http://dx.doi.org/10.5670/oceanog.2009.71, 2009.

Hernandez, F., Blockley, E., Brassington, G. B, Davidson, F., Divakaran, P., Drévillon, M., Ishizaki, S., Garcia-Sotillo, M., and other 17 co-authors: Recent progress in performance evaluations and near real-time assessment of operational ocean products, J. Oper. Oceanogr., 8, 221-238, https://doi.org/10.1080/1755876X.2015.1050282, 2015.

Hu, C., Lee, Z., and Franz, B. A.: Chlorophyll-a algorithms for oligotrophic oceans: A novel approach based on three-band reflectance difference, J. Geophys. Res., 117, C01011, doi:10.1029/2011JC007395, 2012.

IFREMER / IDM / SISMER - Scientific Information Systems for the SEA: North East Atlantic Ocean - Eutrophication and Ocean Acidification aggregated datasets 1921/2017 v2018. Aggregated datasets were generated in the framework of EMODnet Chemistry III, under the support of DG MARE Call for Tender EASME/EMFF/2016/006 - lot4, https://doi.org/10.6092/459D8254-6C7B-4A0E-9FDB-04EFFE5F5A77, 2018.

Johnson, K., Pasqueron De Fommervault, O., Serra, R., D'Ortenzio, F., Schmechtig, C., Claustre, H., and Poteau, A.: *Processing Bio-Argo nitrate concentration at the DAC Level* (p.). https://doi.org/10.13155/46121, 2016.

Johnson, K. S., Plant, J. N., Coletti, L. J., Jannasch, H. W., Sakamoto, C. M., Riser, S. C., Swift, D. D., Williams, N. L., Boss, E., Haëntjens, N., Talley, L. D., and Sarmiento J. L.: Biogeochemical sensor performance in the SOCCOM profiling float array: SOCCOM BIOGEOCHEMICAL SENSOR PERFORMANCE. *Journal of Geophysical Research: Oceans*, *122*(8), 6416–6436. https://doi.org/10.1002/2017JC012838, 2017.

Lam, F. P. A., Gerkema, T., and Maas, L. R. M.: Preliminary results from observations of internal tides and solitary waves in the Bay of Biscay. http://www.whoi.edu/science/AOPE/people/tduda/isww/text/lam/, 2003.

Lavigne, H., D'Ortenzio, F., Ribera D'Alcalà, M., Claustre, H., Sauzède, R., and Gacic, M.: On the vertical distribution of the chlorophyll a concentration in the Mediterranean Sea: a basin-scale and seasonal approach, Biogeosciences, 12, 5021–5039, https://doi.org/10.5194/bg- 12-5021-2015, 2015.

Lavín, A., Valdés, L., Sánchez, F., Abaunza, P., Forest, A., Boucher, J., Lazure, P., and Jegou, A.-M. : The Bay of Biscay: the encountering of the ocean and the shelf. In: The Sea. Volume 14. Part B. The Global Coastal Ocean: Interdisciplinary

Regional Studies and Synthesis, Edition: First, Chapter: 24, Publisher: Harvard University Press, Editors: A. Robinson, K. Brink, pp.933-999, 2006.

Lazzari, P., Solidoro, C., Salon, S., and Bolzon, G. : Spatial variability of phosphate and nitrate in the Mediterranean Sea: A modeling approach, Deep Sea Research Part I: Oceanographic Research Papers, 108, 39-52, doi: 10.1016/j.dsr.2015.12.006, 2016.

Lellouche, J.-M., Le Galloudec, O., Regnier, C., Levier, B., Greiner, E., and Drevillon, M. : Quality Information Document (CMEMS-GLO-QUID-001-024), http://marine.copernicus.eu/documents/QUID/CMEMS-GLO-QUID-001-024.pdf, 2016.

Lellouche, J.-M., Greiner, E., Le Galloudec, O., Garric, G., Regnier, C., Drevillon, M., Benkiran, M., Testut, C.-E., Bourdalle-Badie, R., Gasparin, F., Hernandez, O., Levier, B., Drillet, Y., Remy, E., and Le Traon, P.-Y.: Recent updates to the Copernicus Marine Service global ocean monitoring and forecasting real-time 1⁄12° high-resolution system, Ocean Sci., 14, 1093-1126, https://doi.org/10.5194/os-14-1093-2018, 2018.

Leonard, B. P.: A stable and accurate convective modelling procedure based on quadratic upstream interpolation, Comput. Method. Appl. M., 19, 59–98, 1979.

~~Longhurst, A.: Ecological geography in the sea. Academic Press, 1998.~~

Madec, G.: "NEMO ocean engine", Note du Pole de modélisation, Institut Pierre-Simon Laplace (IPSL), France, No 27 ISSN No 1288-1619, 2008.

Ludwig, W., Probst, J. L., and Kempe, S.: Predicting the oceanic input of organic carbon by continental erosion, Global Biogeochem. Cy., 10, 23–41, doi:10.1029/95GB02925, 1996.

Madec, G., Delecluse, P., Imbard, M., and Lévy, C.: "OPA 8.1 Ocean General Circulation Model reference manual", Note du Pole de modélisation, Institut Pierre-Simon Laplace (IPSL), France, No11, 91pp., 1998.

Madec, G.: NEMO ocean engine. Note du Pôle de modélisation, Institut Pierre-Simon Laplace (IPSL), France. Available at: https://www.nemo-ocean.eu/wp-content/uploads/NEMO_book.pdf, 2008.

Maraldi, C., Chanut, J., Levier, B., Ayoub, N., De Mey, P., Reffray, G., Lyard, F., Cailleau, S., Drévillon, M., Fanjul, E. A., Sotillo, M. G., Marsaleix, P., and the Mercator Research and Development Team: NEMO on the shelf: assessment of the Iberia–Biscay–Ireland configuration, Ocean Sci., 9, 745-771, https://doi.org/10.5194/os-9-745-2013, 2013.

Mayorga, E., Seitzinger, S. P., Harrison, J. A., Dumont, E., Beusen, A. H. W., Bowman, A. F., Fekete, B. M., Kroeze, C., and Van Drecht, G.: Global Nutrient Export from WaterSheds 2 (NEWS 2): model development and implementation, J. Environ. Modell. Softw., 25, 837–853, 2010.

Mignot, A., Claustre, H., Uitz, J., Poteau, A., D'Ortenzio, F., and Xing, X.: Understanding the seasonal dynamics of phytoplankton biomass and the deep chlorophyll maximum in oligotrophic environments: A Bio-Argo float investigation, Global Biogeochemical Cycles, 28, 856–876, https://doi.org/10.1002/2013GB004781, 2014.

Mignot, A., D'Ortenzio, F., Taillandier, V., Cossarini, G., and Salon S.: Quantifying observational errors in Biogeochemical-argo oxygen, nitrate and chlorophyll a concentrations, Submitted to, Geophys. Res. Lett., 2018.

Moore, T. S., Campbell, J. W., and Dowell, M. D: A class-based approach to characterizing and mapping the uncertainty of the MODIS ocean chlorophyll product, Remote Sensing of Environment, 113, 2424-2430, 2009.

Nykjær, L., Van Camp, L.: Seasonal and interannual variability of coastal upwelling along northwest Africa and Portugal from 1981 to 1991. Journal of Geophysical Research, 99(C7):14197, 1994.

O'Dea, E., Furner, R., Wakelin, S., Siddorn, J., While, J., Sykes, P., King, R., Holt, J., and Hewitt, H.: The CO5 configuration of the 7 km Atlantic Margin Model: large-scale biases and sensitivity to forcing, physics options and vertical resolution, Geosci. Model Dev., 10, 2947-2969, https://doi.org/10.5194/gmd-10-2947-2017, 2017.

OSPAR: Quality Status Report 2000: Region IV - Bay of Biscay and Iberian Coast. OSPAR Commission. London. 134 + xiii pp, 2000.

OSPAR: OSPAR integrated report 2003 on the eutrophication status of the OSPAR maritime area based upon the first application of the Comprehensive Procedure. OSPAR Eutrophication Series, publication 189/2003. OSPAR Commission, London, 2003.

OSPAR: Common procedure for the identification of the eutrophication status of the OSPAR maritime area, Tech. Rep. 2013-8., London, U. K. [Available at www.ospar.org/documents?d532957], 2013.

Pelegrí, J. L., and Benazzouz, A.: Coastal upwelling off North-West Africa. In: Oceanographic and biological features in the Canary Current Large Marine Ecosystem. Valdés, L. and Déniz-González, I. (eds). IOC-UNESCO, Paris. IOC Technical Series, No. 115, pp. 93-103. URI: http://hdl.handle.net/1834/9180, 2015.

Perruche, C., Hameau, A., Paul, J., Régnier, C., and Drévillon M.: Quality Information Document (CMEMS-GLO-QUID-001-014), http://marine.copernicus.eu/documents/QUID/CMEMS-GLO-QUID-001-014.pdf, 2016.

Perruche, C., Szczypta, C., Paul, J., and Drévillon, M.: Quality Information Document (CMEMS-GLO-QUID-001-029), http://marine.copernicus.eu/documents/QUID/CMEMS-GLO-QUID-001-029.pdf, 2018.

Piraud, I., Marseleix, P., and Auclair, F.: Tidal and thermohaline circulation in the Bay of Biscay. Geophys. Res. Abstracts, 5, 07058, 2003.

Ribera d'Alcalà, M., Civitarese, G., Conversano, F., and Lavezza, R.: Nutrient ratios and fluxes hint at overlooked processes in the Mediterranean Sea, J. Geophys. Res., 108 (C9), 8106, doi:10.1029/2002JC001650, 2003.

Roether, W., and Well, R.: Oxygen consumption in the Eastern Mediterranean, Deep Sea Res., Part I, 48(6), 1535–1551, 2001.

Rossby, T.: The North Atlantic Current and surrounding waters: At the crossroads. Rev. Geophys., 34, 463–481, doi:https://doi.org/10.1029/96RG02214, 1996.

Saba, V. S., Friedrichs, M. A. M., Antoine, D., Armstrong, R. A., Asanuma, I., Behrenfeld, M. J., Ciotti, A. M., Dowell, M., Hoepffner, N., Hyde, K. J. W., Ishizaka, J., Kameda, T., Marra, J., Mélin, F., Morel, A., O'Reilly, J., Scardi, M., Smith Jr., W. O., Smyth, T. J., Tang, S., Uitz, J., Waters, K., and Westberry, T. K.: An evaluation of ocean color model estimates of marine primary productivity in coastal and pelagic regions across the globe, Biogeosciences, 8, 489-503, https://doi.org/10.5194/bg-8-489-2011, 2011.

Salon, S., Cossarini, G., Bolzon, G., Feudale, L., Lazzari, P., Teruzzi, A., Solidoro, C., and Crise, A.: Marine Ecosystem forecasts: skill performance of the CMEMS Mediterranean Sea model system, Ocean Sci. Discuss., https://doi.org/10.5194/os-2018-145, in review, 2019.

Sathyendranath, S., Brewin, R. J. W., Müeller, D., Brockmann, C., Deschamps, P.-Y., Doerffer, R., Fomferra, N., Franz, B. A., Grant, M. G., Hu C., Krasemann, H., Lee, Z., Maritorena, S., Devred, E., Mélin, F., Peters, M., Smyth, T., Steinmetz, F., Swinton, J., Werdell, J., and Regner, P.: Ocean Colour Climate Change Initiative: Approach and Initial Results, IGARSS 2012, 2024-2027. http://dx.doi.org/10.1109/IGARSS.2012.6350979, 2012.

Schmechtig, C., Poteau, A., Claustre, H., D'Ortenzio, F., and Boss, E.: Processing bio-Argo chlorophyll-A concentration at the DAC level. Ifremer. https://doi.org/10.13155/39468, 2015.

Schneider, B., Bopp, L., Gehlen, M., Segschneider, J., Frölicher, T. L., Cadule, P., Friedlingstein, P., Doney, S. C., Behrenfeld, M. J., and Joos, F.: Climate-induced interannual variability of marine primary and export production in three global coupled climatecarbon cycle models. Biogeosciences. 5: 597-614, 2008.

Schourup-Kristensen, V., Sidorenko, D., Wolf-Gladrow, D. A., and Völker, C.: A skill assessment of the biogeochemical model REcoM2 coupled to the Finite Element Sea-Ice Ocean Model (FESOM 1.3). Geosci. Model Dev. 7: 2769–2802., 2012.

Séférian, R., Bopp, L., Gehlen, M., Orr, J. C., Ethé, C., Cadule, P., Aumont, O., Mélia, D. S. Y., Voldoire, A., and Madec, G.: Skill assessment of three earth system models with common marine biogeochemistry, Clim. Dynam., 40, 2549–2573, doi:10.1007/s00382-012-1362-8, 2013.

Sotillo, M. G., Cailleau, S., Lorente, P., Levier, B., Aznar, R., Reffray, G., Amo-Baladrón, A., Chanut, J., Benkiran, M., and Alvarez-Fanjul, E.: The MyOcean IBI Ocean Forecast and Reanalysis Systems: operational products and roadmap to the future Copernicus Service, Journal of Operational Oceanography, DOI: 10.1080/1755876X.2015.1014663, 2015.

Sotillo, M. G., Levier, B., and Lorente, P.: Quality Information Document (CMEMS-IBI-QUID-005-001), http://marine.copernicus.eu/documents/QUID/CMEMS-IBI-QUID-005-001.pdf, 2018.

Steinacher, M., Joos, F., Frölicher, T. L., Bopp, L., Cadule, P., Cocco, V., Doney, S. C., Gehlen, M., Lindsay, K., Moore, J. K., Schneider, B., and Segschneider, J.: Projected 21st century decrease in marine productivity: a multi-model analysis.Biogeoscience. 7: 979-1005, 2010.

Sverdrup, H.: On conditions of the vernal blooming of phytoplankton. ICES J. Mar. Sci. 18: 287–295. doi:10.1093/icesjms/18.3.287, 1953.

Tagliabue, A., Bopp, L., Dutay, J.-C., Bowie, A. R., Chever, F., Jean-Baptiste, P., Bucciarelli, E., Lannuzel, D., Remenyi, T., Sarthou, G., Aumont, O., Gehlen, M. and Jeandel, C.: On the importance of hydrothermalism to the oceanic dissolved ironinventory. Nature Geoscience. 3: 252 – 256, doi:10.1038/ngeo818, 2010.

~~Takahashi, T., Broecker, W. S., and Langer, S.: Redfield ratio based on chemical data from isopycnal surfaces, J. Geophys. Res., 90, 6907–6924, 1985.~~

Taylor, J. R., and Ferrari. R.: Shutdown of turbulent convection as a new criterion for the onset of spring phytoplankton blooms. Limnol. Oceanogr. 56: 2293–2307. doi:10.4319/lo.2011.56.6.2293, 2011.

Teruzzi, A., Bolzon, G., Salon, S., Lazzari, P., Solidoro, C., and Cossarini, G.: Assimilation of coastal and open sea biogeochemical data to improve phytoplankton simulation in the Mediterranean Sea. Ocean Modell. 132, 46–60. doi: 10.1016/j.ocemod.2018.09.007, 2018.

Thierry, V., Bittig, H., Gilbert, D., Kobayashi, T., Kanako, S., and Schmid, C.: *Processing Argo oxygen data at the DAC level cookbook* (p.). https://doi.org/10.13155/39795, 2016.

Tonani, M., Teruzzi, A., Korres, G., Pinardi, N., Crise, A., Adani, M., et al. : The Mediterranean monitoring and forecasting centre, a component of the MyOcean system, in Proceedings of the Sixth International Conference on EuroGOOS 4-6 October 2011, eds H. Dahlin, N. C. Fleming, and S. E. Petersson (Sopot: Eurogoos Publication), 2014.

~~Torres, R., and Barton, E. D.: Onset of the Iberian upwelling along the Galician coast. Continental Shelf Research, 27(13):1759–1778, 2007.~~

Valdés, L., Alvarez-Ossorio, M. T., Lavín, A., Varela, M., and Carballo, R.: Ciclo anual de parámetros hidrográficos, nutrientes y plancton en la plataforma continental de La Coruña (NO, España). Bol. Inst. Esp. Oceanog., 7 (1), 91–138, 1991.

Valdés, L., and Lavin, A.: Dynamics and human impact in the Bay of Biscay: An ecological perspective p 293-320 in: Sherman, K. and Skjoldal, H.R. (eds), Large Marine Ecosystems of the North Atlantic – Changing States and Sustainability. Elsevier Science, Amsterdam, The Netherlands, 2002.

Vichi, M., Cossarini, G., Gutierrez Mlot, E., Lazzari, P., Lovato, T., Mattia, G., Masina, S.,McKiver, W., Pinardi, N., Solidoro, C., Zavatarelli, M.: The BiogeochemicalFlux Model (BFM): Equation Description and User Manual. BFM version 5 (BFM-V5). Release 1.0, BFM Report series N, 1. March 2013. CMCC, Bologna, Italy,http://bfm-community.eu,p.87, 2013.

von Schuckmann, K., Le Traon, P.-Y., et al: The Copernicus Marine Environment Monitoring Service Ocean State Report, Journal of Operational Oceanography, 9:sup2, s235-s320, DOI: 10.1080/1755876X.2016.1273446, 2016.

von Schuckmann, K., Le Traon, P.-Y., et al.: Copernicus Marine Service Ocean State Report, Journal of Operational Oceanography, 11:sup1, S1-S142, DOI: 10.1080/1755876X.2018.1489208, 2018.

Westberry, T., Behrenfeld, M. J., Siegel, D. A., and Boss, E.: Carbon-based primary productivity modeling with vertically resolved photoacclimation, Global Biogeochem. Cycles, 22(2), GB2024, doi:10.1029/2007GB003078, 2008.

Williams, R. G., McClaren, A. J., and Follows., M. J.: Estimating the convective supply of nitrate and implied variability in export production over the North Atlantic. Global Biogeochem. Cycles 14: 1299–1313. doi:10.1029/2000GB001260, 2000.

Wong, A., Keeley, R., Carval, T., & Argo Data Management Team: Argo Quality Control Manual for CTD and Trajectory Data. https://doi.org/10.13155/33951, 2015.

Wooster, W. S., Bakun, A., Mclain, D. R.: Seasonal Upwelling Cycle Along the Eastern Boundary of the North-Atlantic. Journal of Marine Research, 34(2):131–141, 1976.

Zalezak, S. T.: Fully multidimensional flux-corrected transport algorithms for fluids, J. Computat. Phys., 31, 335–362, 1979.

Figure 11: The logo of Copernicus Publications.

1200

Table 1: Synthesis table for Chl-a (mg Chl m^{-3}) and NPP (mg C m^{-2} d^{-1}) assessment against satellite derived estimations. Mean and standard deviation, Mean Error $= \langle (model - obs) \rangle$, RMSE $= \sqrt{\langle (model - obs)^2 \rangle}$, Percent Bias (%) $= |Mean\ Error / Mean\ Obs|$ and correlation are computed for the IBI Extended Domain, using model and observations averaged over the length of the simulation (2010-2016).

Variable	**Dataset**	**Mean ± std**	**Mean Error**	**RMSE**	**Percent Bias (%)**	**Correlation**
Chl-a	IBI36	0.615 ± 0.69				
	ESA OC-CCI	0.555 ± 0.63	0.06	0.42	10.8	0.81
NPP	IBI36	441.7 ± 203.5				
	VGPM	871.5 ± 577.2	-429.8	636.7	49.3	0.65
	Eppley	557.5 ± 358.3	-115.8	295.3	20.8	0.66
	CbPM	518.1 ± 660.96	-76.4	602.78	14.7	0.45

1215

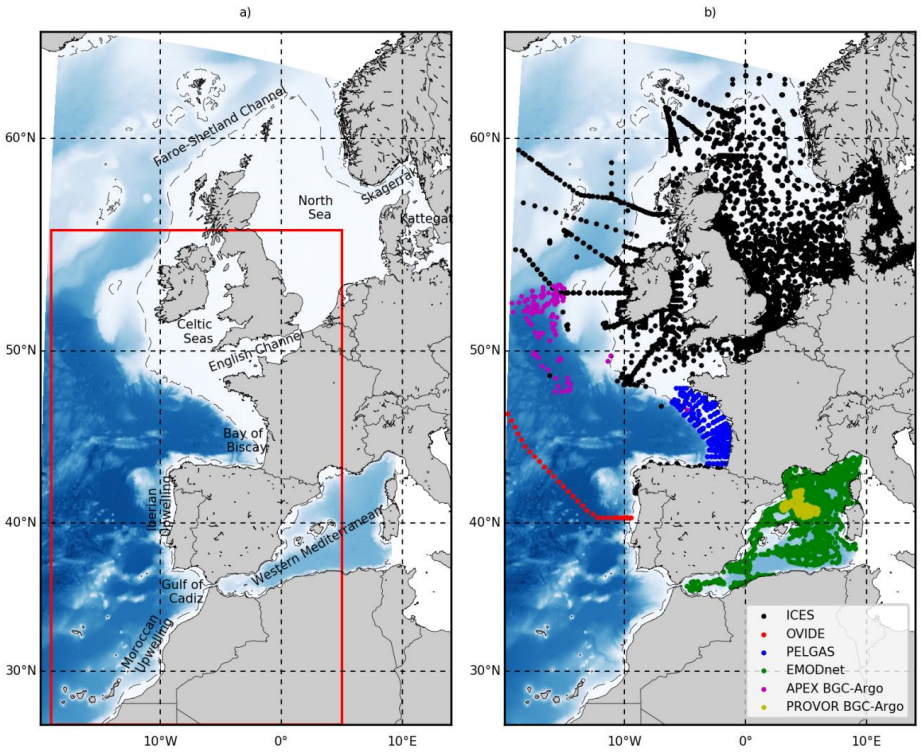
a)
b)
60°N
50°N
40°N
30°N
10°W
0°
10°E
Faroe-Shetland Channel
North Sea
Skagerrak
Kattegat
Celtic Seas
English Channel
Bay of Biscay
Iberian Upwelling
Western Mediterranean
Gulf of Cadiz
Moroccan Upwelling
ICES
OVIDE
PELGAS
EMODnet
APEX BGC-Argo
PROVOR BGC-Argo

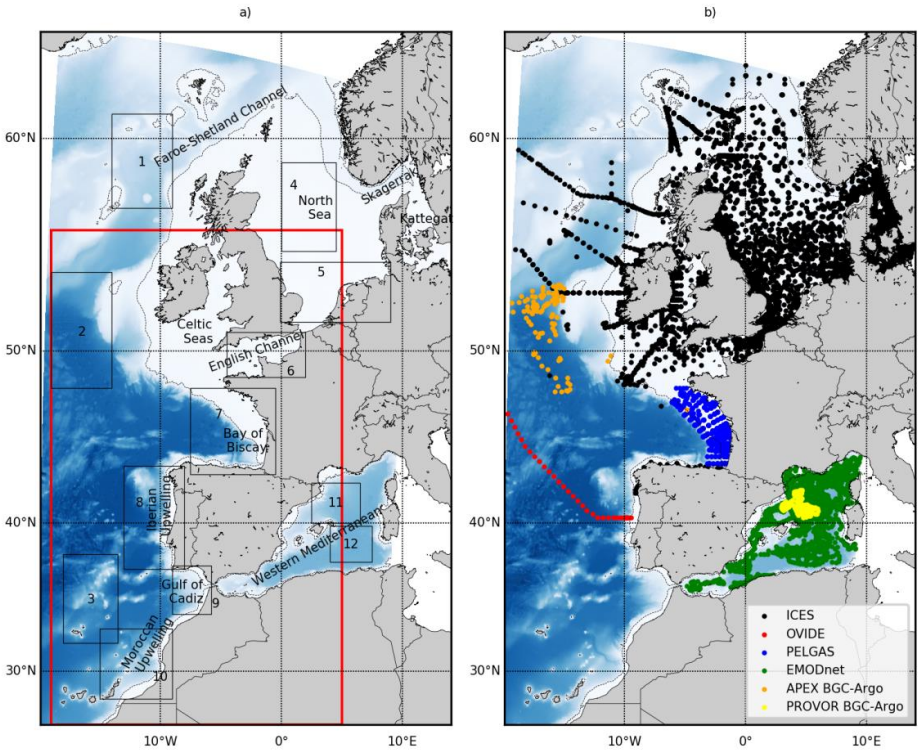

Figure 1. a) IBI Extended Domain on a curvilinear grid and IBI Service Domain extend~~s~~ing from -19°E to 5°E and 26°N to 56°N on a regular grid (red rectangle). The 12 back boxes represent the different areas described in Section 2 and used for evaluation in Section 4. They represent the North Atlantic (boxes 1, 2, 3), North Sea (boxes 4 and 5), English Channel (box 6), Bay of Biscay (box 7), Iberian upwelling (box 8), Gulf of Cadiz (box 9), Moroccan upwelling (box 10) and Western Mediterranean (boxes 11 and 12. b) Location of in-situ biogeochemical data used for validation. ICES data are in black, OVIDE section ~~is in red,~~and ~~-~~PELGAS data of the North-East Atlantic EMODnet dataset are respectively in red and blue, ~~are in blue, -~~the Mediterranean Sea EMODnet ~~product~~ dataset ~~of the EMODnet~~ is in green, the APEX BGC-Argo float in the Atlantic is in ~~Magenta~~orange, and PROVOR BGC-Argo float in the Mediterranean is in yellow. The font represents the bathymetry and dashed line is the 200 m isobath delimiting the shelf region.

1230

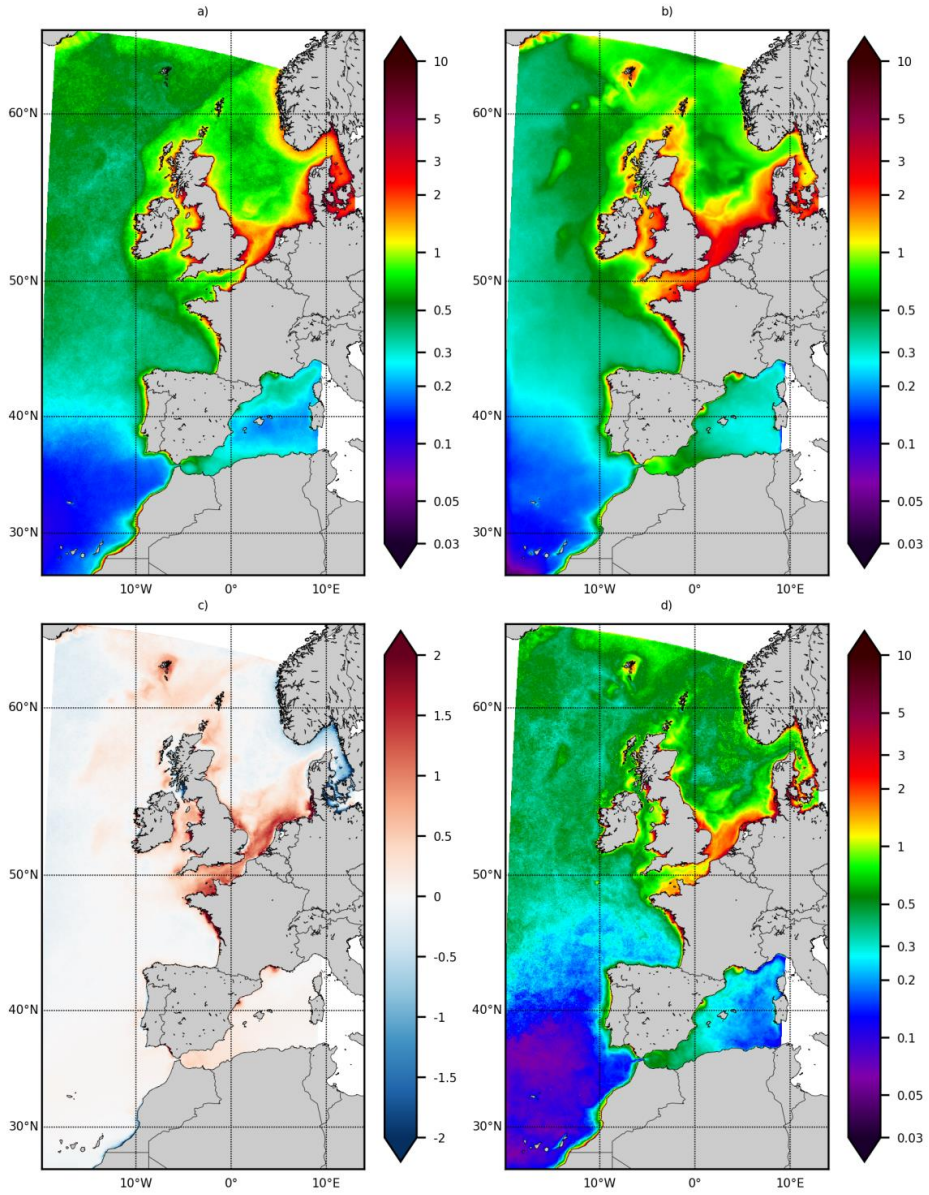
a)
b)
c)
d)
60°N
50°N
40°N
30°N
10°W
0°
10°E
10
5
3
2
1
0.5
0.3
0.2
0.1
0.05
0.03
2
1.5
1
0.5
0
-0.5
-1
-1.5
-2

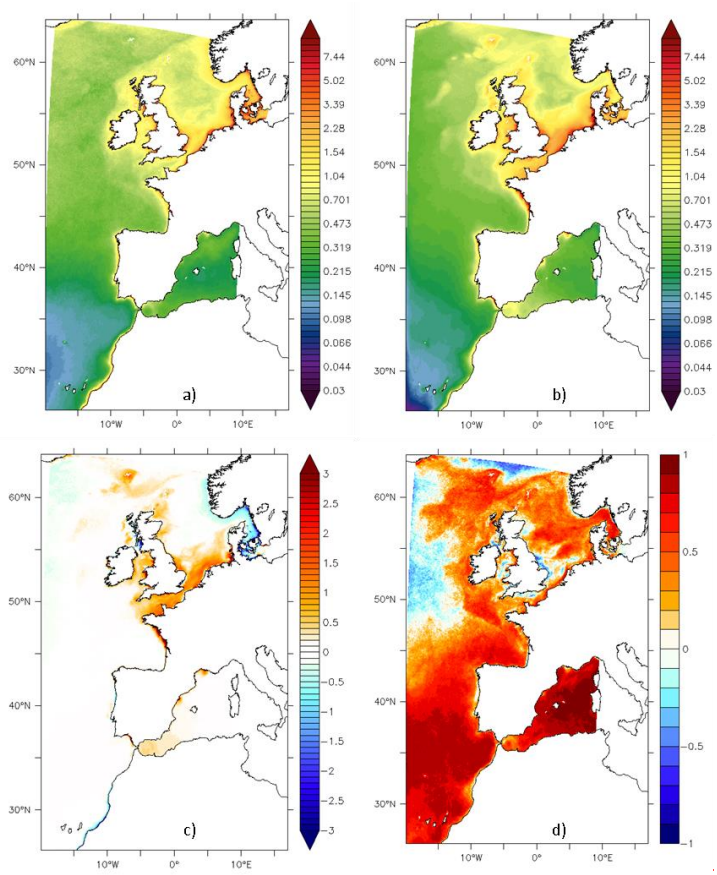

Figure 2. Sea surface Chl-a. ~~-~~a) annual average of ESA OC-CCI ocean colour product, ~~-~~b) annual average of IBI36, ~~and~~ c) averaged bias of Chl-a ~~(model – observation)~~ $(model - obs)$ and and d) RMSE ($\sqrt{\langle (model - obs)^2 \rangle}$), all expressed ~~$\sqrt{\langle \; \rangle}$, all expressed~~ in mg Chl m^{-3}. ~~- d) Temporal correlation between the model and the observation.~~ Statistics are computed from monthly fields between 2010 and 2016. ~~and the model is masked as a function of the data.~~

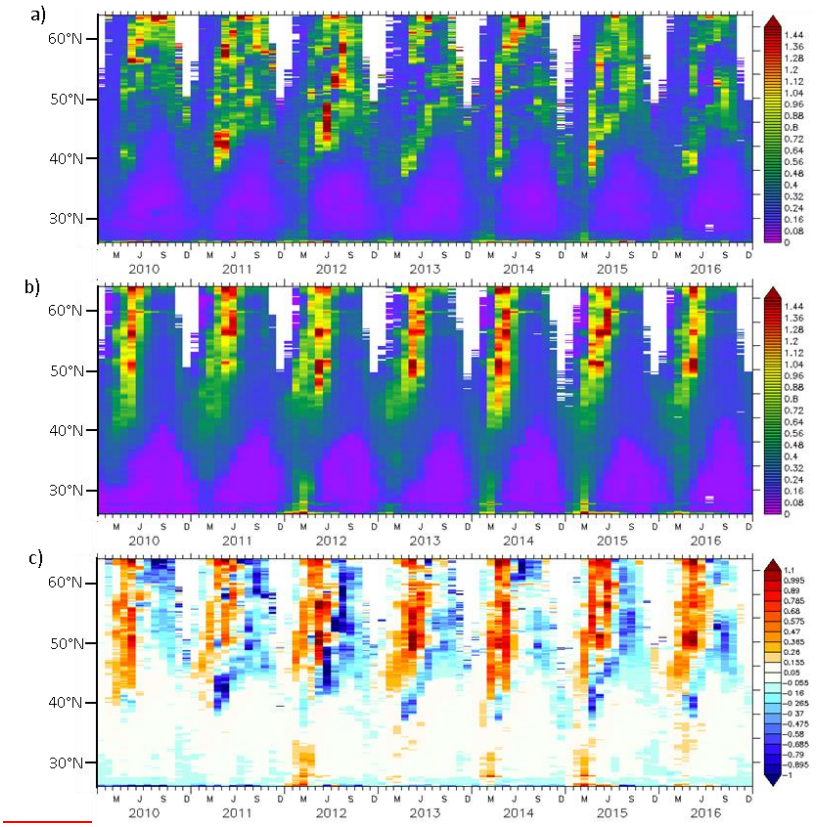
a)
60°N
50°N
40°N
30°N
M J S D M J S D M J S D M J S D M J S D M J S D M J S D
2010 2011 2012 2013 2014 2015 2016
1.44 1.36 1.28 1.2 1.12 1.04 0.96 0.88 0.8 0.72 0.64 0.56 0.48 0.4 0.32 0.24 0.16 0.08 0
b)
60°N
50°N
40°N
30°N
M J S D M J S D M J S D M J S D M J S D M J S D M J S D
2010 2011 2012 2013 2014 2015 2016
1.44 1.36 1.28 1.2 1.12 1.04 0.96 0.88 0.8 0.72 0.64 0.56 0.48 0.4 0.32 0.24 0.16 0.08 0
c)
60°N
50°N
40°N
30°N
M J S D M J S D M J S D M J S D M J S D M J S D M J S D
2010 2011 2012 2013 2014 2015 2016
1.1 0.995 0.89 0.785 0.68 0.575 0.47 0.365 0.26 0.155 0.05 −0.055 −0.16 −0.265 −0.37 −0.475 −0.58 −0.685 −0.79 −0.895 −1

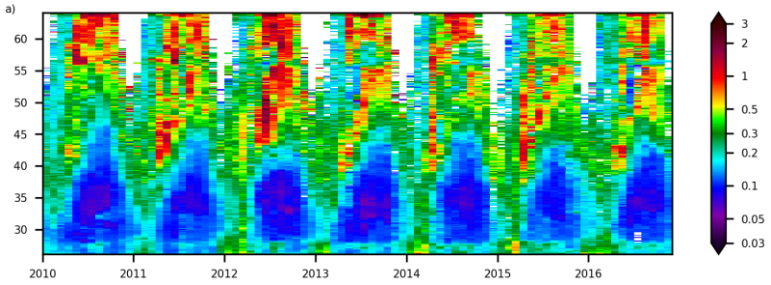
a)
60
55
50
45
40
35
30
2010 2011 2012 2013 2014 2015 2016
3 2 1 0.5 0.3 0.2 0.1 0.05 0.03

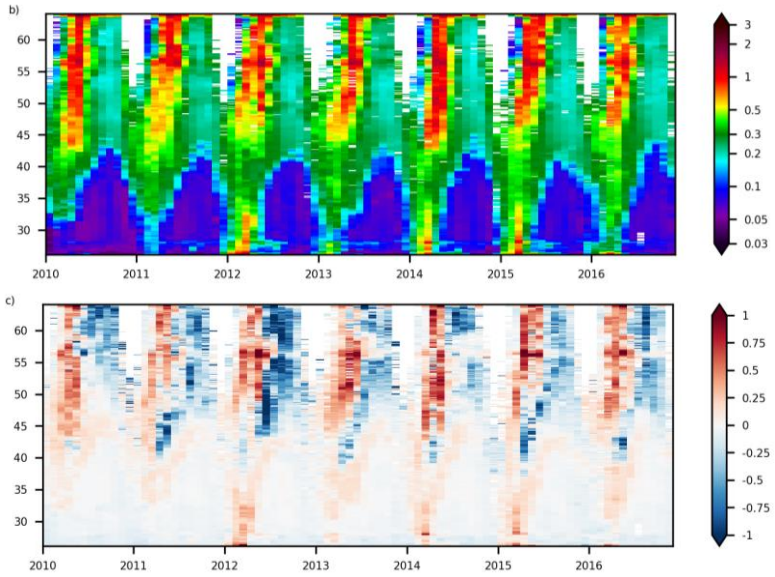

Figure 3. Hovmöller diagram for sea surface Chl-a at 15°W between 2010 and 2016. a) ESA OC-CCI ocean colour product, b) IBI36 and c) bias of Chl-a $(model - obs)$~~(model – observation)~~, all expressed in mg Chl m^{-3}. Monthly fields between 2010 and 2016 are used.~~The model is masked as a function of the data.~~

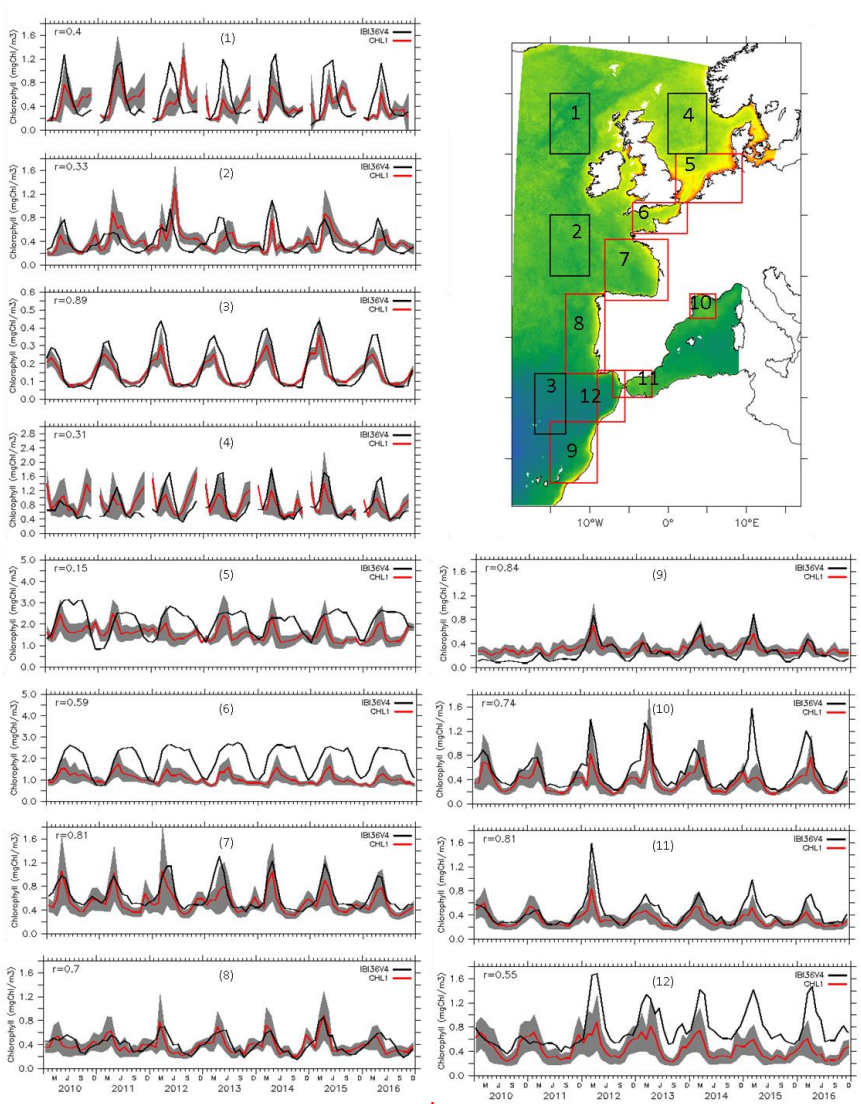
r=0.4
(1)
IBI36V4
CHL1
Chlorophyll (mgChl/m3)
r=0.33
(2)
r=0.89
(3)
r=0.31
(4)
r=0.15
(5)
r=0.59
(6)
r=0.81
(7)
r=0.7
(8)
r=0.84
(9)
r=0.74
(10)
r=0.81
(11)
r=0.55
(12)
1
2
3
4
5
6
7
8
9
10
11
12
10°W
0°
10°E
M J S D M J S D M J S D M J S D M J S D M J S D M J S D
2010
2011
2012
2013
2014
2015
2016

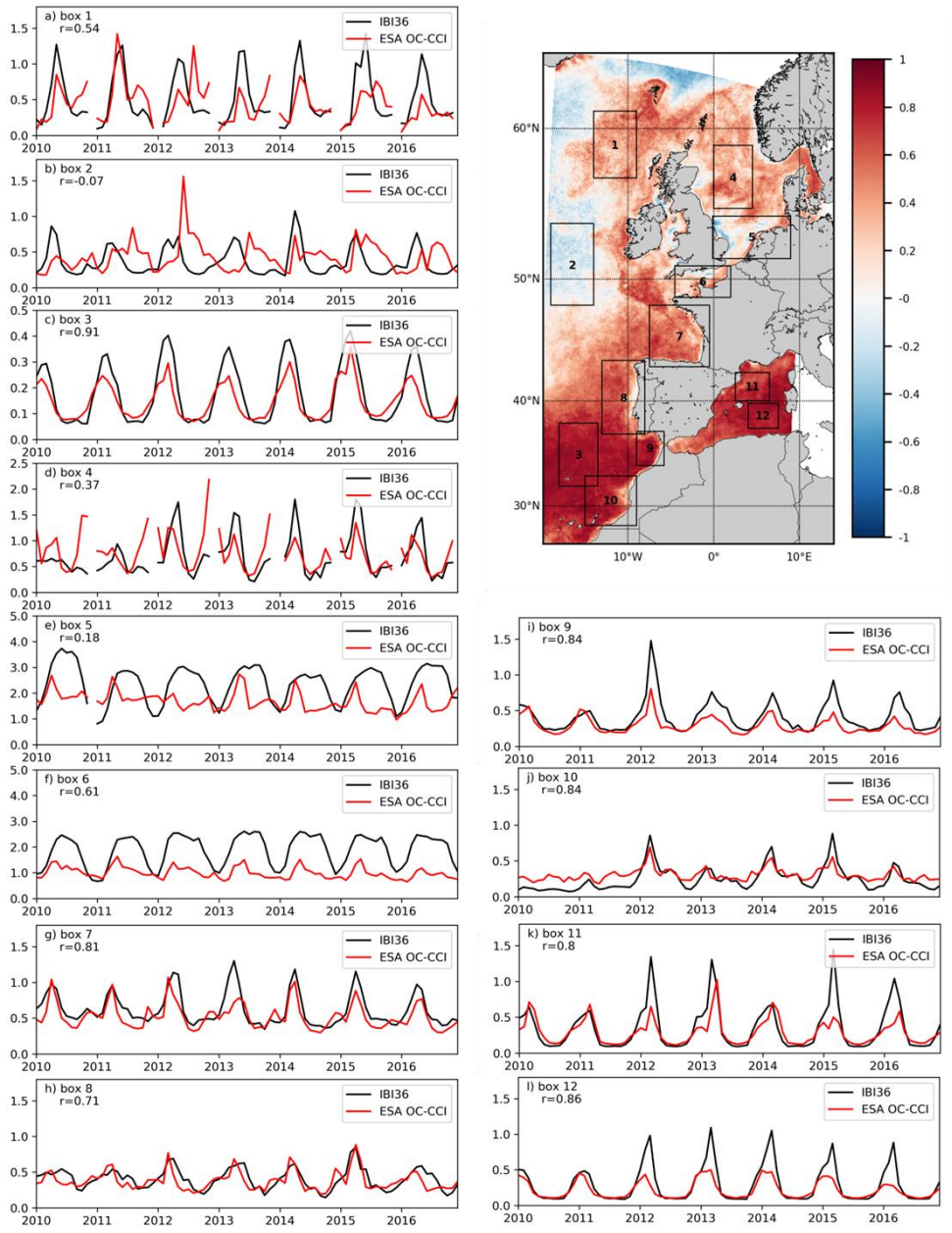

Figure 4. T~~T~~ime series of Sea surface Chl-a (mg Chl m^{-3}) between 2010 and 2016. IBI36 is in black and ESA OC-CCI ocean colour product in red ~~with associated error in grey~~. ~~Concentrations~~ Chl-a is ~~are~~ averaged over the 12 ~~small~~ boxes ~~as~~ defined in Figure 1 and reported to the map on the top-right. The correlation between the model and the data is indicated in the top-left of each time series. The top-right panel represents the spatial distribution of temporal correlation between the model and the observation. ~~The model is masked as a function of the data.~~ Note the different scales in y-axis. ~~The correlation between the model and the data is indicated in the top-left of each panel.~~

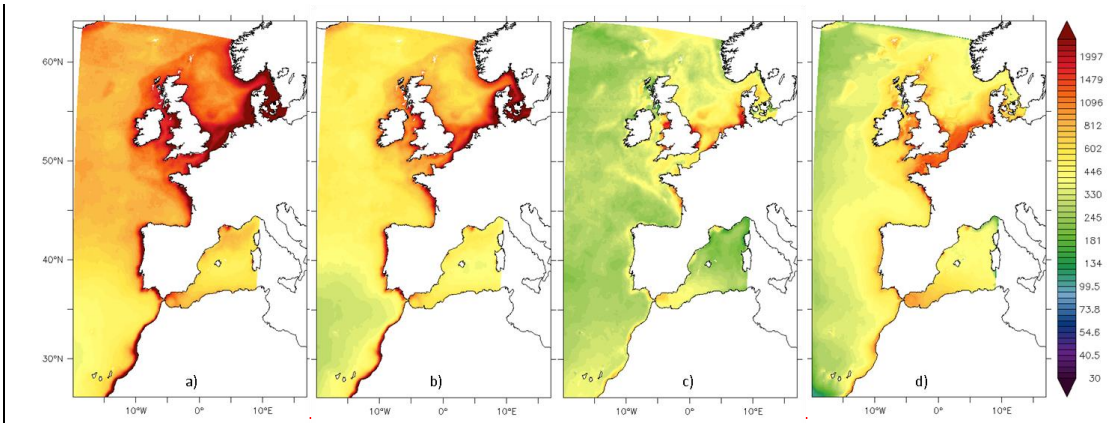
60°N
50°N
40°N
30°N
10°W
0°
10°E
a)
b)
c)
d)
1997
1479
1096
812
602
446
330
245
181
134
99.5
73.8
54.6
40.5
30

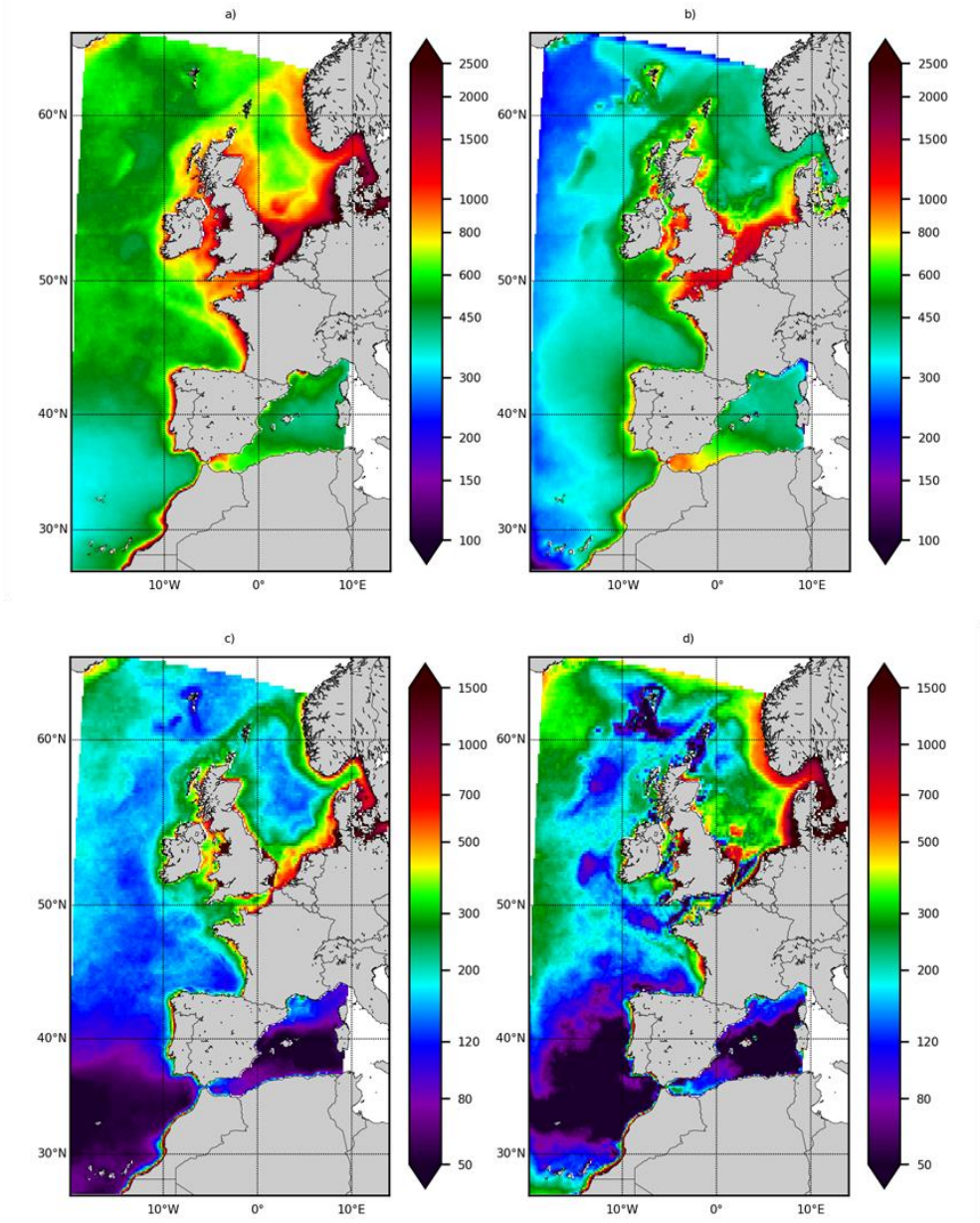

Figure 5. Depth integrated ~~net primary production~~NPP (mg C m^{-2} d^{-1}). a) Mean of the three NPP products (~~Annual average for a)~~ VGPM, ~~b)~~ Eppley-VGPM and ~~, c)~~ CbPM)~~,~~ ~~and b~~d) IBI36, ~~,~~ c) standard deviation of the three NPP products, and d) bias ($IBI36 - mean\ NPP\ poducts$). ~~Averages~~Statistics are computed from monthly fields between 2010 and 201~~5~~6.~~, and the model is masked as a function of the data.~~

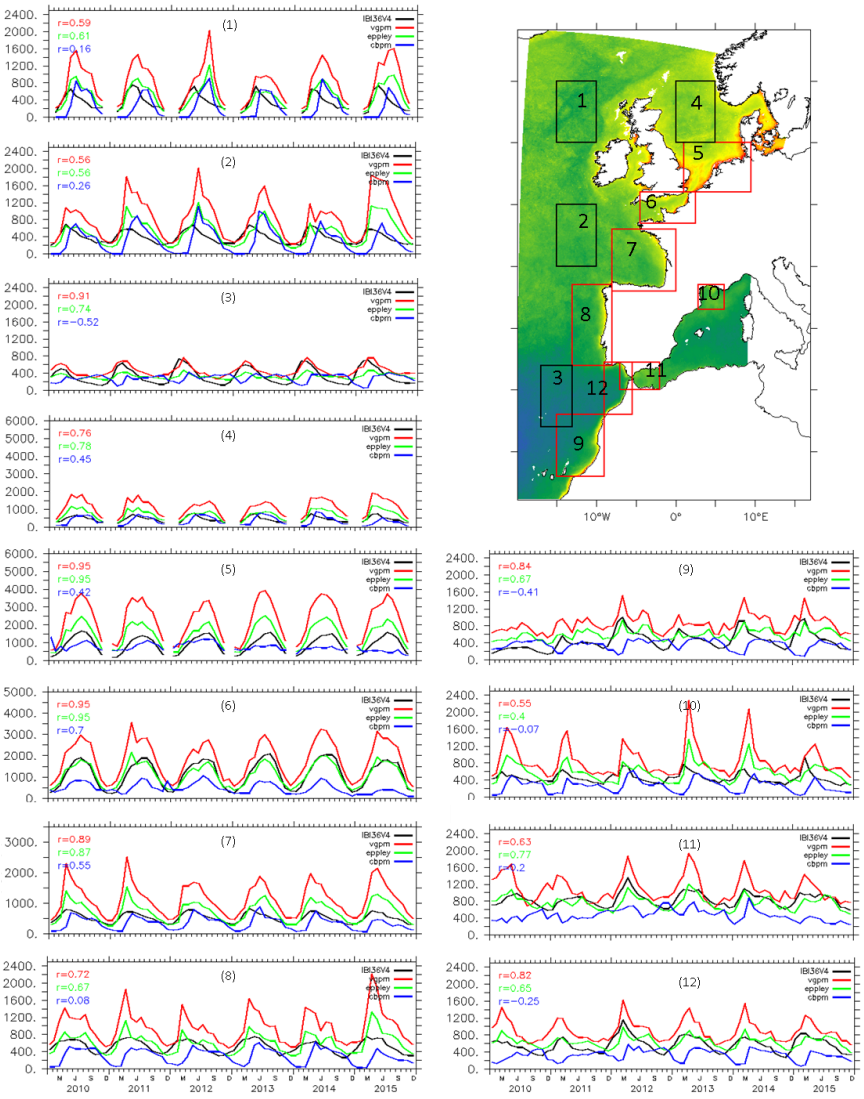
(1)
r=0.59
r=0.61
r=0.16
(2)
r=0.56
r=0.56
r=0.26
(3)
r=0.91
r=0.74
r=−0.52
(4)
r=0.76
r=0.78
r=0.45
(5)
r=0.95
r=0.95
r=0.42
(6)
r=0.95
r=0.95
r=0.7
(7)
r=0.89
r=0.87
r=0.55
(8)
r=0.72
r=0.67
r=0.08
(9)
r=0.84
r=0.67
r=−0.41
(10)
r=0.55
r=0.4
r=−0.07
(11)
r=0.63
r=0.77
r=0.2
(12)
r=0.82
r=0.65
r=−0.25
vgpm
eppley
cbpm
2010
2011
2012
2013
2014
2015
10°W
0°
10°E

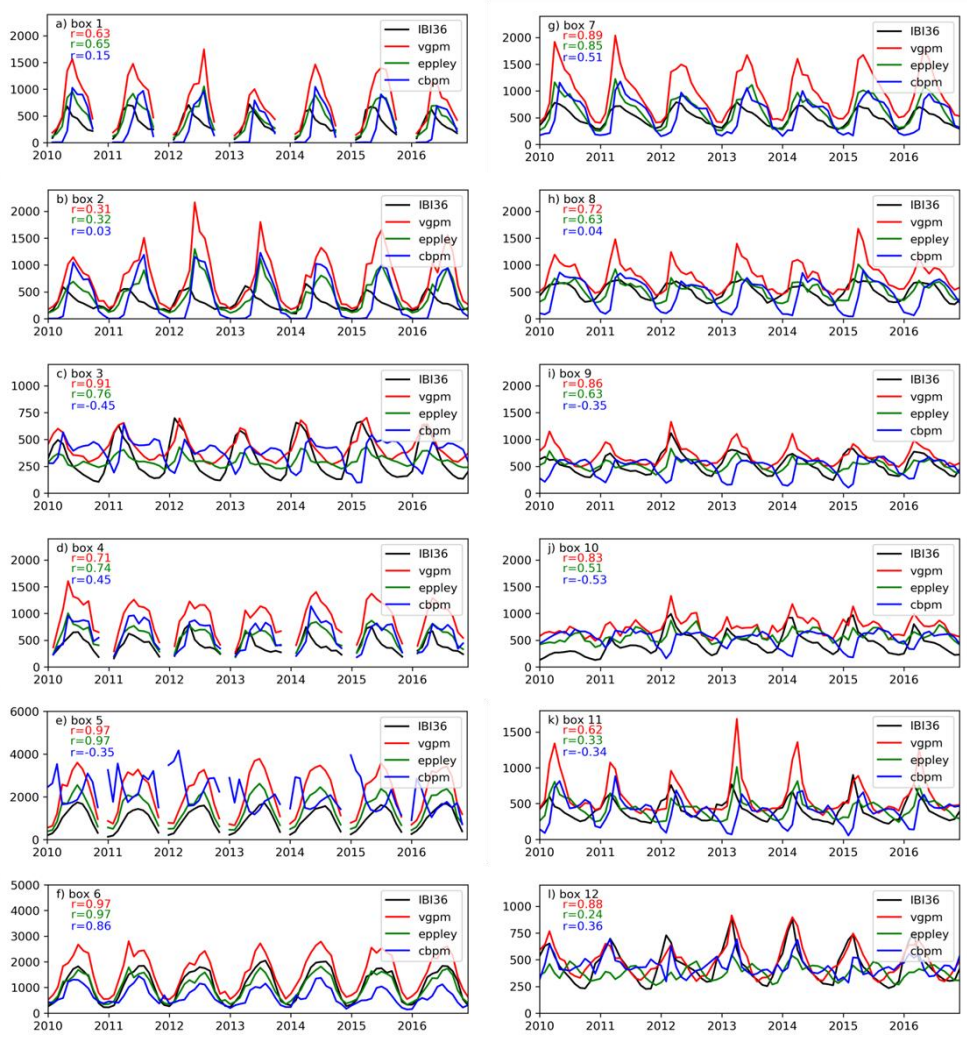

Figure 6. Time series of depth integrated ~~net primary production~~NPP (mg C m^{-2} d^{-1}) between 2010 and 201~~5~~6. IBI36 is in black, VGPM in red, Eppley-VGPM in green and CbPM in blue. NPP is averaged over 12 small boxes ~~as~~ defined in ~~the map on the top right~~Figure 1. ~~The model is masked as a function of the data.~~ Note the different scales in y-axis. The correlation between the model and the NPP products (using corresponding colours) is indicated in the top-left of each panel.

1280

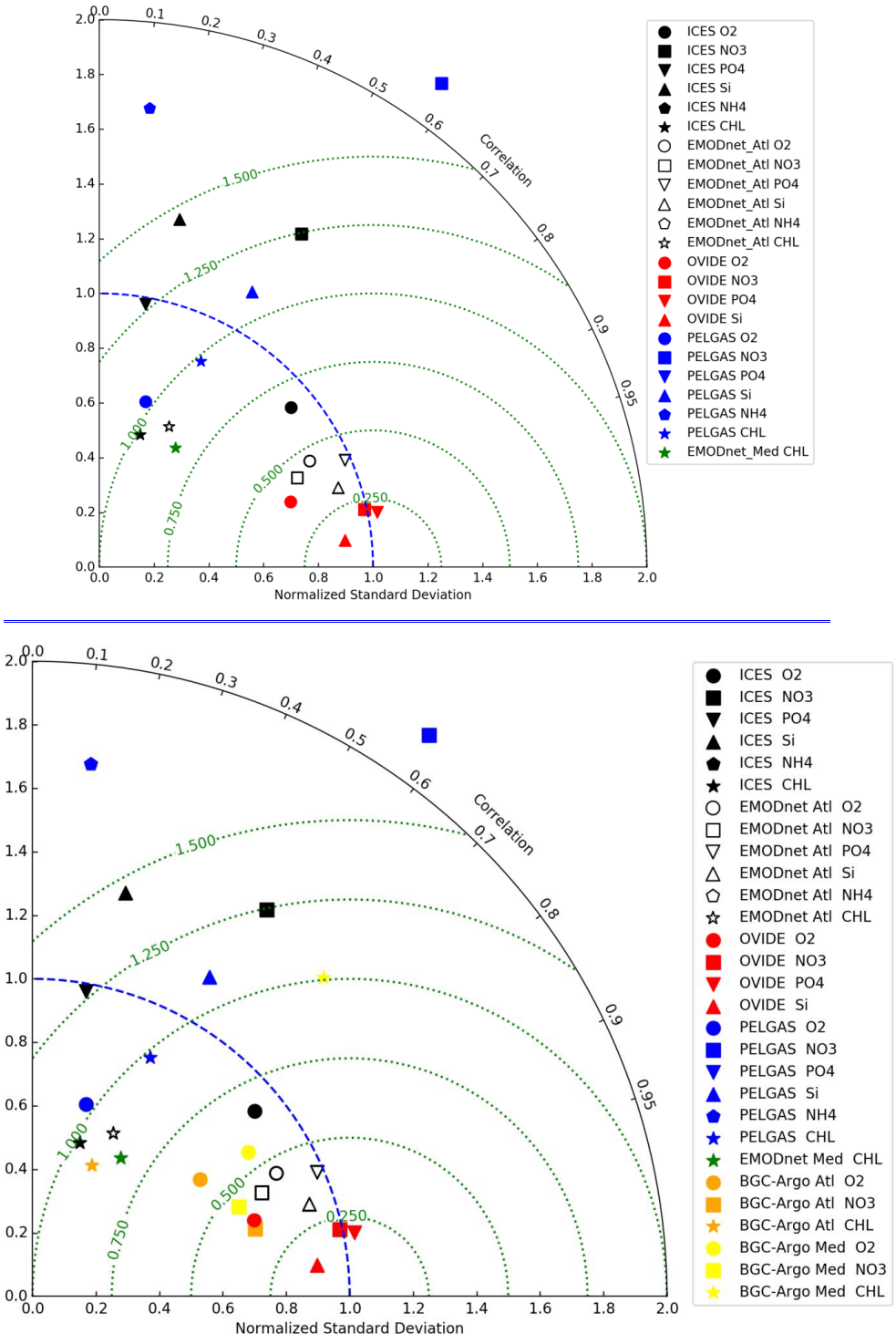

Figure 7~~16~~. Taylor diagram summarizing the skill of the IBI36 system to estimate the main biogeochemical variables: oxygen (circle), nitrate (square), phosphate (triangle pointing upwards), silicate (triangle pointing down), ammonium (pentagone) and Chl-a (star) from ICES (black), North Atlantic EMODnet product (white), OVIDE (red), PELGAS (blue),

Mediterranean EMODnet product (green), APEX BGC-Argo in the Atlantic (orange) and PROVOR BGC-Argo in the Mediterranean (yellow).

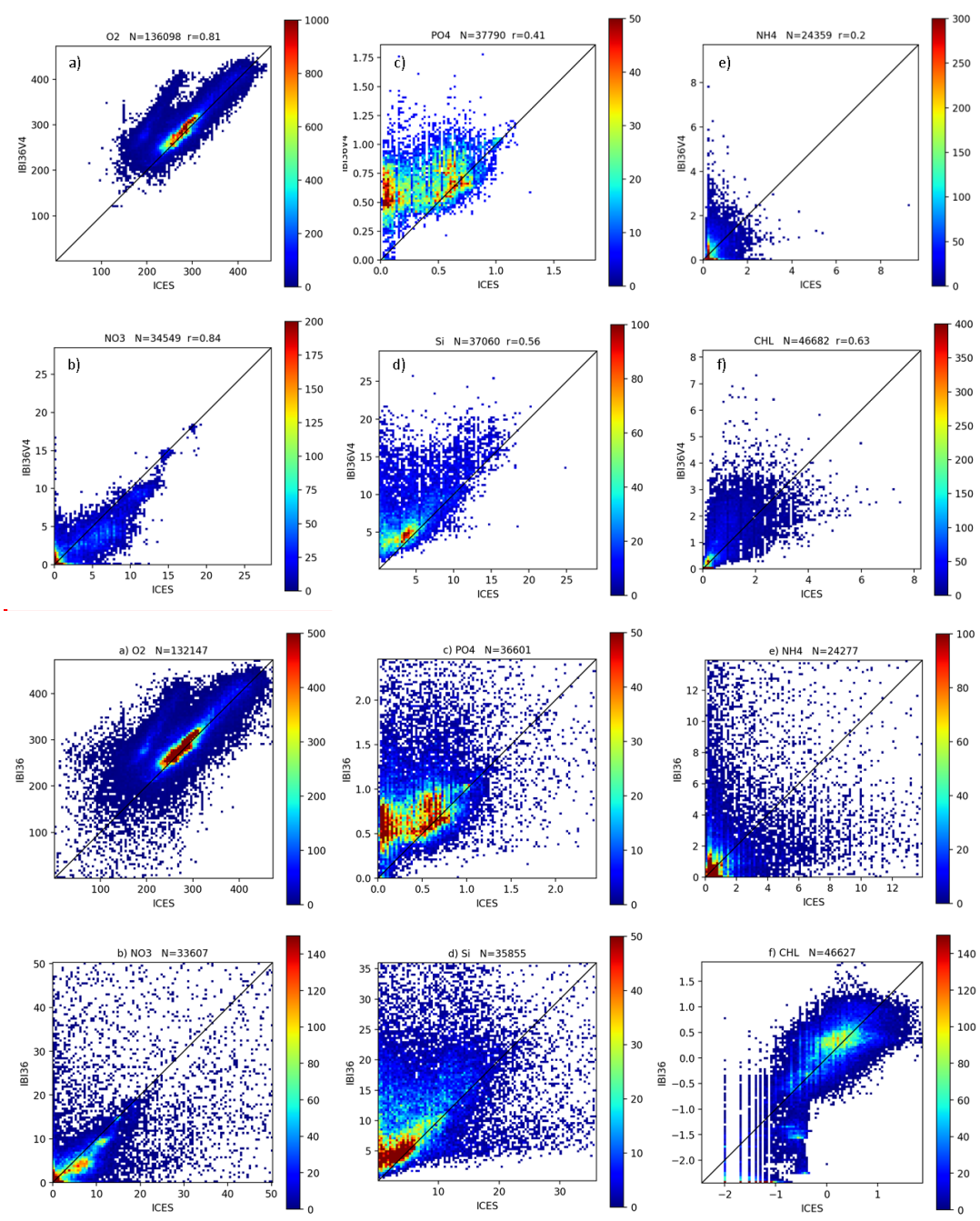

Figure 8~~7~~. Density plots for a) oxygen ~~(a)~~, b) nitrate ~~(b)~~, c) phosphate ~~(c)~~, d) silicate ~~(d)~~, e) ammonium ~~(e)~~, and f) log10(Chl-a) ~~(f)~~. ICES data are on the x-axis and IBI36 on the y-axis. Oxygen and nutrients are expressed in µmol l^{-1} ~~and Chl-a in mg Chl m^{-3}~~. Each axis is divided in 100 bins and colorbar represents the density of the match-ups (number of overlapping points). Note the different scales for the variables. ~~Low-density points are removed (density lower than the threshold of 5), some extrema are then not visible here.~~ N indicates the total number of match-ups~~, and r the Pearson correlation coefficient~~. Daily averaged IBI36 outputs and ICES data are collocated in space and time between 2010 and 2016. All depths are presented, keeping in mind that ICES data are mainly located in the shallow and coastal waters of the Northern seas.

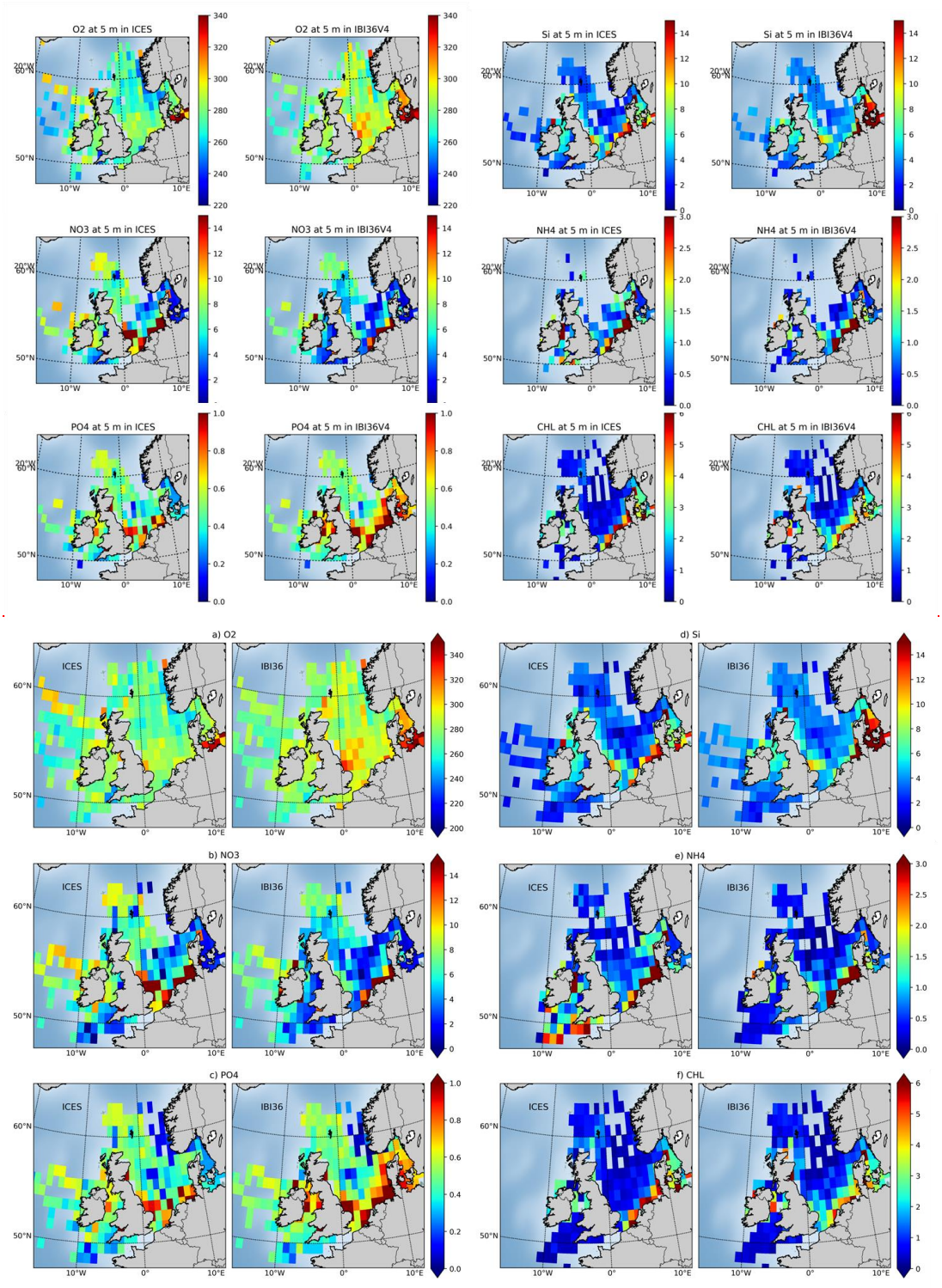

Figure 9~~8~~. Surface concentrations of a) oxygen, b) nitrate, c) phosphate, d) silicate, e) ammonium and f) Chl-a from ICES database (left of each panel) and IBI36 (right of each panel). Oxygen and nutrients are expressed in µmol l^{-1} and Chl-a in mg Chl m^{-3}. Daily averaged IBI36 outputs and ICES data are collocated in space and time between 2010 and 2016. Match-ups

are averaged between 0 and 10 meter depth, gridded and averaged on a horizontal grid of 1°x1° resolution. ~~Grid points containing less than 5 data are excluded.~~

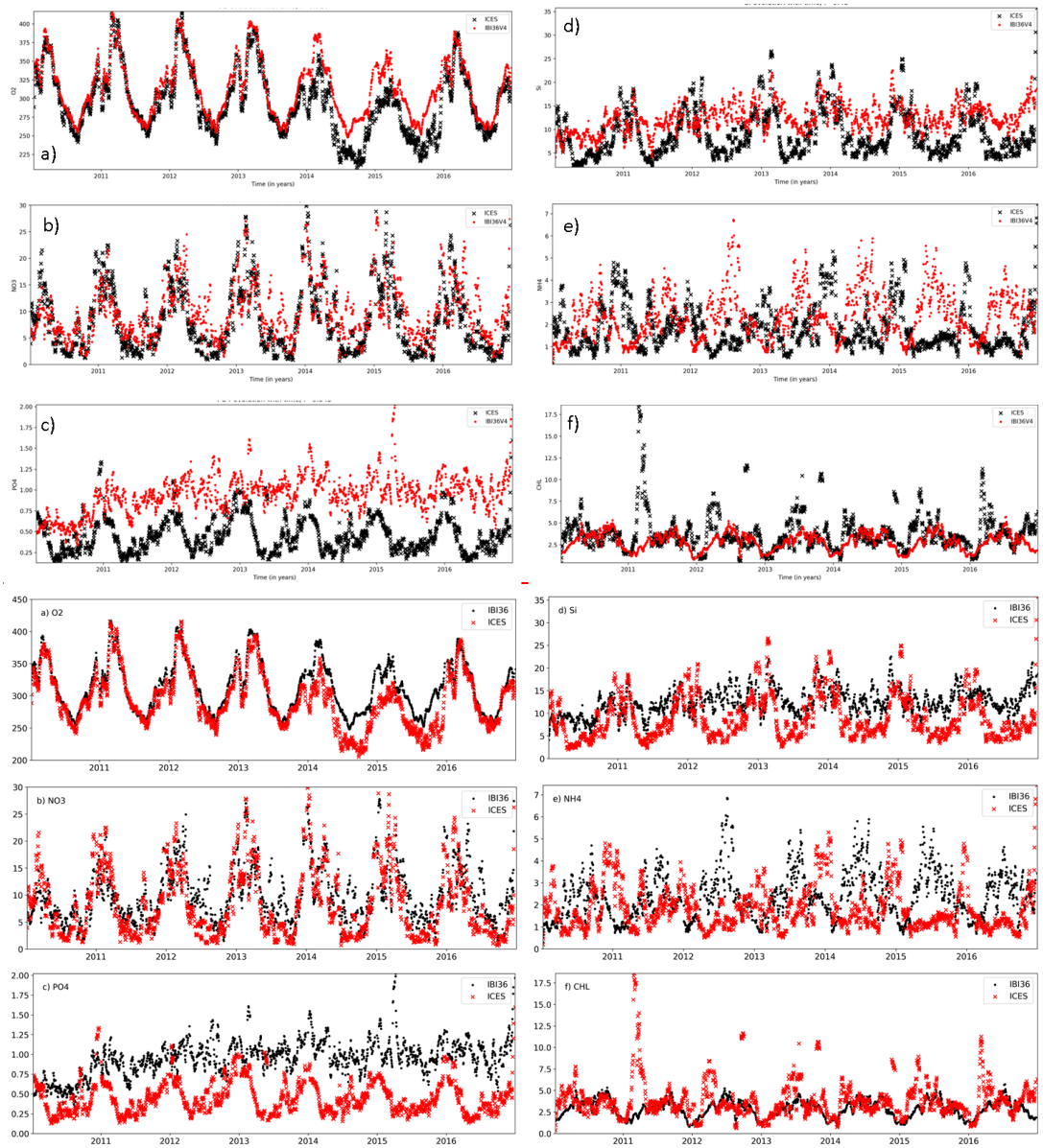

Figure 10~~9~~. Time series of surface concentrations of a) oxygen, b) nitrate, c) phosphate, d) silicate, e) ammonium and f) Chl-a from ICES (red~~black~~) and IBI36 (black~~red~~). Oxygen and nutrients are expressed in µmol l^{-1} and Chl-a in mg Chl m^{-3}. Daily averaged IBI36 outputs and ICES data are collocated in space and time between 2010 and 2016. Match-ups are averaged between 0 and 10 meter depth, and daily averaged. Time series are smoothed using a 10-day window.

1330

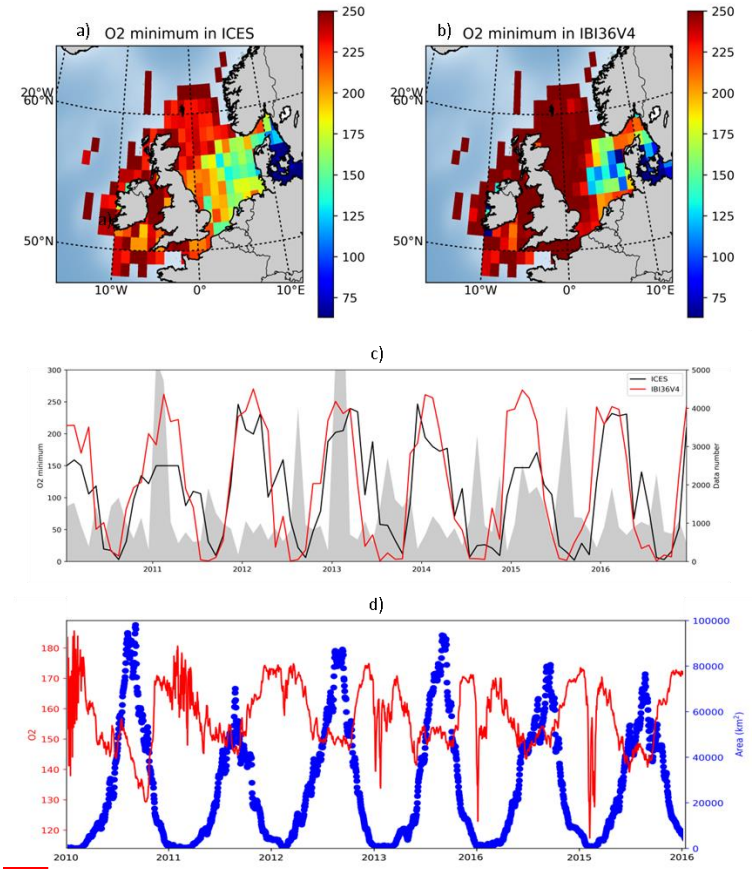
a) O2 minimum in ICES
b) O2 minimum in IBI36V4
20°W
60°N
50°N
10°W
0°
10°E
250
225
200
175
150
125
100
75
c)
ICES
IBI36V4
O2 minimum
Data number
2011
2012
2013
2014
2015
2016
d)
O2
Area (km²)
2010
2011
2012
2013
2016
2015
2016

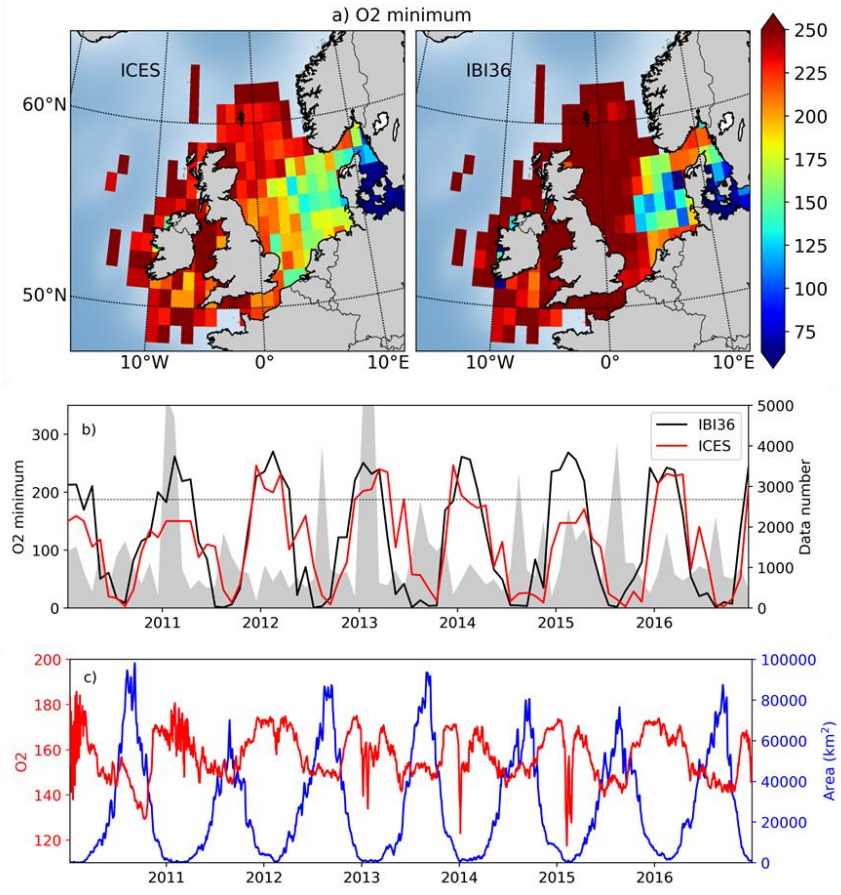

Figure 1~~0~~: a) ~~Areas vulnerable to oxygen deficiency over the continental shelf (bathymetry <= 200m).~~ Minimum oxygen (µmol l^{-1}) in ~~a)~~ ICES data (left) and ~~b)~~ IBI36 col~~-~~located to ICES (right) between 2010 and 2016. b~~c~~) Time series of minimum oxygen (µmol l^{-1}) in ICES data (~~black~~red) and IBI36 IBI36 col~~l~~located to ICES (~~red~~black). The deficiency threshold of oxygen (6 mg l^{-1} or 187.5 µmol l^{-1}) is represented by the dashed line. Number of available data in ICES is added to the right axis (area plot in gray). c~~d~~) Surface area (in km^2) vulnerable to oxygen deficiency, that is where oxygen ~~concentrations~~ decrease below the deficiency threshold ~~of 6 mg l^{-1} (or 187.5 µmol l^{-1}) over the continental shelf~~ (blue; right axis) and associated mean oxygen concentrations (µmol l^{-1}; red; left axis) using the whole ~~in~~ IBI36 simulation (not only IBI36 col~~l~~located to ICES). The three subplots are for the continental shelf (bathymetry <= 200m).

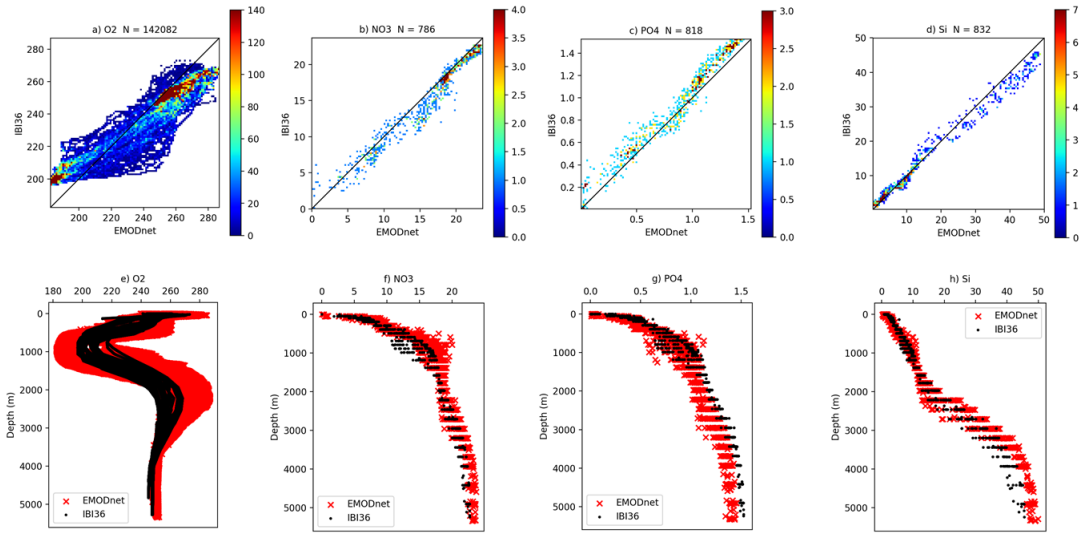
a) O2 N = 142082
b) NO3 N = 786
c) PO4 N = 818
d) Si N = 832
IBI36
EMODnet
e) O2
f) NO3
g) PO4
h) Si
Depth (m)
EMODnet
IBI36

1350

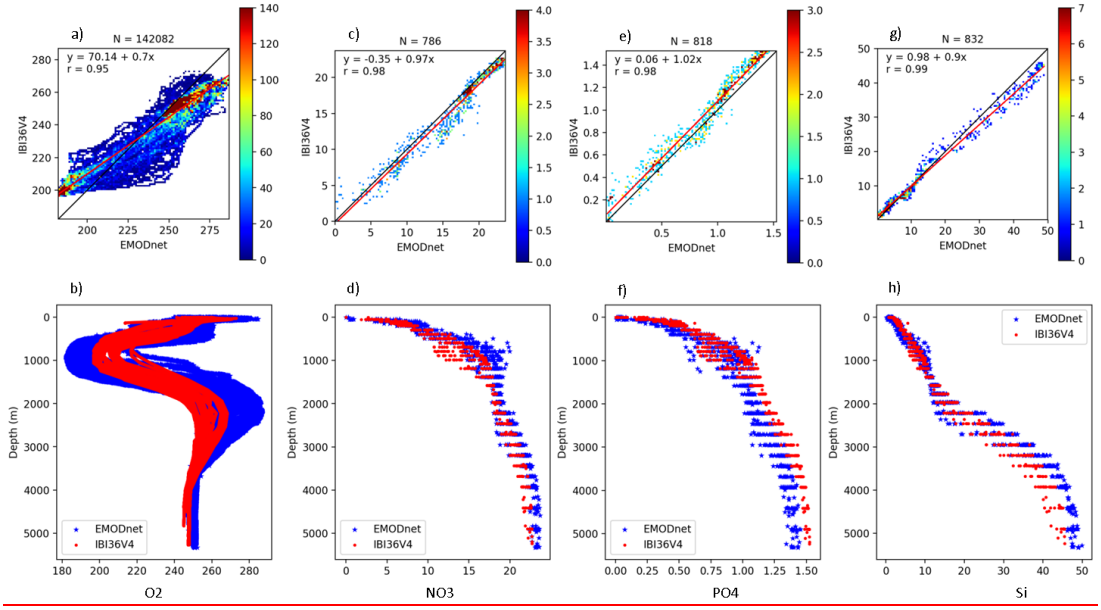
a)
N = 142082
y = 70.14 + 0.7x
r = 0.95
c)
N = 786
y = -0.35 + 0.97x
r = 0.98
e)
N = 818
y = 0.06 + 1.02x
r = 0.98
g)
N = 832
y = 0.98 + 0.9x
r = 0.99
IBI36V4
EMODnet
b)
d)
f)
h)
Depth (m)
EMODnet
IBI36V4
O2
NO3
PO4
Si

Figure 12~~1~~. Density plots (top) and vertical profiles (bottom) for oxygen (a, ~~b~~e), nitrate (~~c~~b, ~~d~~f), phosphate (~~e~~c, ~~f~~g), and silicate (~~g~~d, h) from OVIDE section data (EMODnet dataset~~base~~) and IBI36. All nutrients are expressed in µmol l^{-1}. OVIDE data are on the x-axis and IBI36 on the y-axis of the density plots. Each axis is divided in 100 bins and colorbar represents the density of the match-ups ~~-~~(number of overlapping points). Note the different scales for the variables. N indicates the total number of match-ups, and r the Pearson correlation coefficient. Daily averaged IBI36 outputs and OVIDE section data are collocated in space and time.

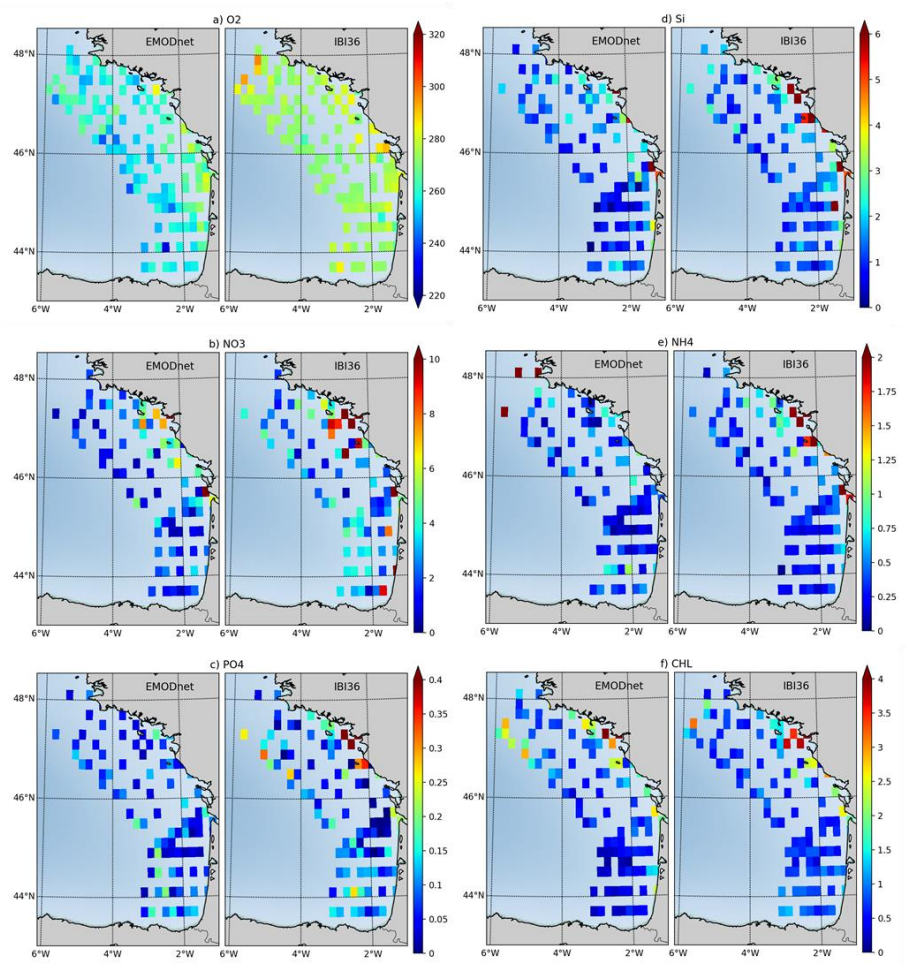
a) O2
EMODnet
IBI36
d) Si
b) NO3
e) NH4
c) PO4
f) CHL
48°N
46°N
44°N
6°W
4°W
2°W

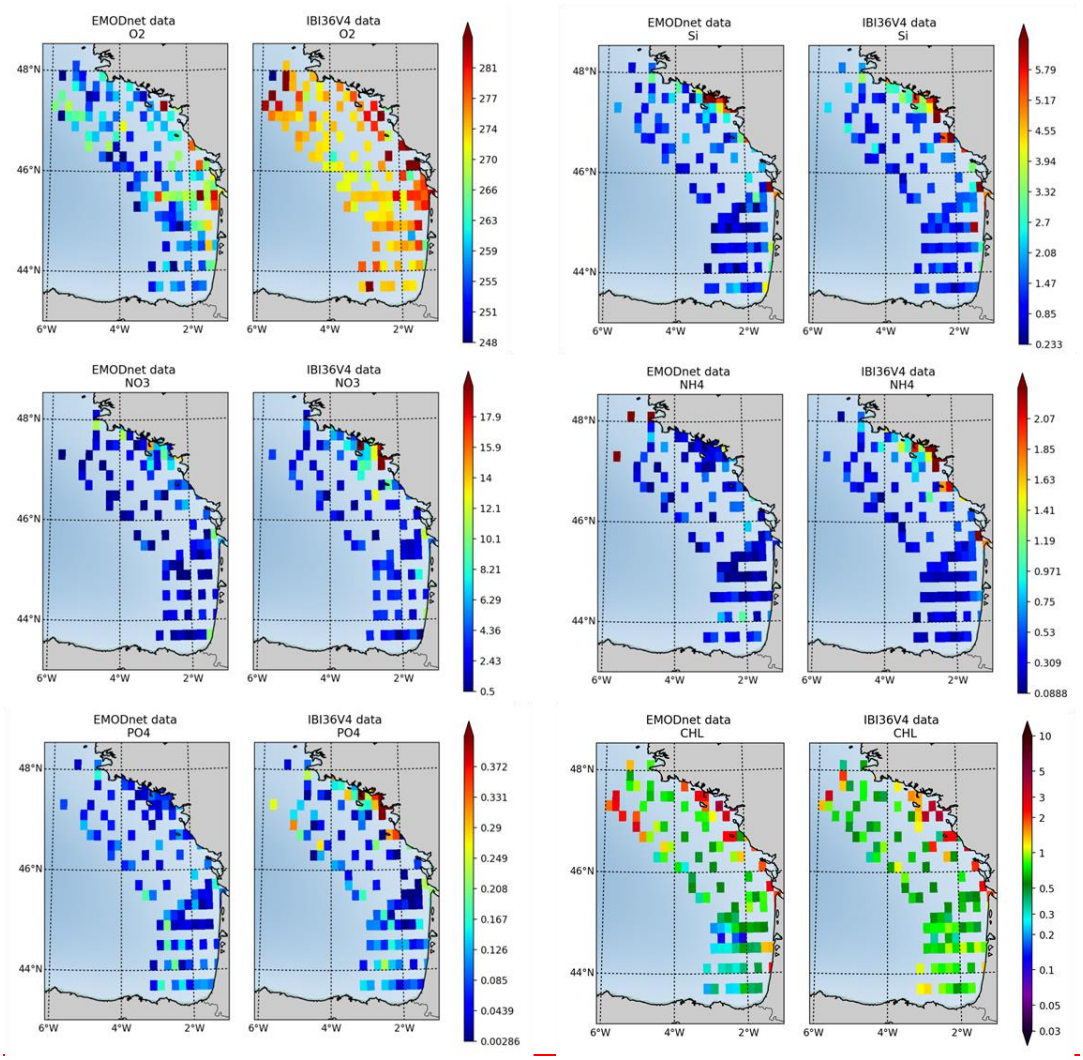

Figure 13~~2~~. Surface concentrations of oxygen (a), nitrate (b), phosphate (c), silicate (d), ammonium (e) and Chl-a (f) from the PELGAS data of the ~~(~~EMODnet database~~)~~ (left of each panel) and IBI36 (right of each panel). Oxygen and nutrients are expressed in µmol l^{-1} and Chl-a in mg Chl m^{-3}. IBI36 and PELGAS data are collocated in space and time between 2010 and 2016. Match-ups are averaged between 0 and 10 meter depth, gridded and averaged on a horizontal grid of 0.~~1~~2°x0.~~1~~2° resolution.

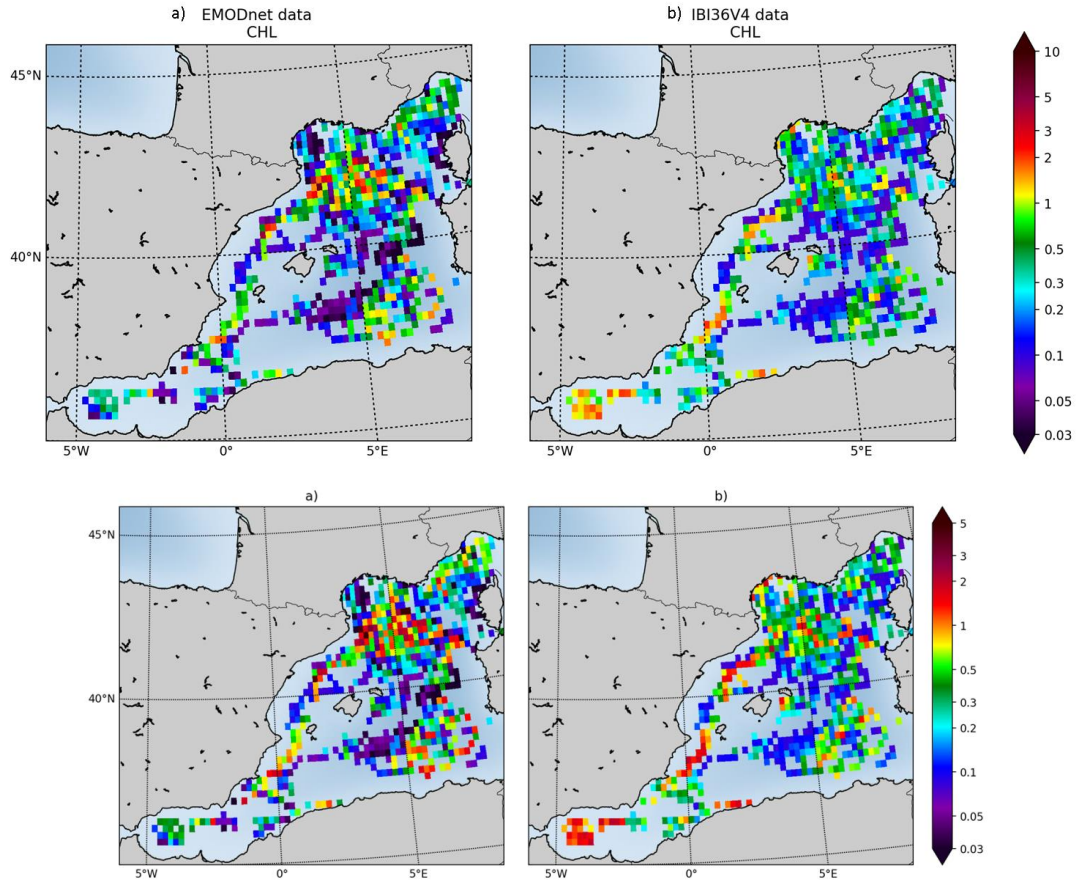

Figure 1[4]~~3~~. Sea surface Chl-a from EMODnet dataset (a) and IBI36 (b) in mg Chl m^{-3}. IBI36 and EMODnet dataset are collocated in space and time between 2010 and 2016. Match-ups are averaged between 0 and 10 meter depth, gridded and averaged on a horizontal grid of 0.2°x0.2° resolution.

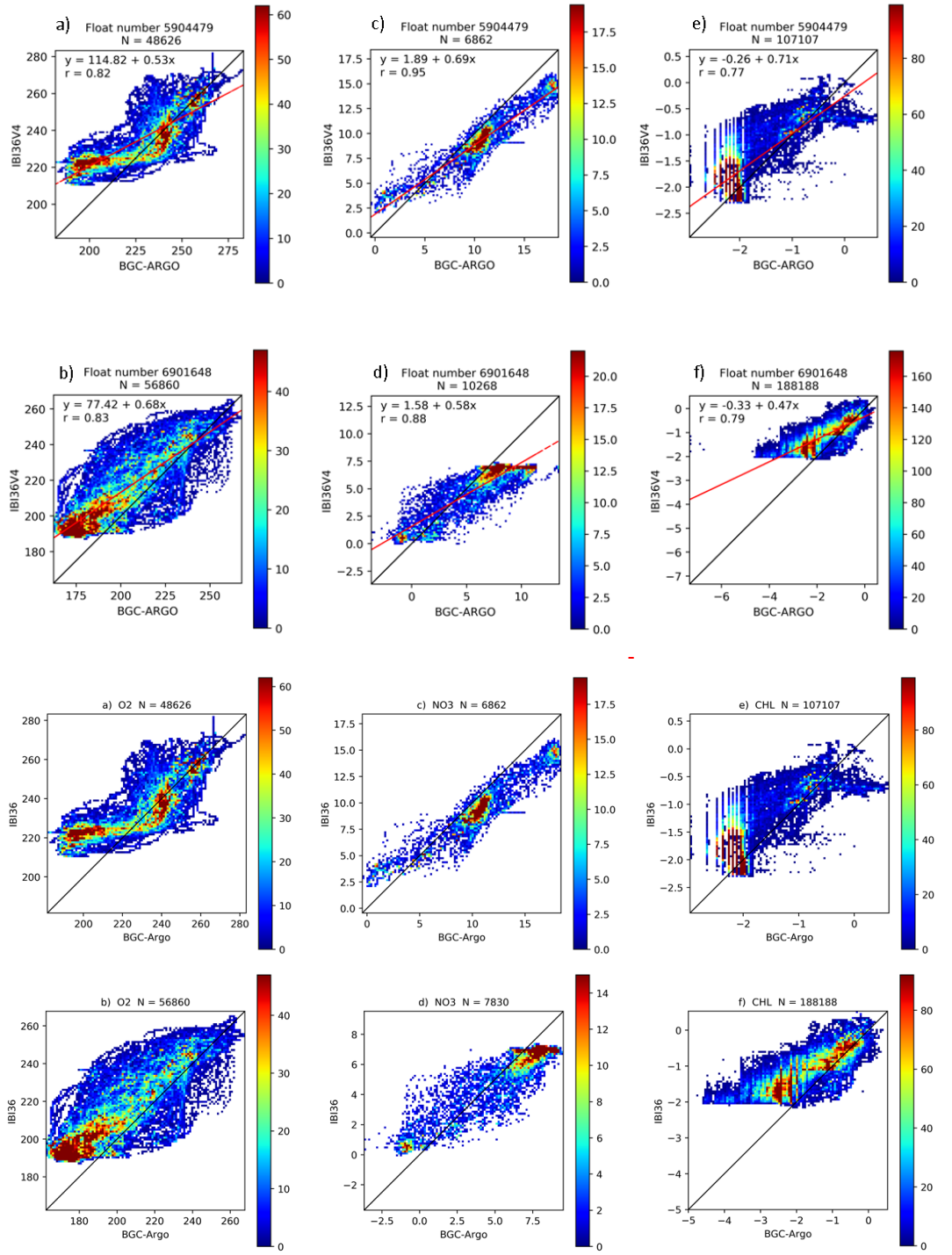

Figure 154. Density plots for oxygen (a, b), nitrate (c, d), and log(Chl-a) (e, f) from BGC-Argo data and IBI36 for the Atlantic (top) and Mediterranean (bottom). Oxygen and nitrate are expressed in µmol l^{-1}. Argo data are on the x-axis and

IBI36 on the y-axis of the density plots. Each axis is divided in 100 bins and colorbar represents the density of the match-ups (number of overlapping points). Note the different scales for the variables. N indicates the total number of match-ups, and r the Pearson correlation coefficient. IBI36 and Argo data are collocated in space and time.

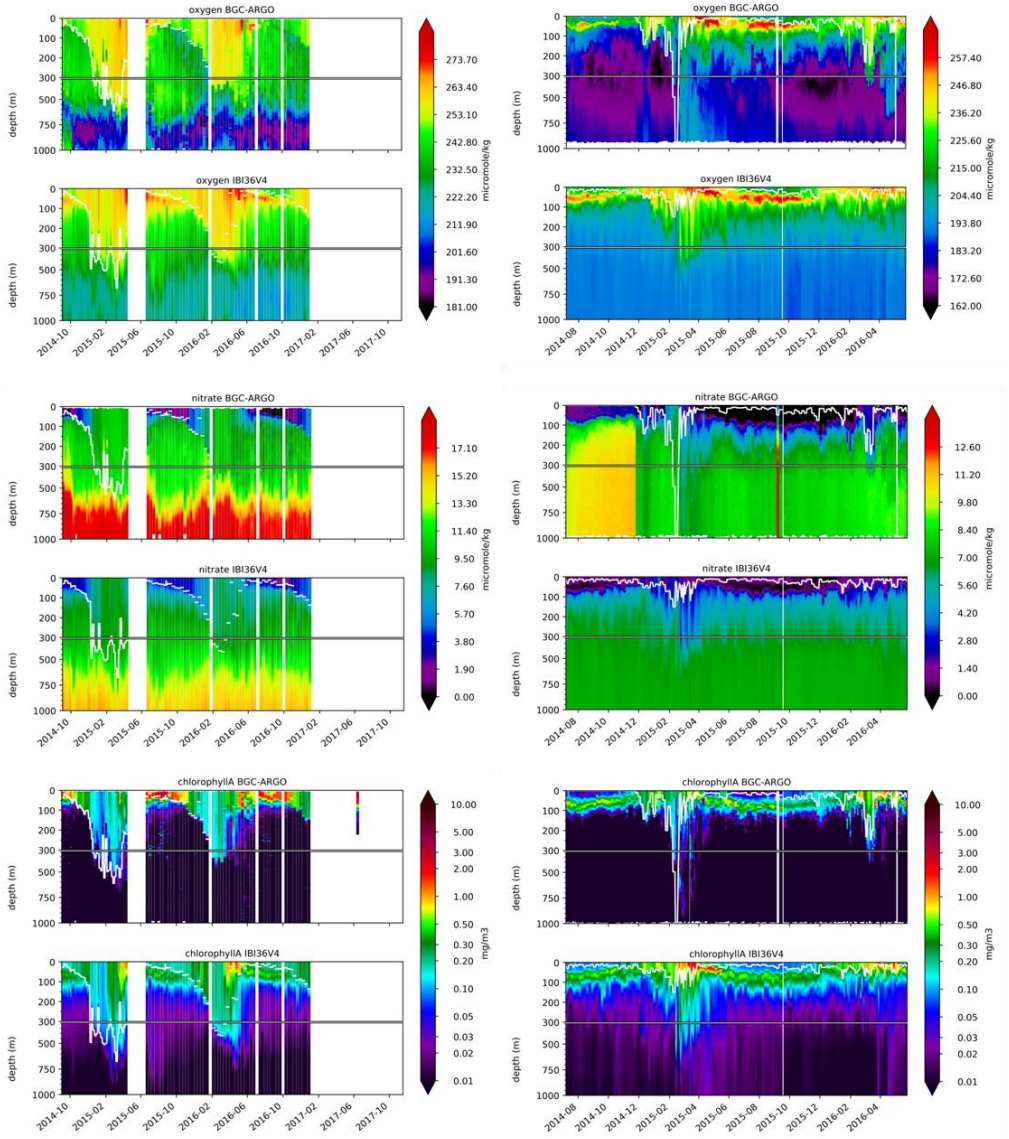
oxygen BGC-ARGO
oxygen IBI36V4
nitrate BGC-ARGO
nitrate IBI36V4
chlorophyllA BGC-ARGO
chlorophyllA IBI36V4
depth (m)
micromole/kg
mg/m3

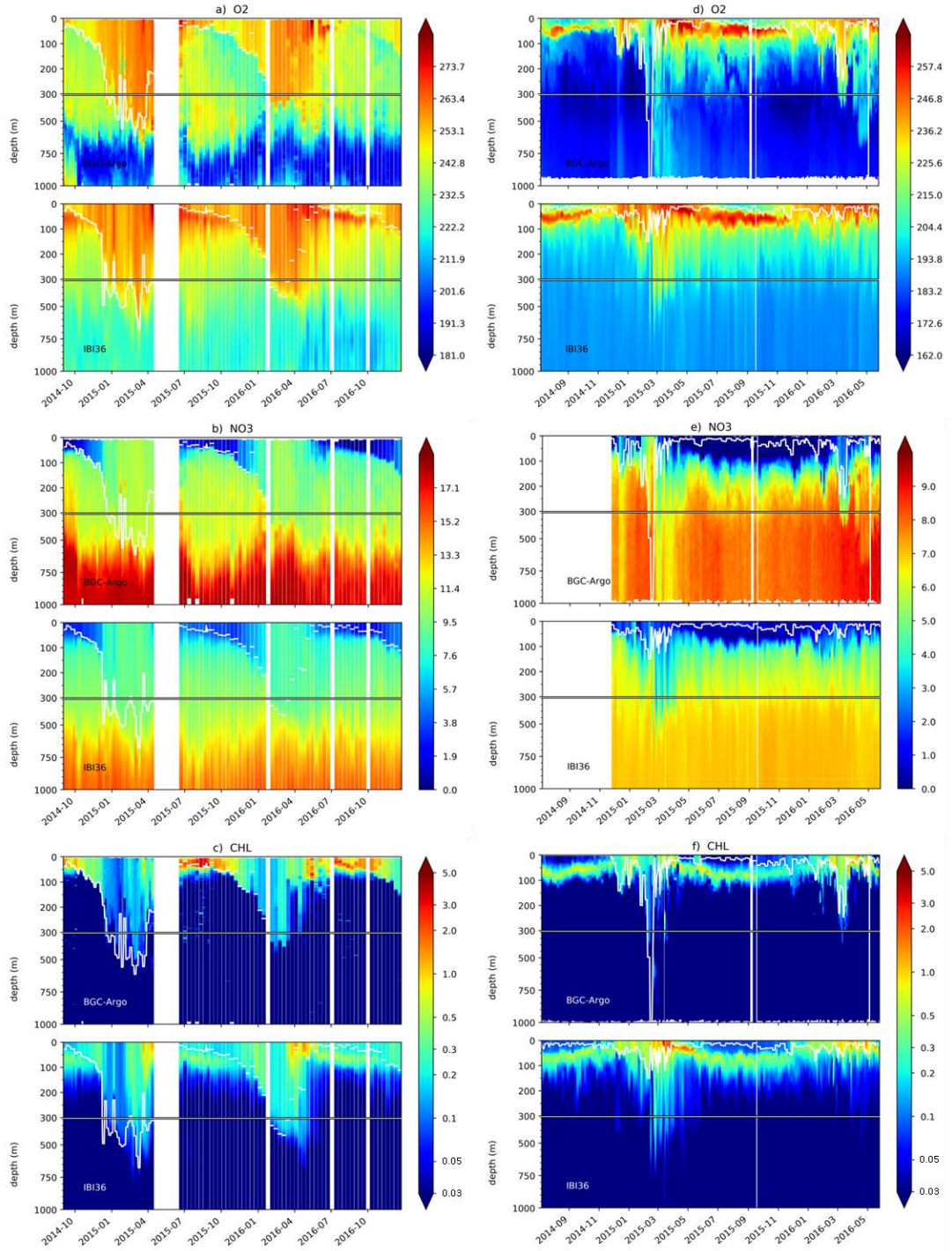

Figure 1~~6~~5. Time series of oxygen (top), nitrate (middle), and Chl-a (bottom) from BGC-Argo data and IBI36 for the Atlantic (left) and Mediterranean (right). Oxygen and nitrate are expressed in µmol l^{-1} and Chl-a in mg Chl m^{-3}. IBI36 and Argo data are collocated in space and time. The white line represents the MLD computed from ~~XXX~~density criterion~~a~~ ~~.~~of

0.03 kg m^{-3} difference from surface.

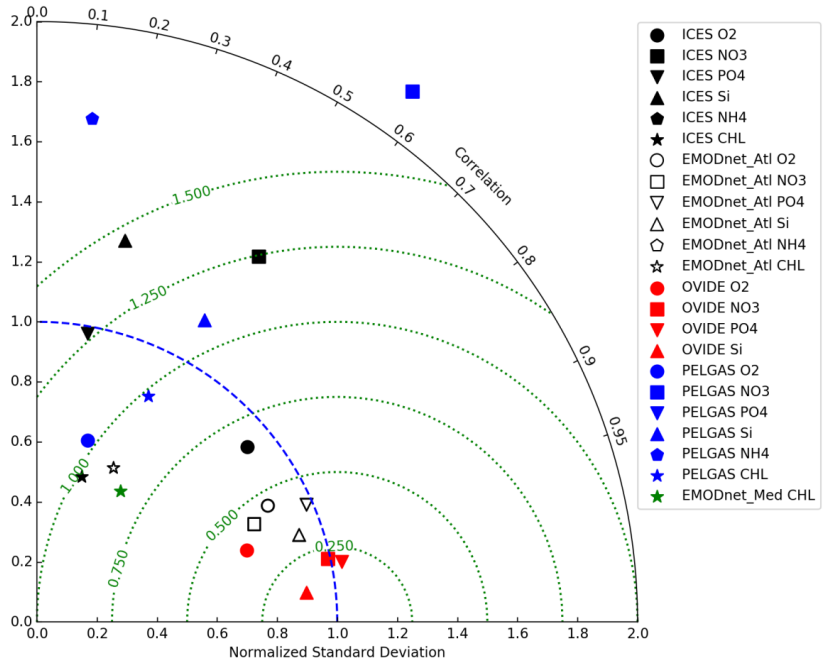

~~Figure 16.~~